NTNU

Norwegian University of
Science and Technology

Power system for electric heating of pipelines

Frode Karstein Novik

Master of Science in Energy and Environment
Submission date: June 2008
Supervisor: Arne Nysveen, ELKRAFT

Norwegian University of Science and Technology
Department of Electrical Power Engineering

Problem Description

In subsea oil production, the well-stream cools down when flowing from the well heads to the platform or onshore process facility. Traditionally chemical inhibitors (methanol) have been used. By insulating the pipeline thermally and heat it by enforcing current through the pipeline, the use of methanol is reduced considerably. This system, the Direct Electric Heating system (DEH) is now qualified and a state-of-the-art hydrate and wax prevention method in the North Sea.

For long pipelines a subsea power supply system is needed. Aker has suggested having a subsea power system combining the power supply to the subsea field and to the DEH system. Each section of the pipeline is a 1-phase electrical load. In the previous semester project work, different concepts related to 3-to-1, 3-to-2 and 3-to-4 phase systems were analysed. The basis for this work is 3-to-2 phase system using either the Scott-T or LeBlanc transformer. The transformer is located subsea close to the pipeline and supplied by a 3-phase subsea cable.

In this master theses the focus is on system modelling and analysis of a subsea power system for heating of long pipelines.

More specific, the master thesis includes:

- Design of possible configurations for DEH which can be used for long step out and for subsea installation.
- Establish a model for the Scott-T transformer in the simulation software SIMPOW for system simulations. Use Dynamic Simulation Language
- Simulations on the DEH power system with the Scott-T implemented during different operational modes (maintain temperature/heating). Investigate the reactive power flow.
- Analyse different fault scenarios in the DEH system with focus on its influence on the main power system, e.g. investigating the degree of unsymmetry in the rest of the power system caused by the failure.

Further details to be clarified with the supervisors during the project work.

Assignment given: 28. January 2008
Supervisor: Arne Nysveen, ELKRAFT

Abstract

Direct electrical heating (DEH) of pipelines is a flow assurance method that has proven to be a good and reliable solution for preventing the formation of hydrates and wax in multiphase flow lines. The technology is installed on several pipelines in the North Sea and has become StatoilHydros preferred method for flow assurance. Tyrihans is the newest installation with 10 MW DEH for a 43 km pipline. However, the pipeline represents a considerable single-phase load which makes the power system dependent on a balancing unit for providing symmetrical conditions. This limits the step out distance and is not suitable for subsea installation.

Aker Solutions has proposed several specially connected transformers for subsea power supply of DEH systems, Scott-T being one of them. The Scott-T transformer is a three-to-two-phase transformer which provides balanced electrical power between the two systems when the two secondary one-phase loads are equal. By implementing this transformer, it can be possible to install the power supply subsea as there is no need for a balancing unit. In addition, the system may be applicable for long step out distances. This is because the pipeline is inductive and can use the reactive power produced by the long cable which also can increase the critical cable length. There are however some limitations to this system using the Scott-T transformer. There is a large variation in the magnetic permeability between individual joints of the pipeline. This can result in different load impedance of the two pipe sections connected to the Scott-T transformer. The result is unbalance in the power system.

The method of symmetrical components is applied to investigate the behavior during unbalanced loading of the Scott–T transformer. The relationship between the negative– and the positive sequence component of the current is used to express the degree of unsymmetry. For the simulations in SIMPOW, the Scott–T transformer is modelled by the use of Dynamic Simulation Language. The simulations on the DSL model give correct and reliable results for analysing the degree of unsymmetry in the Scott–T transformer. When the load impedance of one pipe section is varied, simulation proves that it can change between 0.75 and 1.34 per unit of the other pipe impedance. The Scott–T transformer does still provide electrical power between the two systems which is below the limit for the degree of unsymmetry (15%).

Case 1 and Case 2 introduce two possible configurations for a subsea DEH system with the Scott–T transformer implemented. The configurations include an onshore power supply which is connected to a subsea power system for direct electrical heating and a subsea load at the far end of the subsea cable. The pipeline in Case 1 is 100 km long and is divided into two pipe sections of 50 km which are connected to a Scott–T transformer. The pipeline in Case 2 is 200 km long and is divided into four pipe sections of 50 km each. There are two Scott–T transformers in Case 2.

For normal operation of the subsea load (50 MW, cosfi=0.9) and heating the pipe content from the ambient sea temperature, the results indicate that tap changers are necessary to keep the Scott–T transformers secondary terminal voltage at 25 kV. This meets the requirement in both cases for heating the pipe content from 4°C to 25°C within 48 hours after a shutdown of the process. The degree of unsymmetry is zero for both cases when the system is operated as normal. However, all system simulations indicate that reactive

power compensation has to be included for Case 1 as well as for Case 2 in order to have a power factor of unity at the onshore grid connection.

The fault scenarios indicate that the degree of unsymmetry is dependent on both the type of fault and the power supply in the system. For Case 1, the relationship $|\frac{I_-}{I_+}|$ is only of 3.3% in the subsea cable when there is a short–circuit at DEHBUS3, but as much as 87% at the grid connection. The degree of unsymmetry in the Scott–T transformer is then 67%. This is far beyond the limit for maximum negative sequence component of 15%. The significant unsymmetry in the line between the grid and BUS1 is most likely due to the large power delivered to the fault. During the fault, the reactive power delivered to the system increases from 10.6 Mvar to 131.9 Mvar after the fault, but the active power increases only from 75.2 MW to 87.1 MW. This means that it is most likely the reactive power that contributes to the consequent unsymmetry and negative sequence component of the current.

There are two Scott–T transformers installed in Case 2. If the DEH system is only heating the pipe section closest to shore (at DEHBUS33), simulations show that the three–phase power system becomes unsymmetric which results in different phase currents. The degree of unsymmetry at the grid connection is 32% when only the pipe section at DEHBUS33 is heated. In addition, the unbalance in the three–phase system caused by SCOTT1 involves unbalance in the SCOTT2 transformer as well. The load voltages are not equal in magnitude and dephased of 90 degrees for this mode, but are 32 kV and 35 kV respectively and dephased of 88 degrees. This concludes a very important behavior of the Scott–T transformer.

The simulations conclude that the Scott–T transformer provides symmetrical conditions for both configurations when the two load impedances are equal. However, Case 2 shows an important result when installing two Scott–T transformers in the same system. Unbalanced loading of one of the specially connected transformers gives unsymmetrical conditions in the three–phase system which results in unbalanced load voltages for the other Scott–T transformer.

The analysis is limited to the configurations given for Case 1 and Case 2, but shows typical results when an alternative transformer connection is implemented in a DEH system.

Preface

This master thesis is carried out at the Department of Electrical Power Engineering during spring 2008 and constitutes the final work of the master program of Electric Power Engineering at the Norwegian University of Science & Technology. The master thesis is based on the analysis carried out in the Specialisation project of fall 2007, and documents the work during the last semester.

Aker Engineering & Technology has proposed the subject for this master thesis. It is a part of their step to identify, qualify and select a new design for a more competitive and cost efficient direct electrical heating system.

The figures given throughout the report, such as a transformer and system configurations, have been created using Microsoft Office Visio 2003. The simulations were executed in MATLAB and SIMPOW, and the report was written in the typesetting program LaTeX. The master thesis can be read alone, but it is recommended to be familiar with the main parts in the Specialisation project of fall 2007.

Initially, the objective of the master thesis was to carry out detailed simulations on the DEH system with the specially connected transformers implemented. However, finding a suitable simulation software and establishing a model for the transformer, turned out to be more complex than first expected. Hence, a lot of the work in the thesis regards the modelling of the transformer.

I wish to thank my supervisor Professor Arne Nysveen from the Department of Electric Power Engineering at NTNU for his valuable guidance and instructions of great importance. I would also like to thank my co–supervisor Ole–Johan Bjerknes from Aker Engineering & Technology for sharing his experience and providing literature. Gratitude is also given to Atle Harald Børnes at Statoilhydro for providing data for my DEH system. In addition, I would like to give my thanks to PhD–student Steinar Danielsen for guiding and helping me with the DSL–model for the transformer. Finally, I wish to thank my wife Marte for supporting and motivating me throughout my education by her blessing and cheerful mood.

Trondheim, June 2008

Frode K. Novik

Contents

List of Figures

List of Tables

Chapter 1

Introduction

Direct electrical heating (DEH) is a flow assurance method that has proven to be a good and reliable solution for preventing the formation of hydrates in multiphase flow lines. By now the technology is installed on 16 pipelines in the North Sea, and the experience so far has been very good. The DEH system is installed on pipeline lengths up to 43 km, and the latest installation was installed summer 2007 on the Tyrihans project on a 18" pipeline [1].

The power supply for the traditional DEH system is installed topside on the platform and uses a three–to–three–phase transformer. However, the DEH system with the pipeline as the load represents a considerable single–phase load. It is in most cases desirable to convert the load to a symmetrical three–phase load, and a load balancing unit is therefore implemented in the power supply topside. This requires significant weight and space allocation. Another challenge is that the tendency in the oil industry today is to move oil production into deeper waters which also are located at greater distances from shore. The result is the use of longer pipelines requiring more power for the electrical heating of the pipelines in order to ensure a safe and reliable transport of the hydrocarbons. For long pipelines, a subsea power supply is needed, and today's DEH power supply is not suitable enough.

Aker Solutions has started the process required to qualify DEH load symmetrization by the use of three–to–two–phase transformer connections, and has proposed several alternative transformer connections for analysis [2]. The objective is to enable the design of a more competitive and cost efficient DEH system suitable for subsea installation. SINTEF Energy Research AS has earlier carried out investigations on the proposed three–to–two–phase transformer connections by Aker Solutions [3]. SINTEF recommended in particular to further analyse two configurations, which are presented in the TET5500 Specialisation project [4]. In addition, a third transformer configuration was included in the study.

The basic concepts of different flow assurance methods and especially the direct electrical heating method were also shown in [4]. Furthermore, the DEH system with a three–to–two–phase interface is explained. The three–to–two–phase transformers were analysed, and simulations on the transformer connections were carried out in order to see the effect on the symmetry when the load impedance was varied. The Specialisation Project[4] showed that the Scott–T as well as the Le Blanc transformers give symmetrical three–phase currents when the two load impedances are equal, that is $I_{-} = 0$. In addition, the simulations showed that the Scott–T and Le Blanc configurations responded well to the variations in load impedance.

The main objective of this master thesis and study is to investigate and analyse the

operational characteristics of a DEH system with a specially connected transformer implemented and in addition verify the results found in the Specialisation Project[4]. This includes load flow analysis as well as simulating typical DEH operational modes.

Chapter 2 first gives an explanation of the DEH system as a two–phase load and summarises the analysis of the three–to–two–phase transformers in [4]. In addition, it gives a summary of the MATLAB–results from the investigations on the unsymmetric loading. Chapter 3 focuses on the simulation aspects of a specially connected transformer and in particular the modelling of the transformer.

Different configurations for a subsea DEH–system design are given in Chapter 4. The system simulations for two DEH configurations are presented in Chapter 5 with regards to the load flow and degree of unsymmetry. Typical operational modes for a DEH system and faults are included in the analysis. The transformer model and SIMPOW simulations are discussed in Chapter 6 and a conclusion of the results is given in Chapter 7. The appendices give the additional information required for the transformer modelling and the simulations in SIMPOW. In addition, load flow results are given in the appendix where it is necessary.

Chapter 2

The DEH system and the transformers

Aker Solutions has looked into different transformer connections in order to bring forward alternative solutions regarding power supply for DEH systems. The purpose is to handle the unsymmetry in the power supply that appears due to the pipeline being a considerable single–phase load without a balancing unit. In addition, the transformers can be suitable for long step outs and implemented in a subsea power supply.

This chapter gives initially an explanation of the DEH system as a two–phase load and secondly it summarises the analysis of the alternative transformer connections that were found to be suitable for a three–to–two–phase power supply in the Specialication Project[4]. Finally it shortly presents the main result from the simulations with regards to unsymmetry when there is a change in the load impedance of the transformers.

2.1 The DEH system as a two–phase load

As the pipeline length increases, the demand for electrical power for the DEH system also increases. This is a challenge especially when the power cable of the DEH system is concerned. The longer the pipeline, the higher the voltage has to be applied. This makes the cable insulation exposed to higher voltage, and the insulation thickness has to be increased to withstand it. A solution for longer step out distances, is to divide the pipe length in sections, as shown in Figure 2.1 [5].

Figure 2.1A) shows two half–way–connected sections. The advantage of this solution is that the cable design with a resistive metal screen can be used. The obvious drawback however, is the cost for the extra length of the feeder cable due to the sectioned pipe, additional cable terminations and increased active and reactive power loss due the the extra feeder cable. This requires larger power supply equipment[5].

Figure 2.1B) shows an alternative to the sectioned pipe by the use of a semi conductive screen which drains the charging currents continuously to the sea. This is the most feasibly solution for long pipelines [5].

However, both configurations above depend heavily on a balancing unit for load symmetrisation. For long step outs the power requirement increases which also increases the balancing unit and the space and weight allocation. In addition, this system is not suitable for subsea installation, which limits the distance that is technical and economical feasible for the production even with sectioned pipeline lengths.

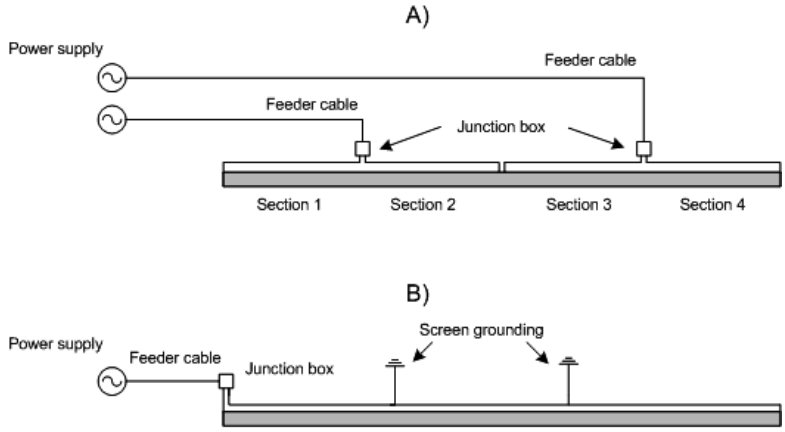

Figure 2.1: DEH with sectioned pipeline

On the other hand, transformers are compared to other types of electrical equipment less complicated to implement in subsea applications. This is due to the robust and compact construction of a transformer, which makes it less vulnerable to the mechanical stress that it is exposed to in a subsea installation.

If a specially connected transformer is used, such as the Scott–T transformer or the Le Blanc transformer, the load symmetrisation unit could be minimised or even eliminated. This is because the Scott–T and Le Blanc transformers are three–to–two–phase transformers which can provide balanced electrical power between a three–phase power system and a two–phase load. There is however some technical characteristics that has to be met in order to provide a fully symmetrical system. It is stated in SINTEF's report that a symmetrical three–phase current is obtained only when the two loads (or sections of pipeline) are equal in impedance and there is 90 degrees phase shift between the two no–load voltages of the transformer [3]. The Scott–T and Le Blanc provides no–load voltages with 90 degrees phase shifted, but the similarities between the loads have to be taken care of during installation of the pipeline.

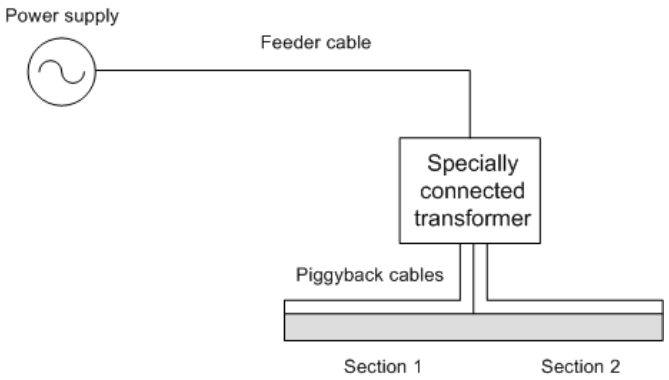

Figure 2.2: DEH system as a two–phase load

The principle of the DEH system as a two–phase load with two sections, is shown in Figure 2.2. The alternative connected transformer is installed subsea at the location of the pipeline. The power supply itself can then be installed topside on a platform, on a

FPSO or at an onshore facility.

The next step, when long step outs are concerned, is to split the pipeline into multiple sections and connect a three–to–two–phase transformer to each section. Figure 2.3 shows a principle sketch.

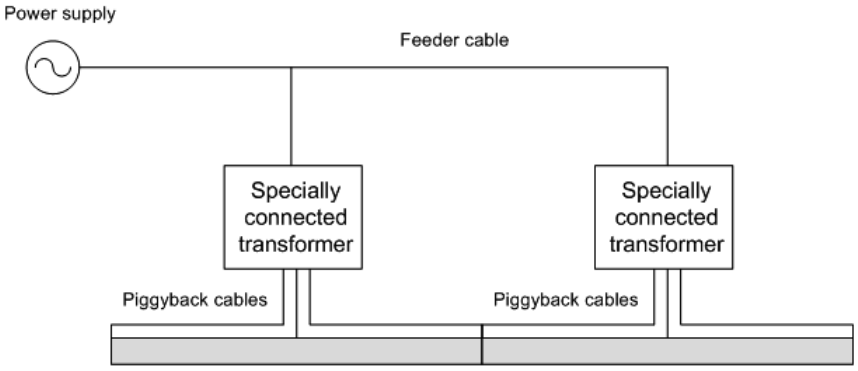

Figure 2.3: DEH system with split pipeline sections

In addition to feed the subsea transformers, the feeder cable can also be connected to a subsea load at the end, e.g a subsea pump, compressor etc. The electrical configuration and terminations of the equipment is depending on the system design and parameters such as distance to field, power requirement as well as available technology and economical interests.

However, an important thing to keep in mind is also the reactive compensation for the DEH system due to the inductive character and the use of reactive power. This has to be considered independent of the transformer and varies with the chosen system design.

2.2 The Scott–T connection

The Scott–T connection is a three–to–two–phase transformer which consists of two separate single–phase transformers connected to one another at the terminal S. The transformer with its winding brought out for connection is known as the "main" transformer, and the other is usually called the "teaser" transformer, see Figure 2.4.

As the terminals A, B and C indicates, it is possible to connect it to a three–phase network. In addition, the high voltage side (three–phase primary side) with its terminal S can be used for grounding. The low voltage side (secondary side) is simply two single–phase windings which may be connected to give two single–phase supplies, three–wire supply or a four–wire supply. This is obtained by different wiring connections of a_1, a_2, b_1 and b_2.

The terminals a_1 and b_2 are connected to give the required three wire supply to the pipeline. The pipeline is in this case divided in two sections Z_{L1} and Z_{L2} as shown Figure 2.2.

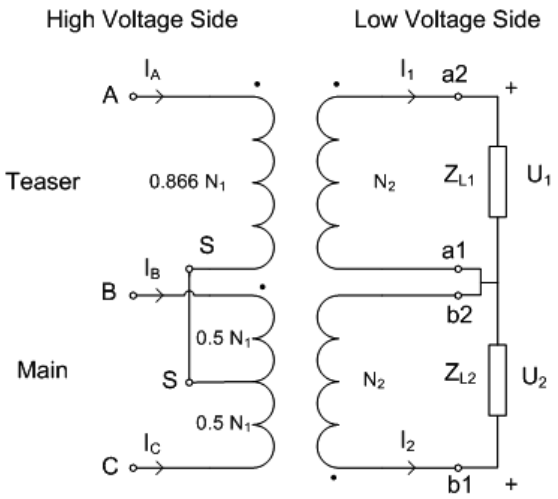

Figure 2.4: Connection diagram for the Scott-T transformer

Voltage and current relationship

If the terminals A, B and C are connected to a three–phase symmetrical power supply with line voltages $U_{AB} = U_{BC} = U_{CA} = U$, the phase diagram becomes as in Figure 2.5. N represents the neutral point of the power supply.

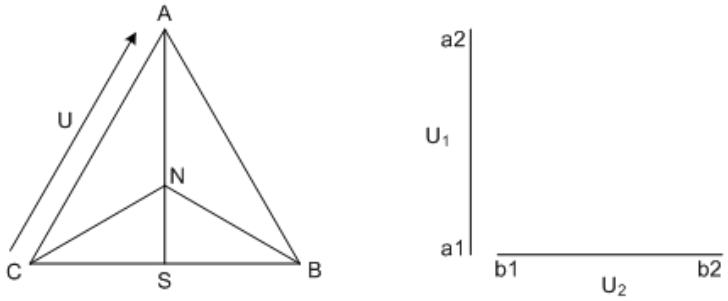

Figure 2.5: Phase diagram for the Scott-T connected transformer when connected to a three–phase symmetrical power supply

By analysing the geometry of Figure 2.5 and the connection diagram in Figure 2.4, it is obvious that U_{BS} and U_{CS} are equal to $0.5U_{BC}$. It can further be shown that the "teaser" voltage U_{AS} is $0.866U$.

The voltage U_{AS} becomes perpendicular to the line voltage U_{BC}. The secondary voltages are in phase with the primary voltages which further also makes the secondary output voltages U_1 and U_2 perpendicular with 90 degrees between them. This is also shown in Figure 2.5. As a result one can state that it is possible to form a three–to–two–phase transformer consisting of two single–phase transformers.Further it can be shown that the number of turns of the Scott–T transformer becomes as indicated in Figure 2.4.

The current relationship in the Scott–T transformer can be deduced by assuming that the transformer is ideal and by loading the secondary side with two equal impedances, which for the sake of simplicity, are resistive. The secondary voltages are assumed equal,

and due to the phase shift of the output voltages on the secondary side, the currents I_1 and I_2 are also shifted 90 degrees from each other.

The relationship between the primary phase currents and the secondary load currents are expressed in Equation 2.1.

$$\begin{aligned} I_A &= \frac{2}{\sqrt{3}}\frac{N_2}{N_1}I_1 \\ I_B &= -\frac{N_2}{N_1}I_2 - \frac{1}{\sqrt{3}}\frac{N_2}{N_1}I_1 \\ I_C &= \frac{N_2}{N_1}I_2 - \frac{1}{\sqrt{3}}\frac{N_2}{N_1}I_1 \end{aligned} \tag{2.1}$$

The load currents are expressed in Equation 2.2.

$$\begin{aligned} I_1 &= \frac{N_1}{N_2}\frac{\sqrt{3}}{2}I_A \\ I_2 &= I_B\frac{N_1}{2N_2} - I_C\frac{N_1}{2N_2} \end{aligned} \tag{2.2}$$

The current phase diagram can be presented as in Figure 2.6, which shows the current relationship in the Scott–T transformer.

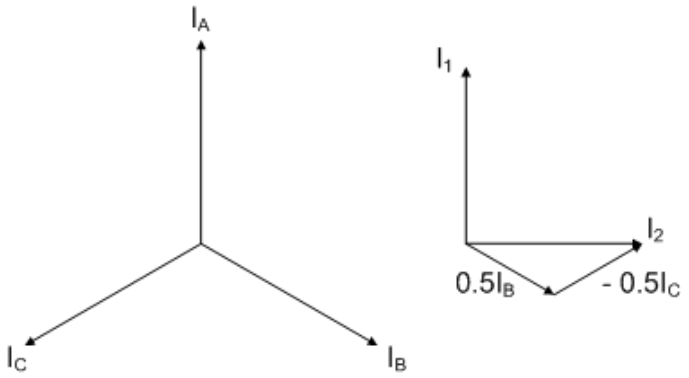

Figure 2.6: Current relationship in the Scott–T transformer

By comparing the current phase diagram in Figure 2.6 and the voltage phase diagram in Figure 2.5, one can see that the output currents I_1 and I_2 on the secondary side are in phase with the output voltages U_1 and U_2.

2.3 The Le Blanc connection

Figure 2.7 shows the winding connections for the Le Blanc transformer. The primary of the transformer is connected in delta, which is the normal interface connection in the case of a step–down unit supplied from a high voltage source [6]. The secondary side has an unbalanced winding structure. Phases A and C have two secondary side windings, but phase B has only one secondary winding. The secondary side can be arranged for

either two–phase three wire or four wire output. For the DEH application, the two loads Z_{L1} and Z_{L2} are connected as shown in Figure 2.7.

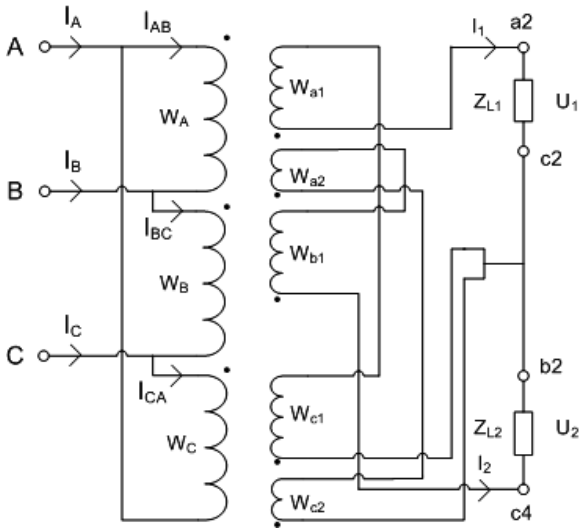

Figure 2.7: Connection diagram for the Le Blanc transformer

Voltage and current relationship

The primary side of the transformer is connected in delta. If the terminals A, B and C are connected to a three–phase symmetrical power supply with the line voltages $U_{AB} = U_{BC} = U_{CA} = U$, the phase diagram of the primary side becomes as in Figure 2.8.

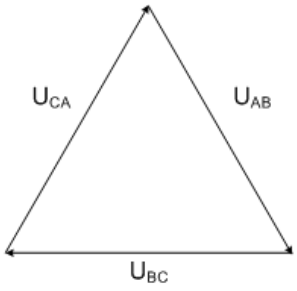

Figure 2.8: Phase diagram for the primary side of the Le Blanc connected transformer when connected to a three–phase symmetrical power supply

The load voltages U_1 and U_2 on the secondary side in Figure 2.7 are found by studying the geometry of the connection diagram and the voltage triangle of the primary side. It can be shown that the load voltages becomes as shown in Figure 2.9.

Note that the output voltages U_1 and U_2 are 90 degrees apart, similar as for the Scott–T transformer in Figure 2.5. The Le Blanc connection provides balanced electrical power between a three–phase and two–phase power system.

The number of turns of the Le Blanc transformer windings must be as in Equation 2.3 to ensure that the secondary side voltage balances the two phases.

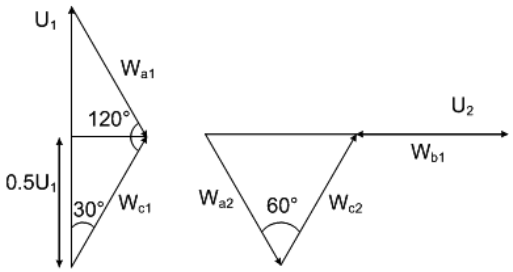

Figure 2.9: Phase diagram for the secondary side of the Le Blanc connected transformer

$$\begin{gathered} N_{W_A} : N_{W_B} : N_{W_C} : N_{W_{a1}} : N_{W_{c1}} : N_{W_{a2}} : N_{W_{b1}} : N_{W_{c2}} \\ 1 : 1 : 1 : \frac{1}{\sqrt{3}} : \frac{1}{\sqrt{3}} : \frac{1}{3} : \frac{2}{3} : \frac{1}{3} \end{gathered} \tag{2.3}$$

By introducing some assumptions to the Le Blanc transformer and the number of turns in Equation 2.3, following relationship between the load currents I_1 and I_2 and the primary line currents is found, see Equation 2.4.

$$\begin{aligned} I_1 &= I_A \frac{\sqrt{3}}{2} \\ I_2 &= I_B + \frac{1}{2} I_A \end{aligned} \tag{2.4}$$

The primary line currents and the secondary load currents can be presented graphically as in Figure 2.10. Note that the load currents are in phase with the load voltages in Figure 2.9.

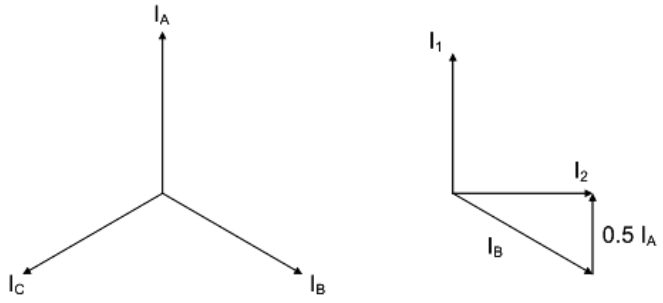

Figure 2.10: Current relationship in the Le Blanc transformer

2.4 Unsymmetric loading of the transformers

The pipeline in a DEH–system consists of several individual pipe joints that are welded into a pipeline. Earlier analysis and measurements performed on large numbers of pipe joints show significant variation of the magnetic permeability for the individual pipe joints. An important effect of the variation in the magnetic permeability is that the

impedance of the pipe varies along the pipe line [5]. This has an effect on the loading of the three–to–two–phase transformers, the degree of unsymmetry in particular.

It is mentioned in Section 2.1 that the two load sections of the pipeline have to be equal in order to ensure balanced symmetrical conditions. In the analysis of the Scott–T and Le Blanc transformers in [4], the degree of unsymmetry is investigated when the impedance of the two loads vary. In addition to these two transformers, a third configuration is also analysed in [4], but the results show an unsatisfactory respond to the variations in impedance and it is not included in the further analysis.

The technique known as "The method of symmetrical components" is used as the point of departure for the analysis of the transformer connections in [4]. Further, the relationship between the negative sequence component and the positive sequence component of the load currents I_1 and I_2 is applied to look into the degree of unsymmetry and tolerance when the load impedance is changed, see Equation 2.5. According to the diagram in Appendix A, maximum allowed value of the continuous negative sequence current is 15% of the positive current[7].

$$\text{Degree of unsymmetry} = |\frac{I_-}{I_+}| \tag{2.5}$$

As a base for the investigations in [4], there are introduced some simplifications regarding the transformers. The resistance and leakage reactance of the transformer are ignored as well as disregarding the saturation of the core. These introduced simplifications imply that the load voltages of the transformer can be determined based on a no–load condition. In addition, magnetizing current is neglected and ampere–turn balance is assumed. It is important to keep in mind that the analysis in [4] considers only the symmetrical conditions of the power transformer and not the DEH system as a whole.

The power factor of a DEH–system is in the order of 0.3 in a piggyback configuration, which is equal to an impedance angle of 72.5 degrees [5]. If the impedance is assumed to be 1 per unit, the resistive and inductive parts of the pipeline impedance are as follows:

$$\begin{aligned} Z = R + jX &= 1e^{(j72.5^\circ)} \\ R = \cos(72.5^\circ)Z &= 0.3p.u \\ X = \sin(72.5^\circ)Z &= j0.954p.u \end{aligned} \tag{2.6}$$

Simulations for four cases are closer analysed[1] by using MATLAB:

1. Resistive loads and changing R_1 between $0.1R_2$ and $5.1R_2$. R_2 is kept at 0.3 (constant)[2]
2. Inductive loads and varying R_1 in the domain $[0.1R_2 - 5.1R2]$, R_2 constant, and $X_1 = X_2 = 0.954$ (constant)
3. Inductive changes. X_1 varies in the domain $[0.1X_2 - 5.1X2]$, $X_2 = 0.954$ (constant), and $R_1 = R_2 = 0.3$ (constant),

[1] The details of the MATLAB programs and simulations can be found in [4]
[2] The values are chosen in order to have a wide variation of impedance

4. Increase one load impedance to simulate the operation with two pipelines of different length. Z_1 varies in the domain $[0.1Z_2 - 5.1Z_2]$, and Z_2 is constant

The load currents I_1 and I_2 are equal for each configuration, and are calculated by the following equations:

$$\begin{aligned} I_1 &= \frac{U_1}{R_1 + jX_1} \\ I_2 &= \frac{U_2}{R_2 + jX_2} \end{aligned} \tag{2.7}$$

Next, expressions for the currents on the primary side as a function of the load currents are found. The current relationship on the primary side however, depends on the transformer configuration and has to be specified for each case. When the primary currents I_A, I_B and I_C are specified, the general equations for the negative and positive sequence component of the currents can be calculated as in Equation 2.8.

$$\begin{aligned} I_- &= \frac{1}{3}(I_A + I_B a^2 + I_C a) \\ I_+ &= \frac{1}{3}(I_A + I_B a + I_C a^2) \end{aligned} \tag{2.8}$$

a is an operator to simplify the notation of the symmetrical components (the positive, negative and zero sequence component of the current).

2.4.1 Summary of the MATLAB results

The MATLAB program in [4] presents the value of $|\frac{I_-}{I_+}|$ as a graph which can be further interpreted to examine the degree of unsymmetry for the transformer configurations. In addition, it gives the values of which the unsymmetry curve and the curve for maximum allowed continuous value intersect. The area enclosed between these two curves can be used as an indication of how much the impedance can be varied for the transformer configurations. It is important to be aware of the simplifications that are introduced earlier, also apply for the simulations. As mentioned earlier, the limit of maximum allowed continuous negative sequence current is 15% of the positive current.

Figure 2.11, Figure 2.12 and Figure 2.13 show the curve shapes for the degree of unsymmetry for case 2, 3 and 4 which are found by using MATLAB. These are the most relevant simulations when it comes to practical use. Notice that the simulations for the Scott–T and the Le Blanc connection are aggregated in order to emphasise the similarities in the unsymmetry for the two transformers. The MATLAB program for case 4 is given in Appendix B.

When the value of R_1 is lower than 0.617, the value of unsymmetry in the Scott–T and Le Blanc configuration is lower than the maximum limit. This means that if R_1 is lower than 205% of R_2, the configurations are stable when regarding maximum allowed continous negative sequence current. However, when R_1 is lower than 0.1, the degree of unsymmetry is about 10% which is fairly high and close to the limit.

Figure 2.12 shows that the degree of unsymmetry is zero when $X_1 = X_2$ and confirms the theory which says that the Scott–T and Le Blanc provides symmetrical conditions

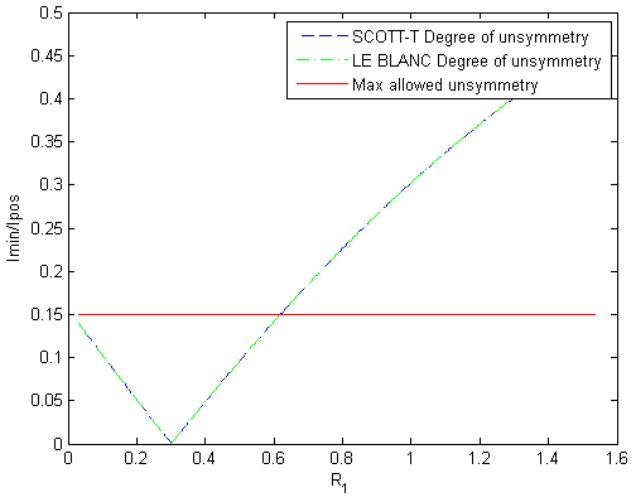

Figure 2.11: Changes in unsymmetry for the Scott–T and Le Blanc transformer when impedances are inductive and R_1 varies

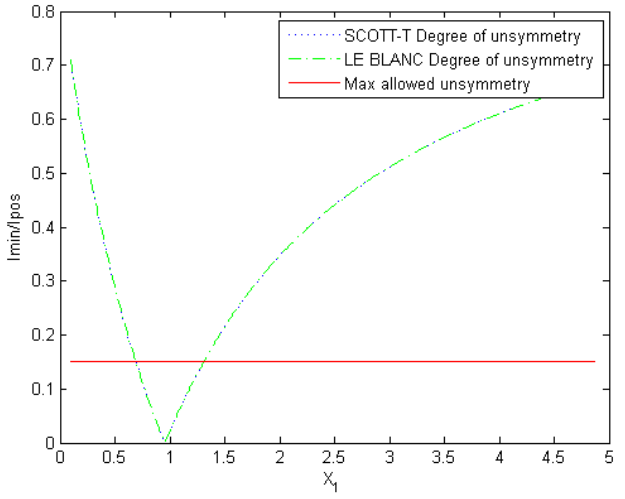

Figure 2.12: Changes in unsymmetry for the Scott–T and Le Blanc transformer when X_1 varies

when the two load impedances are equal. The curves intersect when $X_1 = 0.696$ and $X_1 = 1.297$. The inductance of one of the load can vary between 73% and 136% of X_2 when the resistive parts of the loads are kept constant.

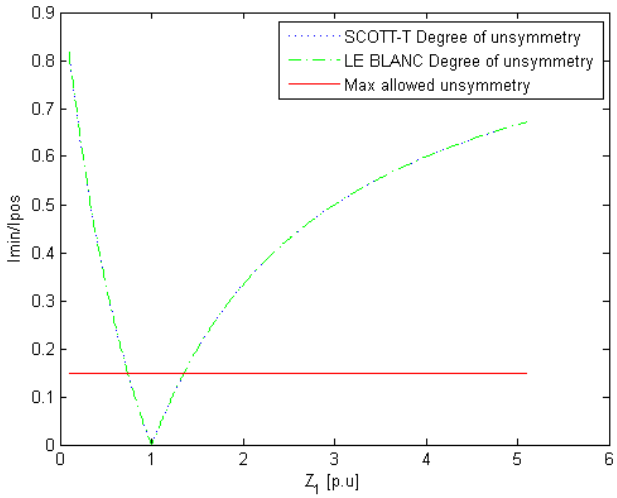

Figure 2.13: Changes in unsymmetry for the Scott–T and Le Blanc transformer when Z_1 varies

The last simulation in Figure 2.13 shows the variation of the unsymmetry when the length of one pipe section varies. The x–axis shows the values of the impedance Z_1. The numbers indicates the length in per unit as well as Z_1 in per unit. The degree of unsymmetry intersects the maximum limit of 15% at 0.740 and 1.351. This means that the length of the pipe line on one of the loads can vary between 74% and 135% of the other to ensure a lower value of the continuous negative sequence current than the limit of 15%. Note that $|\frac{I_-}{I_+}|$ is zero when $Z_1 = Z_2$, which is as expected.

The data obtained in the simulations for the Scott–T and Le Blanc connection are given in Table 2.1.

Table 2.1: Summary of the simulations for the two transformer configurations. The values of R_1 are in per unit of R_2, X_1 in per unit of X_2 and the values for Z_1 are given in per unit of Z_2

Configuration	**Inductive loads, R_1 varies**		**X_1 varies**		**Z_1 varies**	
Variable	R_1min	R_1max	X_1min	X_1max	Z_1min	Z_1max
Scott–T	-	2.05	0.73	1.36	0.74	1.35
Le Blanc	-	2.05	0.73	1.36	0.74	1.35

The values in Table 2.1 are given for the points where the curve of the degree of unsymmetry intersects with the limit of maximum allowed continuous I_-. The column where R_1min is not given, is for the simulations where the curve of $|\frac{I_-}{I_+}|$ do not intersect the maximum allowed continuous I_- on the left side. This is because the value of $|\frac{I_-}{I_+}|$ is lower in that area. The range between the minimum values and the maximum values of R_1, X_1 and Z_1 respectively, is the range where the degree of unsymmetry is lower than the limit of 15% unsymmetry. Table 2.1 gives also an indication of how much the variations in impedance of the two loads can be when it comes to unsymmetry in the power transformer.

From the table it is also evident that the Scott–T and Le Blanc configurations give the same results for the simulations with respect to the degree of unsymmetry. This is shown in the aggregated figures.

Chapter 3

SIMPOW and the transformer model

The main objective of the master thesis is to analyse the operational characteristics of a specially connected transformer implemented in a DEH system. However, the Scott–T and Le Blanc transformers are not initially given in any available power system simulation software library, and must therefore be manually modelled.

Initially, both transformers were supposed to be modelled for simulations in SIMPOW. However, understanding the internal electro technical processes of SIMPOW, the Dynamic Simulation Language and making the model correctly for the simulations, showed to be much more complex and time consuming than first expected. In addition, developing a new electric component for SIMPOW requires verifications to assure that its behavior corresponds to the laws of physics. This added the effort of making a DSL model.

On the other hand, the Scott–T and the Le Blanc transformers are both three–to–two–phase transformers which give symmetrical conditions on the three–phase side when the two loads on the secondary side are equal. In addition, their response to unsymmetric loading is also equal. This is shown during the analysis and results in Chapter 2.4. Based on this, one can assume that the result from a load flow analysis with regards to symmetrical conditions will be the same for the Scott–T and the Le Blanc. This issue has also been discussed with the supervisor. The Scott–T is therefore the only specially connected transformer that is modelled and further analysed in this report.

When it comes to practical application of either the Scott–T or the Le Blanc transformer, the electromechanical design also has to be taken into consideration. One advantage of the Le Blanc transformer compared to the Scott–T is the winding connections. The Le Blanc connection can have three–phase winding connected in star or delta, which offers individual advantages. The Scott–T has two separate halves on the main winding which have to be interleaved in order to minimise leakage reactance effects, resulting in a degree of winding complication. In addition the transformer has to be built as two separate single–phase transformers which makes it bulky and heavy compared to a normal three–phase transformer on the same rating [6].

The Le Blanc transformer, due to its standard design using a three–limb three–phase core, permits more efficient use of the active materials and results in a lighter unit for a given rated kVA. Its main disadvantage is that two of the winding sections must have a turn ratio of $\sqrt{3}$. As only whole numbers of turns can be employed it follows that the choice of turns my be limited in certain cases as well as maximum kVA transformed at any given voltage[6]. Further details on the Scott–T and Le Blanc transformers can be

found in "The J&P Transformer Book" by A. C. Franklin and D. P. Franklin, see [6].

The simulation aspects of the DEH–system is addressed in this chapter with emphasis on modelling the Scott–T transformer in particular. In addition, simulation of the transformer is carried out in SIMPOW and compared with the MATLAB results in Chapter 2.

3.1 Using SIMPOW

The technique known as "The method of symmetrical components" is used in the Specialisation Project[4] to analyse the Scott–T and Le Blanc transformers. Further, the relationship $|\frac{I_-}{I_+}|$ gives the degree of unsymmetry and the result when varying the load impedance on the two–phase side of the transformers. Thus, using the same method and parameters is desirable to verify the results and do simulations on the total DEH–system. It is therefore an advantage to use a program which can handle three–phase models and give output results in terms of symmetrical components. In addition, three–phase models are more suitable in terms of load flow analysis than representing the system in a positive-, negative- and zero sequence equivalent circuit[8]. It is also desirable to use a program which can simulate all the operational modes and failure situations needed.

The specially connected transformer Scott–T is however infrequently used in todays power system, and the simulation software tools available do not include predefined models in that respect. It is therefore necessary to use a software where such a model can be made, and where the requisite data and results can be obtained.

SIMPOW is as computer simulation software designed for use in power system analysis, and has the possibility to implement user defined models. It was started by ABB in 1977 as being developed as a tool to study a new HVDC connection in South America. It is now developed and maintained by STRI AB (Swedish Transmission Research Institute, www.stri.se)[9].

An advantage with SIMPOW is that a user, by means of a so-called Dynamic Simulation Language (DSL), may implement virtually any model of a system element, for instance the specially transformer connections like the Scott–T. The DSL also allows self contained models of processes and systems to be built, simulated and analysed. Hence, SIMPOW may be regarded as a general software for solving a system of differential and algebraic equations and logical conditions[10].For further information of SIMPOW, see the user manual[10].

The SIMPOW program includes several modules for calculations and simulations of a power system:

- Optpow - load flow calculations
- Dynpow - dynamic simulations in phasor and time domain
- Stapow - calculation of short circuit currents
- Dips - reliability calculations
- Dynamic Simulations Language (DSL) - user defined models
- HiDraw - block diagram editior for user defined models

- Addharm - analysis of harmonics
- Tracfeed - analysis of railway power supply

The modules used for the analysis in this report are Optpow, Dynpow and DSL. The input files for Optpow, Dynpow and for making DSL can be made in the text editor "Notepad" or "Textpad". The editor used in this work is "Textpad".

3.1.1 System simulations

The first step in the analysis is to make an Optpow model of the DEH–system which establishes the topology and branches of the system as described in Chapter 4.1. It includes the creation of input data files, i.e. to set values to component parameters in data groups according to the manual, and to execute the basic functions of SIMPOW, see Figure 3.1[10]. This is the base for the load flow analysis. However, as mentioned earlier, the SIMPOW library does not include predefined models for the Scott–T transformer. The model has to be defined using the programming language Dynamic Simulation Language. This is further addressed in Section 3.2.

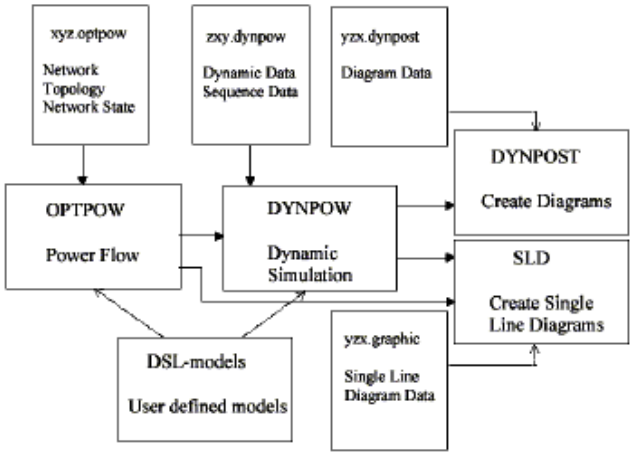

Figure 3.1: The structure of the modules in SIMPOW

When the characteristics of the production sources, transformers, cables, loads and so on are defined in Optpow, the power flow can be calculated which gives the steady state solution of the system. This can be described by the magnitude and phase angle of the node voltages, control variables and other possible state variables. The power flow calculation is further used to study the flow of active and reactive power, the losses, the voltage profile etc. for the given conditions in the DEH–system. In addition, it also provides the initial condition for subsequent analysis on a dynamic model of the system[10].

The next step is to establish a model in Dynpow which can be used to perform dynamic simulations such as load shedding, fault analysis, start–up of motors and so on. The dynamic simulations starts in steady state equal to the power flow in Optpow. Dynamical simulations can be performed with two different representations of AC quantities, Transta and Masta. Transta is used for transient stability models in means of phasor representation and Masta for instantaneous value models using dq0 representation [10].

For the simulations of the DEH–system with the transformer models using DSL, Transta representation is chosen. This is due to the fact that using phasor quantities for describing the models are less complex than instantaneous value models as in the Masta representation. In addition, the DEH system does not include any rotating electrical equipment, and phasor representation is then sufficient for the analysis.

3.2 Modelling the transformer

The first step in modelling the Scott–T connection is to make a DSL model for the transformer which can be used for simulations in SIMPOW. However, in the Specialisation Project[4] the results are obtained based on simplifications regarding the transformer. The resistance and leakage reactance of the transformer are ignored as well as disregarding the saturation of the core. These simplifications are also initially introduced in the progress of developing the DSL model for the Scott–T.

When the transformer model is programmed, the SIMPOW results regarding the unsymmetric loading of the transformer can be compared with the results obtained in [4]. This way, the transformer DSL model is verified and it makes a groundwork for further development including parameters for resistance and reactance. Next, the transformer model can be implemented in the rest of the DEH–system.

3.2.1 Dynamic Simulation Language

The modelling language, DSL, may be used in power system studies for implementing non-standard components of the power system. DSL models can be written both for regulators and primary components (such as transformers). The model is written in DSL-code in a file named zzz.dsl. The model is then compiled and put in a library. The models stored in the library can be used in Optpow, Dynpow, Stapow or independent DSL runs [10]. Figure 3.2[10] shows an example of how to use a DSL model in a Dynpow simulation.

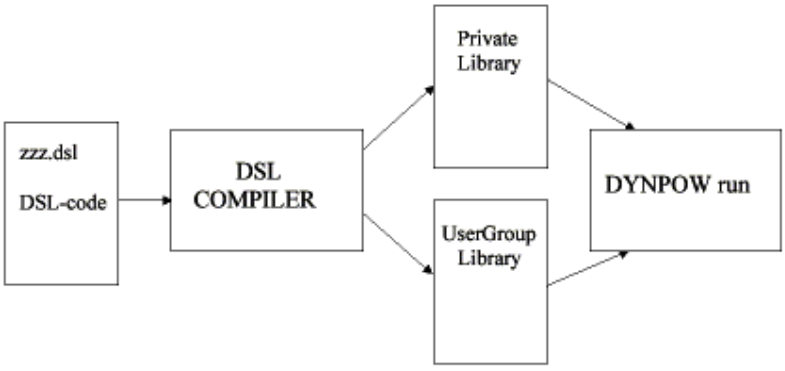

Figure 3.2: Execution of DSL models

SIMPOW has built–in mathematical calculators, which also can handle electro technical equations. This means that the DSL model should contain equations for the relationship

between the current and the voltage in the transformer by means of symmetrical components. In addition, phase quantities can also be utilized when needed as SIMPOW can handle that as well.

When the DSL model is complete, it can be implemented in the Dynpow module for simulations, and the DSL equations are solved simultaneously with all other equations of the total system. For more information about the Dynamic Simulation Language, see Chapter 6 in the SIMPOW manual [10].

3.2.2 The DSL model for the Scott–T connection

A challenge with implementing a DSL model for the specially connected transformer into SIMPOW, is the combination of three– and two–phase side. One solution, is to model the Scott–T connection as a three–winding transformer where the primary side consist of a three–phase winding and the secondary side is two one–phase windings, see Figure 3.3. This way it is possible to do a load flow calculation in Optpow using a standard three–winding transformer, and secondly implement the user defined model for the specially connected transformer in Dynpow. More important, the Optpow simulation initiates a steady state load flow and the initial condition needed for the Dynpow simulations. This means that one first has to run Optpow to do a load flow calculation on the system, and then include the DSL model for the specially connected transformer in Dynpow. This gives the result for the load flow with the Scott–T transformer implemented in the DEH system.

The required inputs for describing the Scott–T connection are equations for the relationship between the voltage and current on the primary– and secondary side of the transformer. In addition, equations which give the symmetrical components for current and voltages on BUS1 is necessary for investigating unsymmetrical loading.

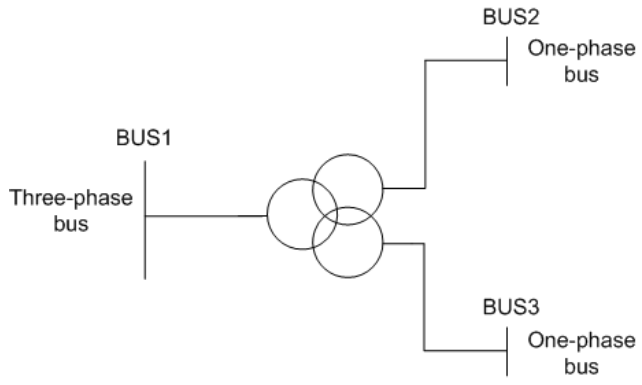

Figure 3.3: SLD for modeling the Scott–T's three–phase and two one–phase sides

The DSL model for the Scott–T connection with the introduced simplifications is given in Appendix C. The model can be divided into three main parts. The first part is a preamble where the process is defined and the declarations of variables and inputs are specified as well as the plotting specifications. The second part is where the transformer is described by means of equations for the voltage and current relationship. The third and last part is a set of equations for plotting the variables that is specified in the preamble.

The second part of the DSL model is the "body" of the transformer, and is addressed next. The first step for describing the Scott–T transformer is the equations for the secondary load currents I_1 and I_2. The equations used in the DSL model for calculating the load currents are given implicitly. They are based on the no–load voltage relationship obtained from the three–phase model of the Scott–T in Figure 2.4 and given in Equation 3.1 and 3.2. By defining the equations for I_1 and I_2 implicitly, SIMPOW uses the voltage relationship to calculate the currents. Note that the equations in Appendix C are defined using the real– and imaginary part of the phase voltages. This terminology is in accordance with Transta representation using phasor quantities.

$$U_1 = \frac{2}{\sqrt{3}}\frac{N_2}{N_1}(U_A - \frac{1}{2}U_B - \frac{1}{2}U_C) \tag{3.1}$$

$$U_2 = \frac{N_2}{N_1}(U_B - U_C) \tag{3.2}$$

However, SIMPOW handles the equations on a per unit basis, and therefore the equations has to be adjusted according to SIMPOW's per unit system. The two voltages U_1 and U_2 are one–phase voltages and their base voltage differ by $\sqrt{3}$ compared to the base voltage for the three–phase side. This results in the following implicit expressions for the load currents:

$$U_1 = \frac{2}{\sqrt{3}}\frac{N_2}{N_1}(U_A - \frac{1}{2}U_B - \frac{1}{2}U_C)\cdot(\frac{1}{\sqrt{3}}) \tag{3.3}$$

$$U_2 = \frac{N_2}{N_1}(U_B - U_C)\cdot(\frac{1}{\sqrt{3}}) \tag{3.4}$$

The second step defines the secondary currents into the transformer and the third step gives the equations for the primary current. Note that for these equations, the symmetrical components are used, see Equation 3.5.

$$\begin{aligned} 3I_+ &= I_A + I_B a + I_C a^2 \\ 3I_- &= I_A + I_B a^2 + I_C a \end{aligned} \tag{3.5}$$

The expressions for the primary phase currents in Equation 2.1 are used in Equation 3.5 together with the rectangular form for the a–operator. The positive– and negative sequence component of the primary current becomes as expressed in Equation 3.6 and 3.7.

$$\begin{aligned} 3I_+ = (\frac{2}{\sqrt{3}}\frac{N_2}{N_1}I_1) + (-\frac{N_2}{N_1}I_2 - \frac{1}{\sqrt{3}}\frac{N_2}{N_1}I_1)(-\frac{1}{2} + j\frac{\sqrt{3}}{2}) + (\frac{N_2}{N_1}I_2 - \frac{1}{\sqrt{3}}\frac{N_2}{N_1}I_1)(-\frac{1}{2} - j\frac{\sqrt{3}}{2}) \\ \Rightarrow 3I_+ = \sqrt{3}\frac{N_2}{N_1}I_1 - j\sqrt{3}\frac{N_2}{N_1}I_2 \\ I_+ = \frac{1}{\sqrt{3}\frac{N_2}{N_1}}I_1 - j\frac{1}{\sqrt{3}\frac{N_2}{N_1}}I_2 \end{aligned} \tag{3.6}$$

$$
\begin{aligned}
3I_- = (\frac{2}{\sqrt{3}}\frac{N_2}{N_1}I_1) + (-\frac{N_2}{N_1}I_2 - \frac{1}{\sqrt{3}}\frac{N_2}{N_1}I_1)(-\frac{1}{2} - j\frac{\sqrt{3}}{2}) + (\frac{N_2}{N_1}I_2 - \frac{1}{\sqrt{3}}\frac{N_2}{N_1}I_1)(-\frac{1}{2} + j\frac{\sqrt{3}}{2}) \\
\Rightarrow 3I_- = \sqrt{3}\frac{N_2}{N_1}I_1 + j\sqrt{3}\frac{N_2}{N_1}I_2 \\
I_- = \frac{1}{\sqrt{3}\frac{N_2}{N_1}}I_1 + j\frac{1}{\sqrt{3}\frac{N_2}{N_1}}I_2
\end{aligned}
\tag{3.7}
$$

The same adjustment regarding the per unit base values in the DSL model has to be considered. The final expressions for the phase currents then becomes:

$$
\frac{1}{\sqrt{3}} \cdot I_+ = \frac{1}{\sqrt{3}\frac{N_2}{N_1}}I_1 - j\frac{1}{\sqrt{3}\frac{N_2}{N_1}}I_2 \tag{3.8}
$$

$$
\frac{1}{\sqrt{3}} \cdot I_- = \frac{1}{\sqrt{3}\frac{N_2}{N_1}}I_1 + j\frac{1}{\sqrt{3}\frac{N_2}{N_1}}I_2 \tag{3.9}
$$

The complete DSL model for the Scott–T transformer and comments are given in Appendix C.

3.3 Transformer simulations

In order to use and analyse the DSL model for the Scott–T connection, it is necessary to establish a power system with the transformer implemented. Initially, the objective is to carry out simulations on the DSL model which give the same results as in the Specialisation Project[4]. This requires only a simple power system with a voltage source, the specially connected transformer and two loads.

To verify that the DSL model is correct, a hand calculated example is given in Appendix C which is further compared with results from simulations in SIMPOW, see Appendix C. The system consists of a swing bus, a Scott–T transformer and two equal loads at unity power factor. By comparing the results, it can be concluded that the DSL model for the lossless Scott–T transformer is correct. The currents on both the primary– and secondary side are the same for the hand calculations and for the DSL simulations. In addition, from the simulations with the DSL model in Dynpow, the load voltages on the secondary side are equal in magnitude, and 90°out of phase. This is, as pointed out in the analysis in Chapter 2, the characteristic property of the Scott–T transformer. Taking a closer look at the symmetrical components, the negative and zero sequence components of the current are zero, but the positive sequence current is equal to the primary phase currents. This gives a symmetrical system.

Next, the loads on the secondary side is varied in order to analyse the degree of unsymmetry. These values are further compared with the MATLAB results from the Specialisation Project given in Table 2.1.

3.3.1 Comparing SIMPOW simulations with MATLAB results

The system for simulations in SIMPOW is given in the single line diagram (SLD) in Figure 3.4.

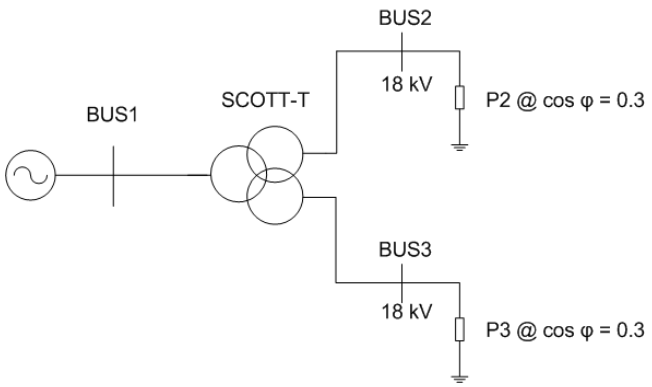

Figure 3.4: SLD for the power system simulations with the Scott–T transformer

System specifications:

- S_{Base} = 2 MVA
- U_{BUS2} = 18 kV
- U_{BUS3} = 18 kV
- PF = 0.3

The voltages at BUS2 and BUS3 are typical DEH–voltage levels, and the power factor is also typical for such a system[5]. A power factor of 0.3 gives an impedance angle of 72.5°. Based on theses values, the impedance of the loads can be calculated.

If the impedance of each load is equal to one per unit and the impedance angle is 72.5°, the resistance and reactance are as in Equation 3.10:

$$\begin{aligned} Z = R + jX = 1e^{(j72.5^\circ)}p.u \\ R = \cos(72.5^\circ)Z = 0.3p.u \\ X = \sin(72.5^\circ)Z = j0.954p.u \end{aligned} \tag{3.10}$$

To calculate the impedance into physical values, a reference value for the impedance is needed, see Equation 3.11. n is referring to the number on the bus of interest.

$$\begin{aligned} Z_{Base(n)} = \frac{{U_n}^2}{S_{Base}} \\ Z_{Base(2)} = \frac{(18kV)^2}{2MVA} = 162\Omega \end{aligned} \tag{3.11}$$

The physical value of the impedance is then:

$$\begin{aligned} Z_n &= Z_{pu} \cdot Z_{(Base-n)} \\ Z_2 &= 1e^{(j72.5^\circ)} \cdot 162\Omega \\ Z_2 &= 162e^{(j72.5^\circ)}\Omega = 48.7 + j154.5\Omega \end{aligned} \tag{3.12}$$

The physical value of the active and reactive power can be found by further using the impedance value.

$$\begin{aligned} S &= P + jQ \\ S &= U \cdot I^* = \frac{U^2}{Z^*} \\ S &= \frac{(18kV)^2}{162e^{j72.5}} \\ S &= 2e^{j72.5^\circ} MVA \\ S &= (0.60 + j1.91)MVA \end{aligned} \tag{3.13}$$

The active power P and the reactive power Q are found in Equation 3.13. Active power $P = 0.60MW$ and $Q = 1.91$ Mvar.

The MATLAB results in Chapter 2.4 show how the degree of unsymmetry changes when one of the load impedance is changed. In addition, Table 2.1 gives the values for where the degree of unsymmetry intersects the maximum allowed continuous negative sequence component of the current. The same graphical presentation can be presented in SIMPOW by using the Dynpow module. The load at BUS2 in Figure 3.4 is chosen to be the load which varies. By using the data groups "LOADS" and "TABLES" in Dynpow, one can specify the variance of the load in per unit. Seeing that variance in the MATLAB simulations where from 0.1 – 5.1 per unit, the same is specified for the SIMPOW calculations. The DSL model for the transformer, is the same as in Appendix C.

Changes in unsymmetry for Scott–T when the active power at BUS2 changes

First, the Scott–T transformer is analysed when the two loads are inductive, and the load at BUS2 is varied between $[0.1P_3 - 5.1P_3]$ which is equal to $[0.03pu - 1.53pu]$. The obtained values from the calculations in Equation 3.13 are used as inputs in Optpow, and the file is given in Appendix D. By running the Optpow calculations, a load flow analysis calculates the steady state value for the Dynpow calculations. The Dynpow file is also given in Appendix D.

After the Dynpow calculation is done, the "Curves"–function is used to present the simulations graphically. The DSL model for Scott–T also includes equations for plotting the positive– and negative component of the current in the transformer. In addition, the load at BUS2 and BUS3 can be plotted in per unit. Figure 3.5 shows the interface in Dynpow for choosing the plotting variabls.

The objective is to plot the degree of unsymmetry by means of the relationship $|\frac{I_-}{I_+}|$ as a function of changing the load on BUS2 in per unit. This is done by first selecting the load at BUS2 (P_2) as the independent variable. Secondly, the variable IN1–PU and

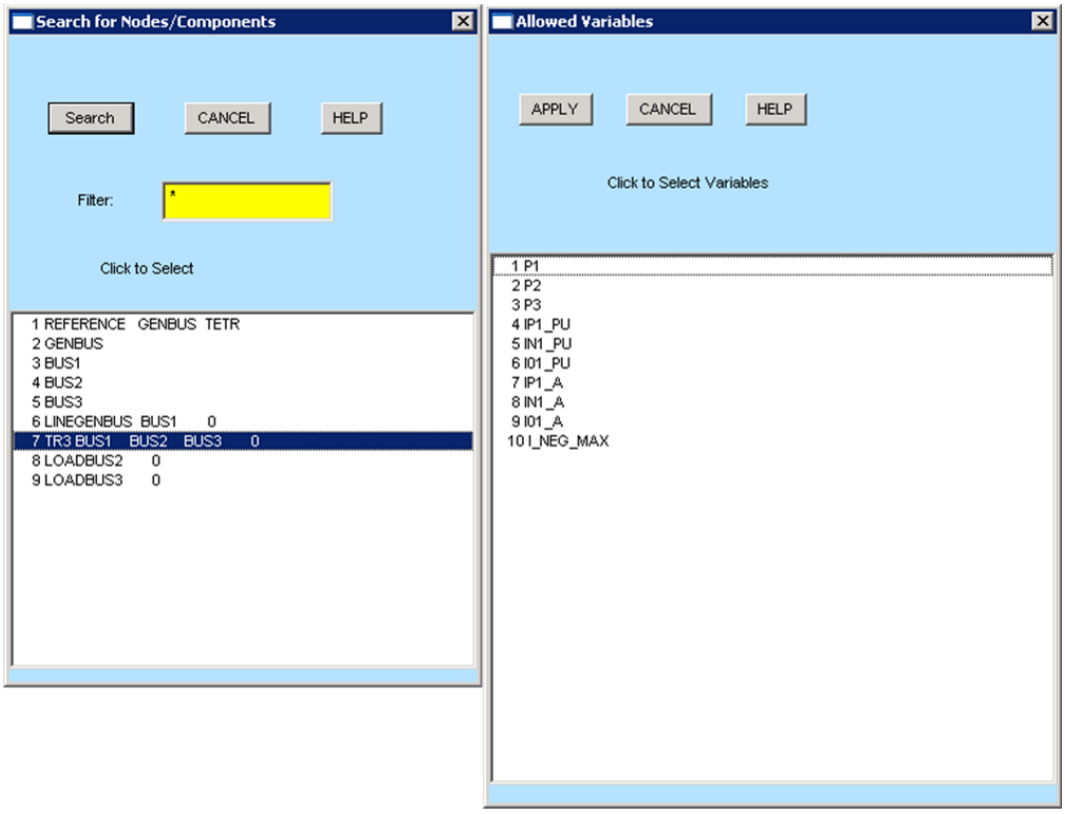

Figure 3.5: Interface in Dynpow for plotting diagrams

IP1–PU for the Scott-T transformer are selected for the negative– and positive value of the current. The relationship between the negative– and positive sequence is generated by dividing IN1–PU by IP1–PU in the "Creating diagram" window. Finally, the variable I–NEG–MAX is selected in order to plot the maximum value of the continuous negative sequence component. The "Creating diagram" window appears then as in Figure 3.6.

Note that the value of IN1–PU in Figure 3.6 is divided by IP1–PU. The box is marked with a blue color.

When "Create diagram" is chosen, the result is presented in SIMPOW as in Figure 3.7. Note that it is very important to specify the same plotting specifications for the curves. The x–axis and the y–axis must have the same minimum and maximum value for both curves. This makes the graphically presentation have the same references.

The red line in Figure 3.7 is the limit for maximum continuous value of I_- which is 0.15 in per unit. The black line shows how the relation $|\frac{I_-}{I_+}|$ develops as the load P_2 changes. The red box in Figure 3.7 marks the intersection between the two curves which is produced by clicking with the mouse pointer. Note that the intersection point is when $P_2 = 0.61pu$. This means that the degree of unsymmetry is 15% when P_2 is 2.033 pu of the load at BUS3 which is 0.3 pu. The result from the MATLAB simulations in Figure 2.11 is 2.05 pu, but the deviation is only caused by the unprecisely function of finding the intersection in the Dynpow curve.

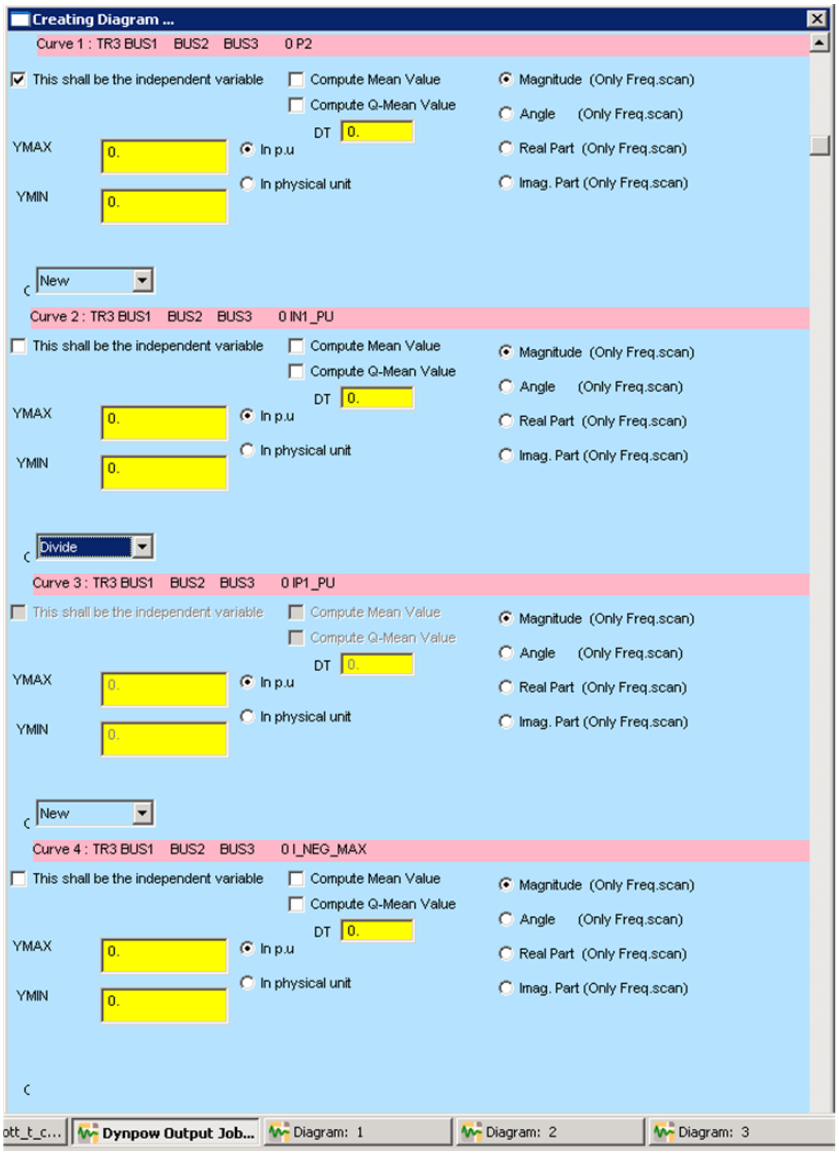

Figure 3.6: Interface when specifying and creating the plot for degree of unsymmetry

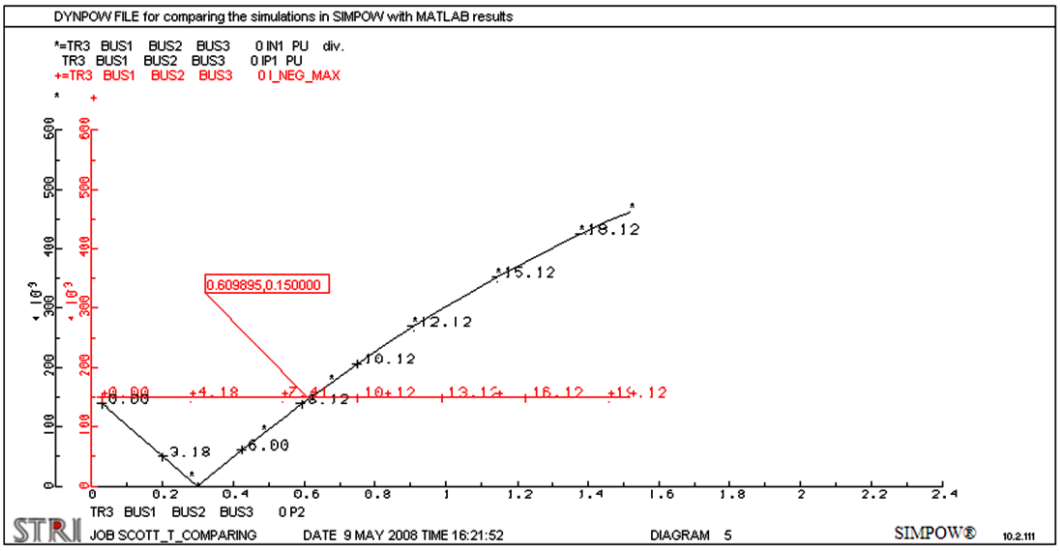

Figure 3.7: SIMPOW result when varying the active power at BUS2

Changes in unsymmetry for Scott–T when the reactive power at BUS2 changes

The second mode for simulations in SIMPOW, is when the reactive power at BUS2 varies and the load at BUS3 is kept constant. The variance for Q_2 is $[0.1Q3 - 5.1Q3]$ which in per unit is $[0.095 - 4.865]$. The Optpow– and Dynpow file for this mode is given in Appendix D.2.

The degree of unsymmetry is given in Figure 3.8.

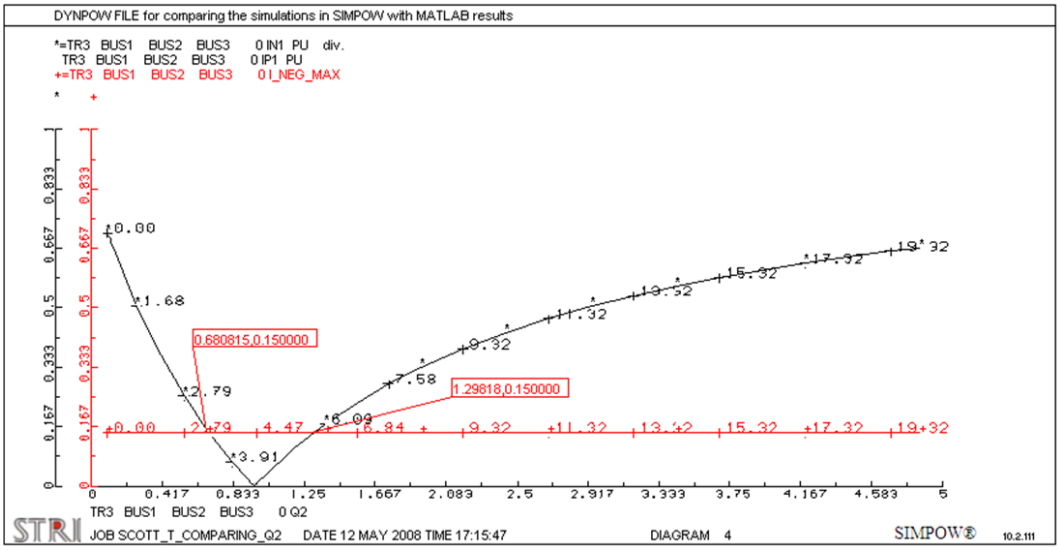

Figure 3.8: SIMPOW result when varying the reactive power at BUS2

The intersection points are when Q_2 is 0.68 and 1.30 of Q_3. The value of Q_3 in per unit is 0.954 which means that the degree of unsymmetry is lower than the maximum allowed value of 15% when Q_2 is 0.71 and 1.36 per unit of Q_3. The values from MATLAB are

0.73 and 1.36. The deviation of the minimum value of Q_2 is due to the inprecisely way of finding the intersection directly in the curves in SIMPOW.

Changes in unsymmetry for Scott–T when the the total impedance at BUS2 changes

The last simulation for comparing MATLAB and SIMPOW results, is when the total impedance Z_2 varies between $[0.1Z3 - 5.1Z3]$. This is equivalent to the situation if the pipeline part at BUS2 is different in length or impedance compared to the pipeline connected at BUS3. Figure 3.9 shows the result from the simulation in SIMPOW. The Optpow file is the same as for the simulations in Figure 3.7 and Figure 3.8, but the Dynpow fileis edited to specify the load changes, see Appendix D.3.

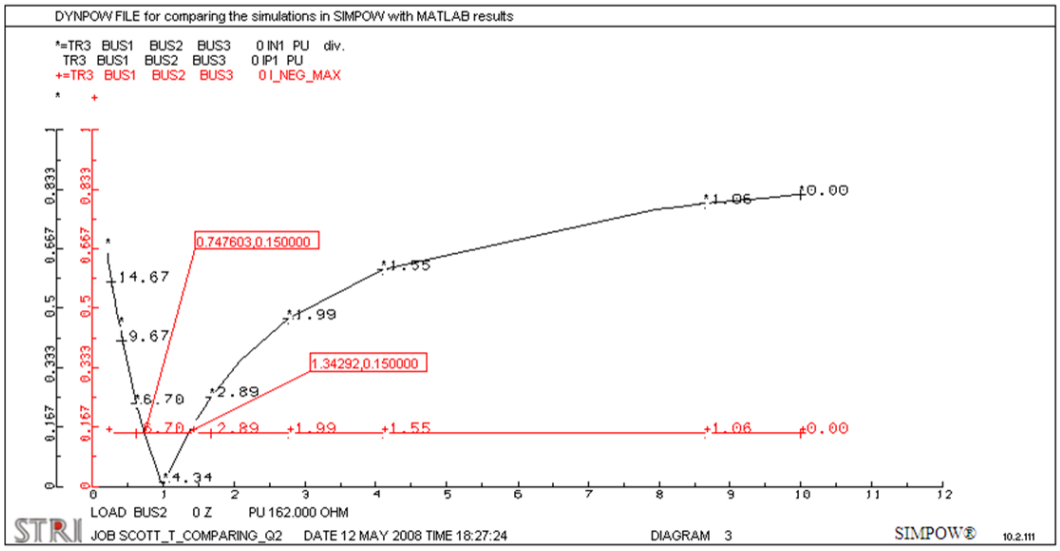

Figure 3.9: SIMPOW result when varying the apparent power at BUS2

Note that the impedance at BUS2 is used as the variable for this simulation. It is given in per unit along the x–axis. The intersection points are when Z_2 is 0.75 and 1.34 per unit of Z_3. This is also the same at the MATLAB result.

To sum up, the simulations in SIMPOW give the same results as in the MATLAB calculations in the Specialisation Project[4]. The small deviations are due to the inaccurate method for finding the intersection points in SIMPOW.

3.4 Scott–T including losses

The DSL model for the Scott–T transformer in Section 3.2 is a simplified model for the transformer. It ignores both resistance and reactance in the transformer as well as disregarding the saturation of the core. However, such an ideal transformer can never be made for practical use, but well designed power transformers can come quite close. It is therefore desirable to include parameters that makes the DSL model account for the losses that occurs during operation of the transformer.

The approximate equivalent circuit of a real transformer often includes both the resistance and leakage reactance of the transformer windings in addition to the core losses in terms of magnetizing resistance and reactance. However, for practical engineering applications, a transformer model which includes the short–circuit impedance is a good approximation for a real transformer. This is due to the fact that under normal circumstances, the magnetizing current causes a negligible voltage drop in the winding[11].

The model for the Scott–T transformer is implemented in SIMPOW as a three–winding transformer with one three–phase primary winding and two one–phase secondary windings. Between the windings one can therefore define the short–circuit impedance $Z_{sc} = ER_{nm} + EX_{nm}$ where ER and EX are the short–circuit resistance and reactance and where nm denotes the windings in concern. For linear conditions one can, based on measurements, establish the equivalent circuit for a three–winding transformer which is given in Figure 3.10 [12].

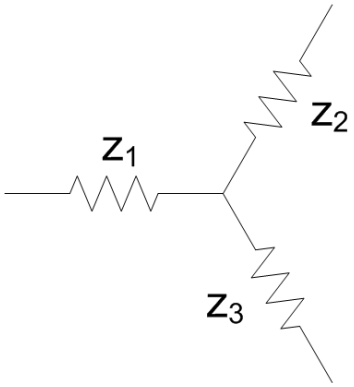

Figure 3.10: Per phase equivalent circuit for a three–winding transformer

The three short–circuit impedances Z_1, Z_2 and Z_3 are fictional quantities introduced to calculate the voltage drop in the transformer when all the windings are connected to a grid. The values for the impedances are found using the expressions in Equation 3.14 [12].

$$\begin{aligned} Z_1 &= \frac{1}{2}(z_{12} + z_{13} - z_{23}) \\ Z_2 &= \frac{1}{2}(z_{12} - z_{13} + z_{23}) \\ Z_3 &= \frac{1}{2}(-z_{12} + z_{13} + z_{23}) \end{aligned} \tag{3.14}$$

z_{12}, z_{13} and z_{23} represents the inductance between the three windings and are are found from short–circuit and open–circuit measurements. The values of the impedances can be used to control the short–circuit currents and the voltage drop across the transformer. However, for the simulation aspect in SIMPOW, the values for the Scott–T transformers short–circuit impedances are set equal to $Z_{sc} = ER + EX = 0.005 + j0.07pu$[13].

Unfortunately, including the short–circuit impedance in the DSL model for Scott–T is quite complex. This is due to the need of local node declarations for giving the internal voltage drop in the transformer. Seeing that the main objective is to analyse the DEH system in total, and not only the specially connected transformer, a simplified method

is introduced. The base for the model is to use the lossless DSL model explained in Section 3.2, and include the voltage drop in the three windings in terms of line impedances that are connected to the primary winding and the two secondary windings respectively. This makes it easier for including the losses in the Scott–T as well as it is less time consuming. The single–line diagram for the Scott–T transformer including the short circuit impedances is shown in Figure 3.11.

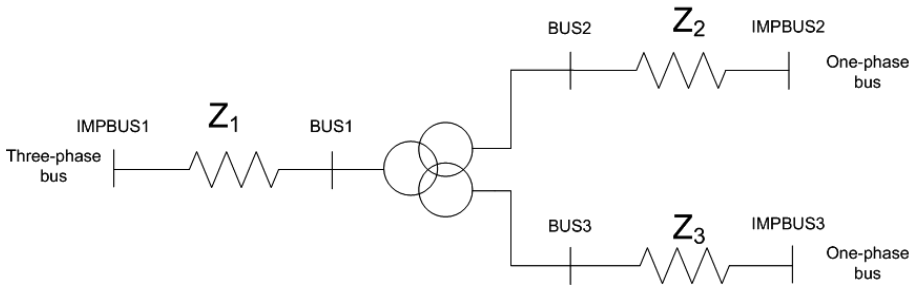

Figure 3.11: SLD for modelling the Scott–T including the short circuit impedances

The nodes IMPBUS1, IMPBUS2 and IMPBUS3 are the nodes which are used in SIMPOW for connecting the Scott–T transformer including the losses to the surrounding power system.

When making models for computer simulations, it is important to verify that the model is programmed correctly and that it is in accordance with the laws of physics. Therefore an example with the Scott–T transformer including the losses is given where the primary side is connected to a voltage source and the secondary terminals are short circuited. Further, hand calculations are carried out to investigate the internal voltage drop and the short circuit currents. Finally the hand calculations are compared with simulations in SIMPOW. It is worth mentioning that it is very important to keep in mind the phase difference of the buses. BUS1 is a three–phase node and BUS2 and BUS3 are one–phase nodes.

The configuration for the example is given in Figure 3.12.

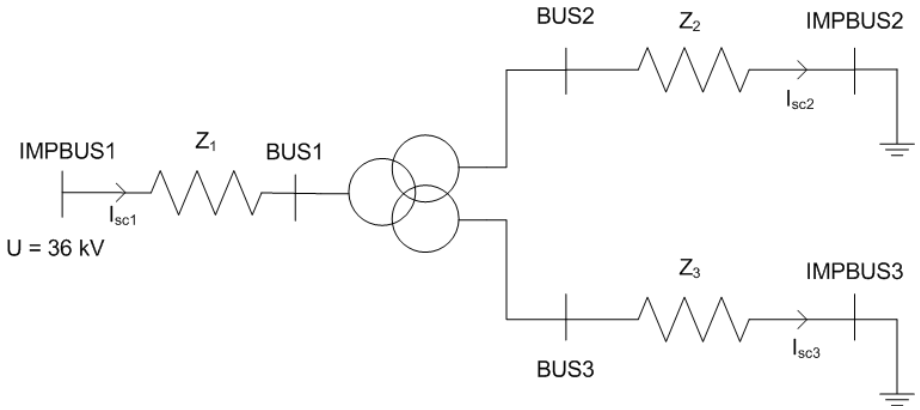

Figure 3.12: System configuration for short circuit calculations of the Scott–T

Transformer nominal data:

- Sn = 2 MVA

- Un(BUS1) = 36 kV
- Un(BUS2) = 18 kV
- Un(BUS3) = 18 kV
- $Z_1 = Z_2 = Z_3$ = ER + EX = $0.005 + j0.007$ p.u

The short–circuit resistance and reactance are given in per unit of the transformer nominal values, and have to be calculated with respect to those. The base value for Z_1 on the primary side is given in Equation 3.15.

$$Z_{Base1} = \frac{Un(BUS1)^2}{Sn} = \frac{(36kV)^2}{2MVA} = 648\Omega \tag{3.15}$$

The base value for the two secondary windings are equal because their nominal terminal voltage is the same, see Equation 3.16.

$$Z_{Base2} = Z_{Base3} = \frac{(18kV)^2}{2MVA} = 162\Omega \tag{3.16}$$

By using the base values for the impedance, one can calculate the values for the three short–circuit impedances Z_1, Z_2 and Z_3 in ohm according to Equation 3.17.

$$Z[\Omega] = Z_{Base} \cdot Z_{pu} \tag{3.17}$$

This gives:

$$\begin{aligned} Z_1 &= (0.005 + j0.07) \cdot 648\Omega = 3.24 + j45.36\Omega = 45.5e^{j85.9}\Omega \\ Z_2 &= (0.005 + j0.07) \cdot 162\Omega = 0.81 + j11.34\Omega = 11.4e^{j85.9}\Omega \\ Z_3 &= (0.005 + j0.07) \cdot 162\Omega = 0.81 + j11.34\Omega = 11.4e^{j85.9}\Omega \end{aligned} \tag{3.18}$$

Next, the short–circuit currents I_{sc2} and I_{sc3} in Figure 3.12 are found by using Equation 3.19. Note that the expression for the short–circuit current on the secondary side is adapted to the one–phase buses.

$$I_{sc} = \frac{U_{pre-fault}}{3 \cdot Z_f} \tag{3.19}$$

Before the short–circuit, the transformer is assumed unloaded, hence the pre–fault voltage at BUS2 and BUS3 is 18 kV. The impedance to ground is the short circuit impedance of the windings seeing that the secondary terminals are grounded directly. The short–circuit currents for the two secondary buses become as expressed in Equation 3.20.

$$I_{sc2} = \frac{18kV}{3 \cdot 11.4e^{j85.9}} = 526.3e^{-j85.9}\text{A} \tag{3.20}$$

Note that the calculated current angle is referred to its node voltage. The short–circuit current in BUS3 is equal to I_{sc2} but is, as shown in Chapter 2.2, 90°out of phase, see Equation 3.21.

$$I_{sc3} = I_{sc2} - 90^\circ = 526.3e^{-j175.9}\text{A} \tag{3.21}$$

The short–circuit current I_{sc1} on the three–phase primary side is calculated by referring the impedances on the secondary side to the primary side. The notation Z_2' and Z_3' are used for referring the two secondary impedances to the primary side and by considering the turn ratio t between the primary– and secondary windings.

$$\begin{aligned} Z_2' &= Z_2 \cdot t^2 = Z_2 \cdot (\frac{36kV}{18kV})^2 = 3.26 + j45.48 \\ Z_3' &= Z_3 \cdot t^2 = Z_3 \cdot (\frac{36kV}{18kV})^2 = 3.26 + j45.48 \end{aligned} \tag{3.22}$$

The short–circuit current I_{sc1} is further calculated using the expression in Equation 3.25.

$$I_{sc1} = \frac{U_{pre-fault}}{Z_{total}} \tag{3.23}$$

The value for Z_{total} is the sum of Z_1 and the parallel connected impedances Z_2' and Z_3' referred to the primary side.

$$\begin{aligned} Z_{total} &= Z_1 + \frac{Z_2' \cdot Z_3'}{Z_2' + Z_3'} \\ \Rightarrow Z_{total} &= 4.87 + j68.1\Omega = 68.2e^{j85.9}\Omega \end{aligned} \tag{3.24}$$

By using the value for the total impedance and Equation 3.23, the value for I_{sc1} is calculated, see Equation 3.25.

$$I_{sc1} = \frac{36kV}{\sqrt{3} \cdot 68.2e^{j85.9}}\Omega = 304.8e^{-j85.9}\text{A} \tag{3.25}$$

Next, the internal voltage on BUS1 in Figure 3.12 can be found by using I_{sc1} and Z_1, see Equation 3.26. Note that the voltage is given in phase–to–phase value.

$$\begin{aligned} U_{BUS1} &= U_{IMPBUS1} - \sqrt{3} \cdot I_{sc1} \cdot Z_1 \\ U_{BUS1} &= 36kV - \sqrt{3} \cdot 304.8e^{-j85.9}\text{A} \cdot 45.5e^{j85.9}\Omega \\ U_{BUS1} &= 12kV \end{aligned} \tag{3.26}$$

The secondary winding voltages on BUS2 and BUS3 in the Scott–T transformer are then finally found by using the turn ratio t:

$$\begin{aligned} U_{BUS2} &= \frac{U_{BUS1}}{t} = \frac{12kV}{2} = 6kV \\ U_{BUS3} &= \frac{U_{BUS1}}{t} = \frac{12kV}{2} = 6kV \end{aligned} \tag{3.27}$$

For the simulations in SIMPOW, an Optpow– and Dynpow file for the configuration in Figure 3.12 has to be made to establish the load flow of the initial conditions, as well

as for the short–circuit faults on the the secondary side. The SIMPOW files are given in Appendix D.4. Note that the lossless DSL model for Scott–T deduced in Section 3.2 is used to represent the transformer. The short circuit impedances Z_1, Z_2 and Z_3 are given by lines which includes resistance and reactance equal to the calculated values for the transformers ER and EX.

The simulations in SIMPOW with the Optpow– and Dynpow file in Appendix D.4 give the following result presented in a SLD diagram from the Dynpow–calculations, see Figure 3.13[1].

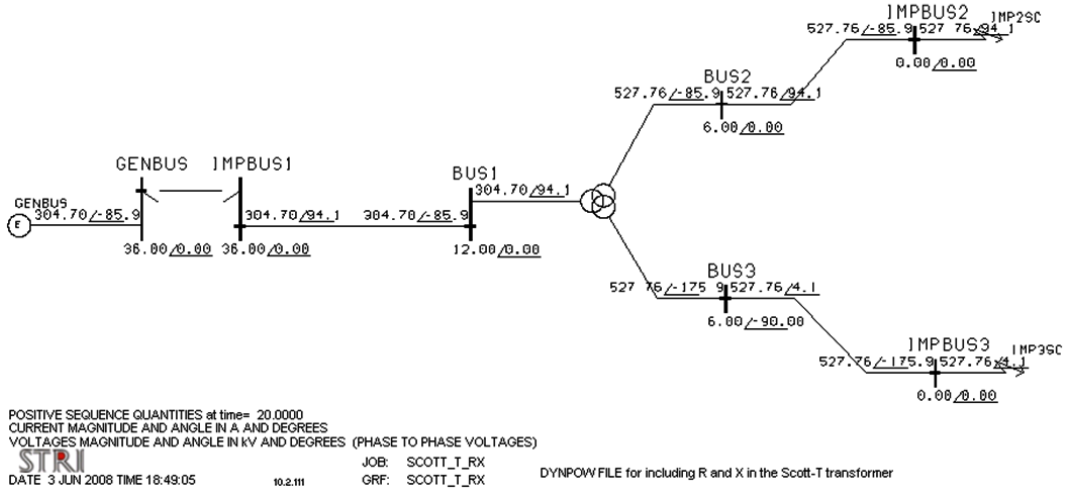

Figure 3.13: Results from simulations in SIMPOW presented in a SLD

The values given above the lines is the amplitude and angle of the phase current that flows in the line. Note that the reference direction is into the node. The value below the nodes are the node voltages in phase–to–phase value and its angle.

By comparing the values from the single–line diagram with the results from the hand calculations, the similarities are revealed. The currents that flows due to the short circuit is equal as well as the voltages on the nodes. Note that the amplitude of the currents on the one–phase side is 527Aand on the primary side 304A. This is natural seeing that the voltage on the primary side is lower than the secondary side. In addition, the short–circuit impedance causes a voltage drop on the primary side due to the short circuit on the secondary load terminals.

[1]In the figure it looks like GENBUS and IMPBUS 1 are not connected, but that is only a graphical error. STRI AB was contacted, but the problem was not solved

Chapter 4

DEH system design

The analysis in Chapter 2.4 and Chapter 3.3 focuses on the Scott–T transformer respectively. The simulations show how the degree of unsymmetry varies as the load impedance changes, but the results are limited to the transformer and does not include the DEH system.

Further research of the Scott–T transformer implemented in a DEH system is necessary to investigate the operation as a whole. Possible system configurations for this analysis is then necessary. Two feasible DEH configurations for subsea power supply are presented in this chapter.

4.1 DEH system design

Direct electrical heating has been, after several studies and research projects, selected as the preferred solution for the prevention of hydrate formation and wax deposition in subsea oil production [5]. There is a lot of factors which are important when designing such a system, especially when it comes to the safety and reliability of the installation.

So far, the power supply for the DEH system is installed topside on a platform which also includes a load balancing unit and compensation for the reactive load. However, by the use of an alternative transformer such as the Scott–T transformer, it can be possible to install the transformer subsea in a template close to the pipeline to be heated without the need for a balancing unit. The power supply itself can be located either onshore or on a topside installation (e.g platform, FPSO). In addition, implementing the Scott–T transformer can prove to be a good solution for long step outs as well. This is due to the fact that the pipeline is a very inductive load using a great deal of reactive power. Long step outs require long cables which produce reactive power. A well designed DEH system can therefore be operated without the need for huge reactive compensation seeing that the pipeline consumes the reactive power from the cable.

When designing an electrical installation, it is always necessary to consider the technically and economically feasible solutions. In addition, for an offshore subsea system, there are multiple standards end requirements which also influences the electrical design. Issues regarding subsea technology and available electrical equipment is an important part of the engineering. However, for the further investigations on the DEH system with the specially connected transformer, two simple configurations are established as the base cases for the analysis. The objective is to analyse the electrical operations of the total subsea system, and the engineering part of the installation has to be dealt with later.

Normally, complex calculations related both to thermal and electrical issues have to be done to specify the power requirements for a DEH system. In addition, the pipeline material and dimension are two variables that influence heavily on the DEH power system. This makes it very important to have the detailed data for the pipeline before carrying out the power system calculations and dimensioning. For the sake of simplicity and convenience, a given set of data for a typical North Sea pipeline is used, see Table 4.1[14].

Table 4.1: Pipeline data for a typical North Sea pipeline

Pipeline material	**Pipeline ID**	**Pipeline wall thickness**	**External coating**	**U–value of isolation**	**Pipeline length**
13 Cr[a]	275 mm	17 mm	50 mm	5 W/m^2K	40 km

[a]SML 13 Cr I SFDP, 2.5% Mo according to DnV OS–F101

The requirements for the DEH system are:

1. Keep the pipe content above 25°C during shutdowns
2. Heat the pipe content from 4°C to 25°C within 48 hours

The electrical data for meeting the requirements are given in Table 4.2.

Table 4.2: Electrical data for the pipeline

Impedance	**Supply voltage**	**Required current**
3.2 + j12.5 Ω	18 kV/20 kV (maintain/heating)	1500 A(heating)

Note that the impedance of the DEH system given in Table 4.2 is for both the piggyback cable and the pipeline. In other words, it is the impedance as seen from the terminals where the piggyback cable is connected. In addition, the specifications given in the table are for a 40 km pipeline. Re–calculations and modifications are done where it is necessary for adjusting the parameters according to the DEH configurations in this analysis. For instance, the power requirements and the impedance of the load are scaled up to be appropriate for longer pipelines.

4.1.1 Case I

Figure 4.1 shows the DEH system design which is the base case for further study and simulations[15]. The system is divided between an onshore and a subsea installation, and the pipeline to be heated is 100 km long.

BUS1 is the interface to the regional power system. Transformer $T12$ provides galvanic isolation between the onshore and subsea part of the system. This transformer can also be a three–winding transformer if it is necessary to have two different voltage levels for BUS3 and BUS4. The 100 km power supply cable between BUS2 and BUS3 is a three–phase cable which can be used to supply a compressor or pump at BUS3, typically 50 MW. The feeder cable for the DEH is chosen to be connected between the onshore station and the subsea installation at BUS4. $T4$ is the specially connected transformer.

As the figure indicates, the pipeline has been divided into two sections. In addition to the electrical parts in Figure 4.1, reactive power compensation might have to be included.

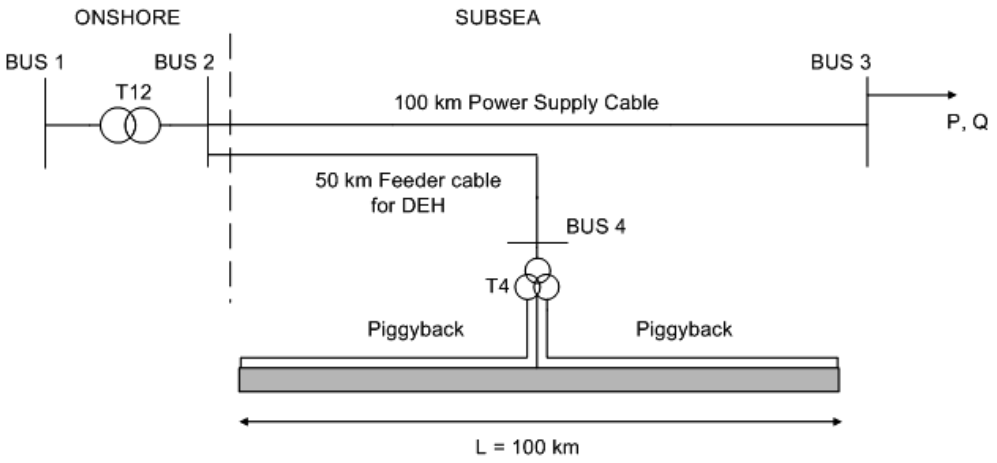

Figure 4.1: DEH system configuration for Case I

Statnett, which is the company managing the power grid in Norway, requires a power factor of unity at the interface connection (PF = 1)[15], which means no flow of reactive power. The power supply can also be on an FPSO, but are in this study chosen to be installed onshore.

4.1.2 Case II

The configuration for Case II, is designed for a 200 km long pipeline, see Figure 4.2. The same applies for this design when it comes to the power supply interface at BUS1 and the load at BUS3. However, there are two specially connected transformers in this configuration. In addition, there are two cable branches at the power supply cable connecting the two transformers at BUS4 and BUS5 and the DEH system to the power supply onshore.

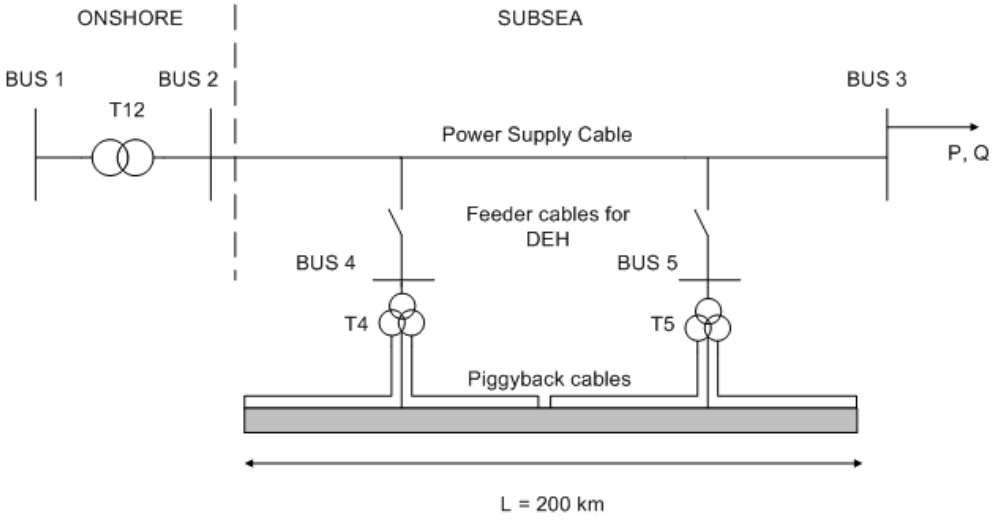

Figure 4.2: DEH system configuration for Case II

An alternative to the configuration in Figure 4.2, is to have the power supply cables for

the transformers at BUS4 and BUS5 as shown in Figure 4.3.

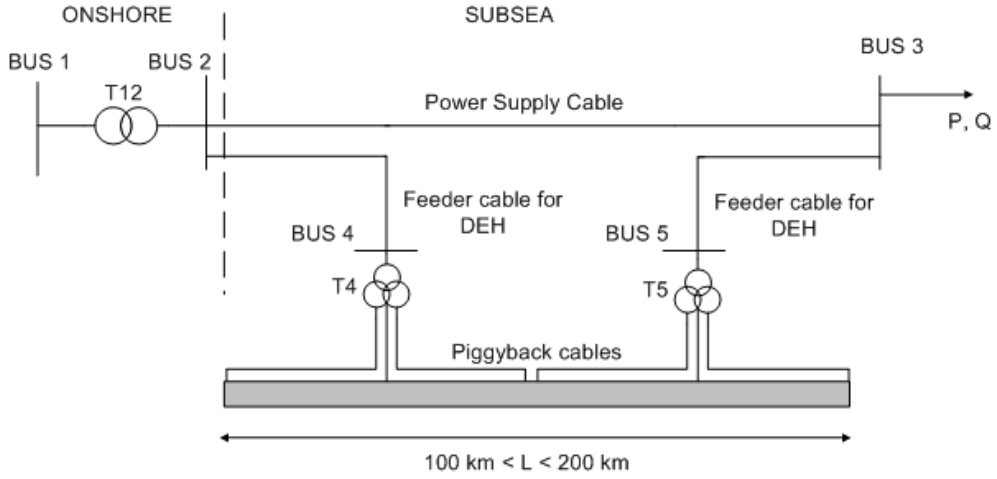

Figure 4.3: Alternative configuration for Case II and pipeline shorter than 200 km

The system design in Figure 4.3 may show to be the preferred configuration for pipeline lengths between 100 and 200 km. This is due to the length of the feeder cables for the DEH. However, the alternative configuration is not included in any further analysis.

Chapter 5

System simulations

When planning, designing and engineering an electric power network, system simulations are of great value for investigating both the electro technical characteristics as well as the health, environmental and security effects. Several studies have to be carried out in order to verify that an electrical system is functional and operating according to given standards and regulations. That is, load flow analysis, insulation coordination, stability studies, reliability as well as contingency studies are important in that matter.

This chapter presents simulations of the DEH system with the specially connected transformer. The configurations described in Chapter 4.1 are the DEH systems that are analysed. Typical operational modes for a DEH system are introduced and load flow analysis is carried out to investigate the voltage relationships, degree of unsymmetry and reactive power flow. In addition, some fault scenarios are simulated. Seeing that this work is primarily a case study, the focus is on the analysis of the DEH system and not the detail engineering including technical and economical estimations. In addition, the given operational modes are meant to give an indication of what to expect for a few typical scenarios when implementing a three–to–two–phase transformer.

5.1 Simulation modes

Chapter 4.1 describes the DEH systems that are analysed, Case 1 and Case 2 respectively. In addition, two requirements of the DEH system are given.

1. Keep the pipe content above 25°C during shutdowns
2. Heat the pipe content from 4°C to 25°C within 48 hours after a shutdown

The initial focus of the simulations is to analyse the effect of implementing the Scott–T transformer to the DEH system. According to Table 4.2, the heating mode requires the higher voltage and is therefore the dimensioning mode for the electrical equipment in terms of electrical stress and degradation. The specifications for heating the pipe content from 4°C to 25°C within 48 hours after a shutdown is therefore chosen as the point of departure for the system simulations.

The analysis for Case 1 and Case 2 includes:

1. Load flow analysis on the systems for heating the pipe content during different operations
2. Analyse the influence of faults such as a short–circuit or load outage
3. The effect of reactive power compensation

The parameters that are investigated are:

- Voltage levels in the system
- Degree of unsymmetry ($|\frac{I_-}{I_+}|$)
- Reactive power

The different modes for Case 1 and Case 2 are further explained in Section 5.2 and Section 5.3.

It is in particularly interesting to investigate the degree of unsymmetry on the nodes that are connected to the grid and the subsea load. In addition, the reactive power flow is also an interesting parameter as the pipeline is greatly inductive and the cables highly capacitive.

As explained in [4] the negative component of the current does not contribute to useful power, but may cause overheating and damages of the equipment in a network. In addition, the negative sequence component has the opposite phase direction as the positive sequence component which can be a severe problem for a motor. However, the influence on electrical equipment from the negative sequence component depends also on the design and function of the equipment.

Table 4.1 gives the data for a 40 km DEH pipeline and Table 4.2 gives the electrical data for the two operational requirements for maintaining and heating the pipeline. The voltage on the load terminals for maintaining the temperature is 18 kV and 20 kV for heating the pipeline. However, by the very fact that the pipeline in Case 1 and 2 are 100 km and 200 km, the data has to be re–calculated. This is done for each case in Section 5.2 and Section 5.3.

5.2 Case 1

The configuration for Case 1 in Figure 4.1, Chapter 4.1, is the first DEH system that is analysed with the Scott–T transformer implemented. The single line diagram for Case 1 is given in Figure 5.1.

As shown in the figure, the transformer between the onshore- and subsea power system is a tree–winding transformer. This makes it possible to have different voltage levels on the bus supplying the DEH system at BUS3 and for the subsea load at the node LOADBUS.

The three nodes DEHBUS1, DEHBUS2 and DEHBUS3 are connected to the lossless Scott-T transformer at SCOTTBUS1, SCOTTBUS2 and SCOTTBUS3 by means of three lines for representing the short–circuit impedance of the transformer. The two loads Z_{DEH2} and Z_{DEH3} represents the impedance of the piggyback cable and the pipeline for the two pipe sections connected to the Scott–T transformer.

The nominal voltage level at BUS1 is specified to be 300 kV, as this is a normal voltage level for the regional power grid. The voltage level for the 100 km subsea cable is chosen to be 132 kV and 66 kV for the 50 km feeder cable. The subsea load is 50 MW at a power factor of 0.9, and the system frequency is 50 Hz[13].

The pipeline for Case 1 is 100 km long and is divided into two 50 km sections which are connected to the Scott–T transformer. The input data for this case is re–calculated from

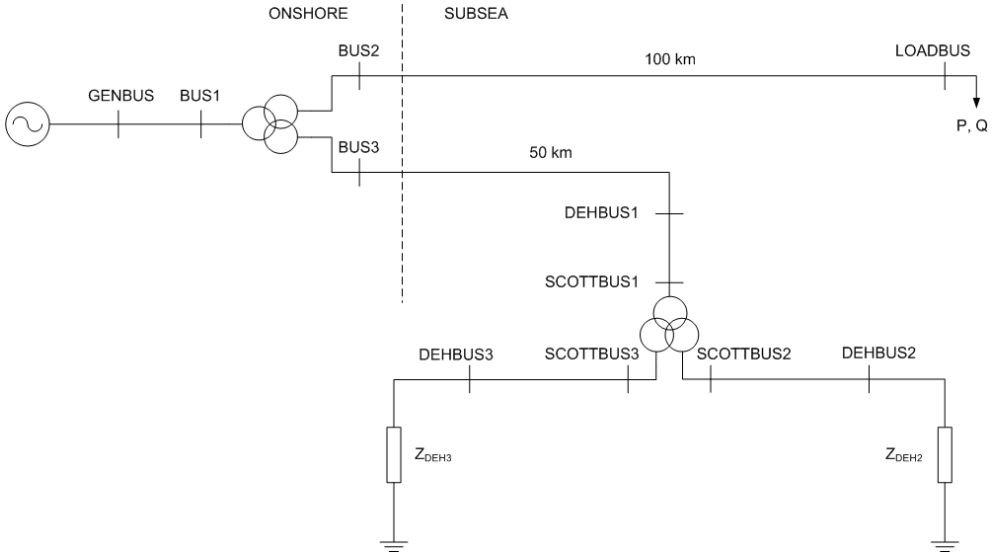

Figure 5.1: Single line diagram for Case 1

the parameters given for the 40 km pipeline in Table 4.2. The impedance of the pipe and the piggyback cable are assumed proportional to the length. Seeing that the two pipe sections in Figure 5.1 are 50 km, the impedance of the pipe sections are a factor of $\frac{50km}{40km} = 1.25$ larger for Case 1. The current required for the 40 km pipeline in Table 4.2 is 1500 A. Assuming the same conditions for the two 50 km pipe section, the voltage also has to be 1.25 larger since the impedance is increased by the same factor. The input data for Case 1 is given in Table 5.1.

Table 5.1: Electrical data for the pipeline in Case 1

Pipeline length	Impedance	Supply voltage	Required current
50 km	4.0 + j15.6 Ω	22.5 kV/25.0 kV (maintain/heating)	1500 A(heating)

The data for the 100 km subsea cable connecting BUS2 and LOADBUS and the 50 km subsea cable between BUS3 and DEHBUS1 are given in Table 5.2[16]. The cables have been investigated to ensure that the voltage drop across the cables are within practical limits and selected after discussions with the supervisor[13].

Table 5.2: Parameters for the subsea cables in Case 1

Subsea cable	Cable type	Rated voltage	AC-resistance at 90°C	Capacitance (per phase)	Inductance (per phase)	Rated current at 90°C
100 km	3x240mm^2 Cu	132 kV	0.097 Ω/km	0.14 µF/km	0.46 mH/km	500 A
50 km	3x630mm^2 Cu	66 kV	0.040 Ω/km	0.27 µF/km	0.35 mH/km	750 A

The parameters for the subsea cables in Table 5.2 have to be adapted to the required specifications in SIMPOW. This is given in Appendix E.1. In addition, the input data for describing the configuration for Case 1 is needed for the simulations in SIMPOW. This is also given in Appendix E.1.

The following modes are analysed:

1. Normal load (50 MW, $cosfi = 0.9$) on LOADBUS. DEH system turned on for heating the pipe content (25 kV)
2. Disconnect the subsea load and keep the 100 km cable no–loaded. DEH system operating for heating
3. Disconnect 100 km cable on BUS2. DEH system operating for heating

In addition, three different fault scenarios are introduced to the system when it is operating at normal load:

i. Short–circuit in the middle of the pipe section at DEHBUS3

ii. Short–circuit on the node DEHBUS3

iii. Disconnect the pipe section at DEHBUS3

In addition, a strategy for improving the system is given in the end of the chapter and a load flow result is presented.

5.2.1 Normal load, DEH heating

Case 1 is first analysed for the situation where the subsea load is running at normal load and the DEH system is turned on for heating the pipe content. The nominal voltage applied to the DEH system is then 25 kV, see Table 5.1.

The Optpow file and Dynpow file for the simulations are based on the values deduced in Appendix E.1 and are given in Appendix F.1.1. The DSL–model for the lossless Scott–T transformer is the same as used before, see Appendix C.

The load flow is calculated with the Scott–T transformer implemented by running the Optpow– and the Dynpow file for Case 1. The result is presented in the single–line diagram from Dynpow, see Figure 5.2. The SLD result is also given in a larger figure in Appendix G which is more appropriate for analysing.

The "lower" values at the nodes in the SLD diagram are the node voltages (phase–to–phase, kV) and the "upper" values are the active– and reactive power (MW, Mvar). Note that the reference direction of the power is into the node. Unfortunately, it looks like the line between GENBUS and BUS1 are disconnected, but that is only a graphical error (STRI AB, who are responsible for SIMPOW was contacted, but the problem was not solved).

The voltage drop across the 100 km cable is calculated in Equation 5.1 and the voltage drop across the 50 km cable is calculated in Equation 5.2.

$$U_{100-drop} = \frac{U_{BUS2} - U_{LOADBUS}}{U_{BUS2}} \qquad (5.1)$$
$$U_{100-drop} = 0.017 = 1.7\%$$

$$U_{50-drop} = \frac{U_{BUS3} - U_{DEHBUS1}}{U_{BUS3}} \qquad (5.2)$$
$$U_{50-drop} = 0.076 = 7.6\%$$

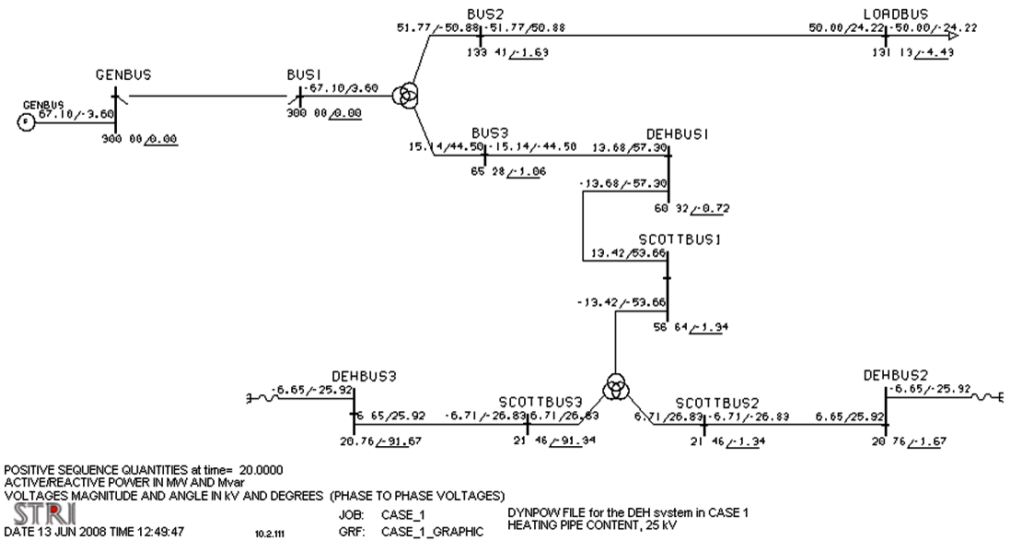

Figure 5.2: Load flow result for Case 1 for normal load and heating the pipeline

The voltage drop across the 100 km cable is lower than the 50 km cable. This is due to high contribution of reactive power from the 100 km cable. In addition the voltage on BUS2 is higher (133.41 kV) than specified in the Optpow file (132.kV). This is due to the same reason of reactive power contribution.

The voltages on the DEHBUS2 and DEHBUS3 are lower than specified in the Optpow file. They are both 20.76 kV, which is only 0.83 per unit of the required 25 kV for heating. The low voltage level is due to the voltage drop across the cable which results in lower voltage supply on the Scott–T primary side. However, the Scott–T transformer supplies two equal load voltages which are 90 degrees out of phase. This is as expected.

An interesting parameter to investigate is the flow of reactive power, Q. Seeing that the node GENBUS is specified as a swing bus in Optpow, it produces or consumes the necessary power and keeps the voltage and phase angle constant. This makes it convenient for analysing the flow of reactive power.

Note that the 100 km cable produces a total of 50.88 Mvar which goes out of BUS2 and through the three–winding transformer. 44.50 Mvar is used by the DEH system connected at BUS3 and only 3.60 Mvar is consumed by the swing bus. The rest of the reactive power is lost in the power transformer. This means that in order to keep the power factor at unity at BUS1 (no flow of reactive power), the need for compensation is 3.60 MVAr. This can be installed on BUS2 by means of a reactor which consumes reactive power. The excessive reactive power from the cable is then dissipated by the reactor and does not go through the three–winding transformer. By using such auxiliary component for compensation, the flow of reactive power through the transformer is minimized, hence it allows a smaller transformer to be installed.

More important, the load flow shows that the reactive power required for the DEH pipelines is produced by the 100 km and the 50 km cable. On the other hand, the current through the two pipelines are only 1360 A, but should have been 1500 A. The low current value is due to the voltage drops along the system which makes the terminal

voltage on the pipeline less than 25 kV. This can be solved by means of tap changers on the Scott–T transformer for optimizing the voltage levels at the load terminals. This is shown in Section 5.2.5. The following simulations are however carried out based on the normal load flow.

The degree of unsymmetry in the power system is zero which means that the Scott–T transformer provides balanced electrical power between the two–phase DEH system and the three–phase power supply.

5.2.2 Disconnecting the subsea load, DEH heating

Next, the subsea load on LOADBUS is disconnected, but the DEH system is operating for heating. The cable is still connected to BUS2, but it is no–loaded. This operation is typical for the system after a shutdown of the production and the pipe content is cooled down to the ambient sea water temperature. The Optpow file is similar to the one given in Appendix F.1.1 and the disconnection of the subsea load is done in Dynpow, see Appendix F.1.2.

Figure 5.3 shows the load flow result from the simulation. It is also given in Appendix G.1.2 in a larger figure.

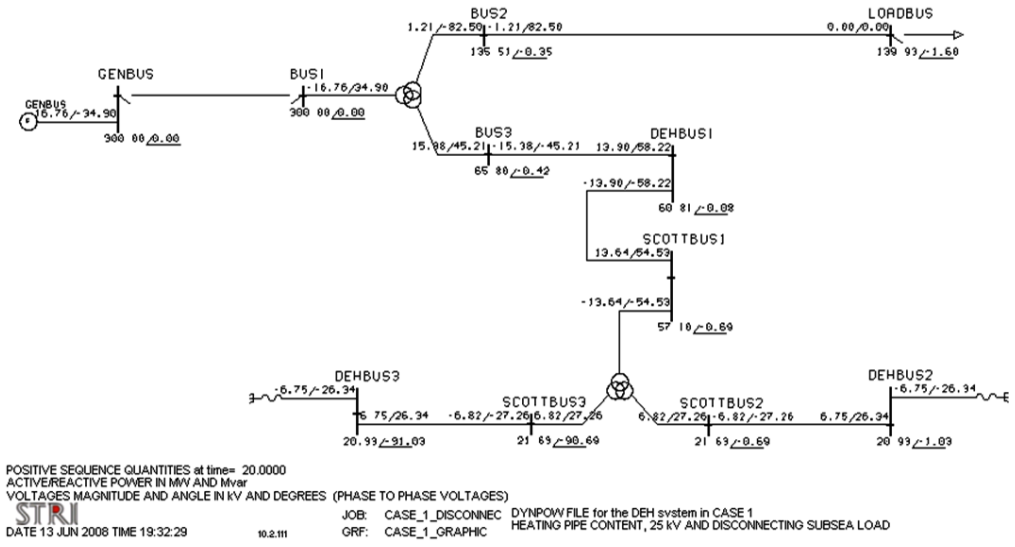

Figure 5.3: Load flow result for Case 1 when the subsea load at LOADBUS is disconnected

Figure 5.3 shows that disconnecting the load at LOADBUS causes the voltage levels to increase. The voltage on LOADBUS increases by 8.8 kV which is 6.7 % higher than during normal load. In addition the voltage on BUS2 increases, but not that much. Disconnecting the load, does also affect the flow of reactive power. BUS1 receives as much as 34.9 Mvar now, which means that there is an excessive of 34.9 Mvar in the system. In addition, the amount of reactive power transported to the DEH system at BUS3 is sllightly higher compared to when the load was operating. As a result, the terminal voltage levels increases.

Figure 5.4 shows the voltages on LOADBUS and BUS2 in per unit before and after the disconnecting the subsea load.

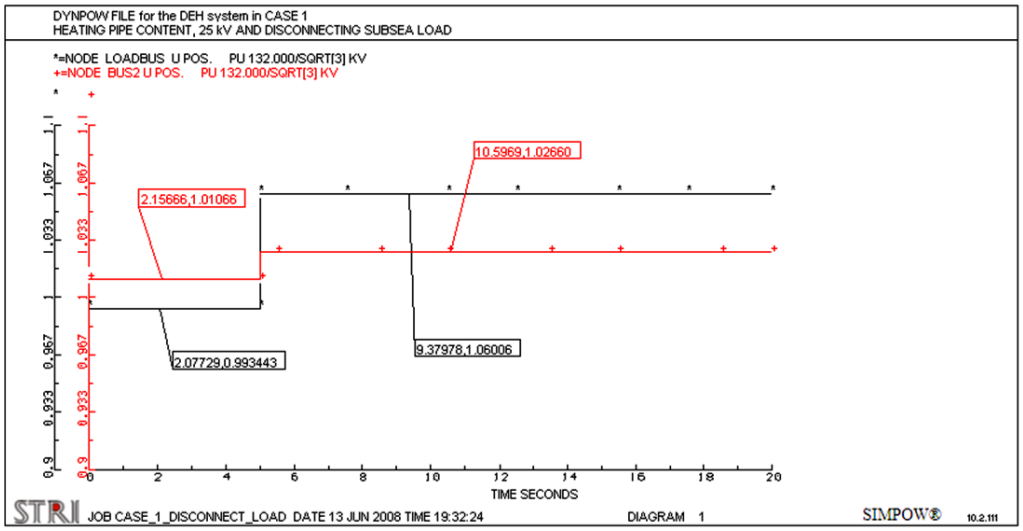

Figure 5.4: The voltages on LOADBUS and BUS2 increase after disconnecting the subsea load at LOADBUS

The subsea load in disconnected after 5 seconds. The red curve is the voltage on BUS2 and the black curve is the voltage on LOADBUS. The boxes give the coordinates of the points in x– and y–direction. x–axis is the time in seconds, and the y–axis is the voltage in per unit. Note that the voltage on LOADBUS increases much more than the voltage on BUS2.

5.2.3 Disconnecting the subsea cable at BUS2, DEH heating

The 100 km cable on BUS2 is disconnected to investigate the influence on the rest of the system. This mode is equivalent to situations when for instance the cable or the subsea load needs to be disconnected for maintenance. The cable is disconnected by using the Dynpow file given in Appendix F.1.3.

Figure 5.5 shows that the subsea cable is disconnected, but the DEH system is still operating. The result is also given in Appendix G.1.3. Unfortunately, it looks like the line between GENBUS and BUS1 is disconnected as well, but that is just a graphical error as explained in Section 5.2.1.

In this mode, the system connected to BUS1 delivers reactive power to the DEH system. This means that there has to be a compensation of 44 Mvar to BUS3 in order to have a power factor of unity at the grid connection. Figure 5.6 shows a diagram from the Dynpow calculation which indicates the change in the reactive power from BUS1.

BUS1 changes from using the excessive 3Mvar from the long cable, to supplying the needed reactive power to the DEH system, 44.6 Mvar (the negative sign in the figure is due to the definition of reference direction). The change is caused by disconnecting the long cable which produces a big part of the required Q to the system. The voltage levels are not changed significantly compared to normal operation.

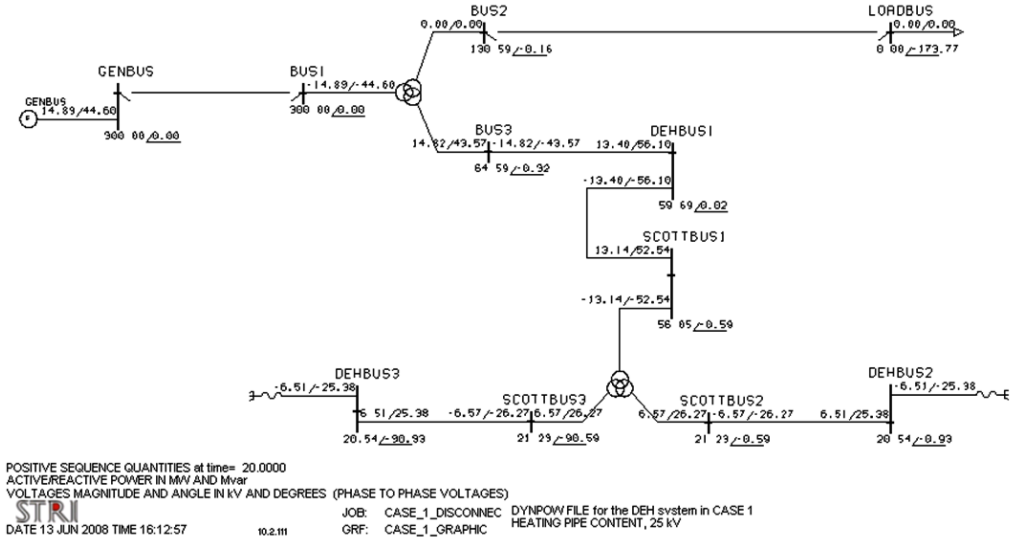

Figure 5.5: Load flow result for Case 1 when the 100 km subsea cable is disconnected at BUS2

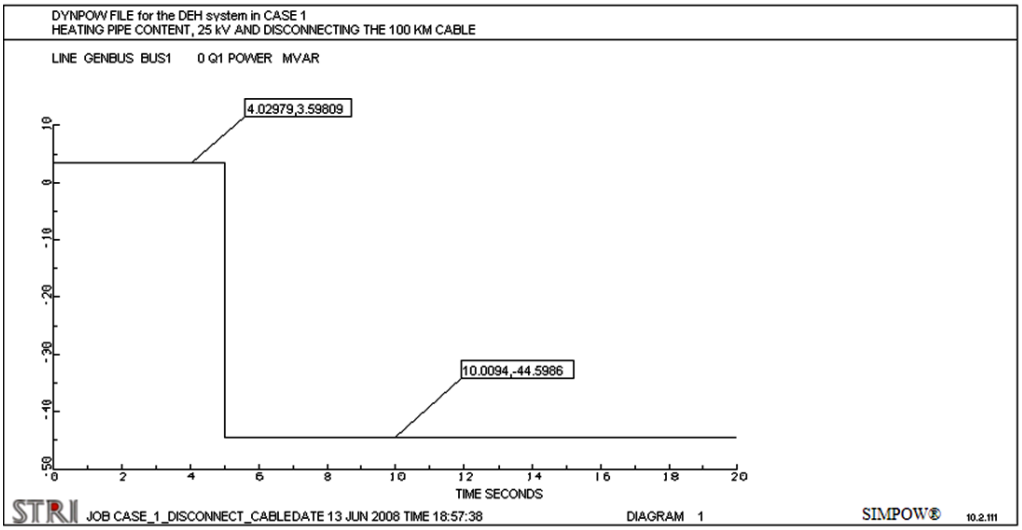

Figure 5.6: Reactive power from BUS1 before and after the disconnection of the 100 km subsea cable

5.2.4 Fault scenarios

The main objective for analysing faults in the configuration for Case 1, is to investigate the degree of unsymmetry. A fault along the pipeline changes the impedance and results in unbalanced loading of the Scott–T transformer. As explained in Chapter 2.1 and Chapter 2.4, unbalanced loading of the Scott–T transformer does not provide balanced electrical power between the two–phase and three–phase system. In addition, such a fault is a challenge for the breakers in a DEH system. This is due to the fact that the system is initially "short–circuited" at the far end of the pipeline and that such a fault might not contribute to a current which the protection equipment is able to detect. The result can be overheating of cables and further complex faults which causes a time consuming maintenance or re–installation of new equipment.

The degree of unsymmetry is examined in the Scott–T transformer and at the nodes BUS1 and LOADBUS as they are connected to the grid and to the subsea load.

Short–circuit in the middle of a pipeline

A short–circuit in the middle of a pipe section halves the pipe impedance of the faulted section which results in unsymmetrically loading of the Scott–T transformer. For the simulations in SIMPOW, the load impedance at DEHBUS3 is divided in two by connecting an equal impedance in parallel, see the Dynpow file in Appendix F.1.4. The Optpow file is the same as used for normal loading.

Figure G.4 in Appendix G.1.4 shows the load flow result for the simulation. The voltage level at the faulted secondary terminal DEHBUS3 decreases after the fault, but the voltage level at the other load terminal DEHBUS2 is stable. The voltage levels in the rest of the system do also decrease. The voltage drop across the 100 km cable is the same as for the normal load situation (1.7%), but the voltage drop in the 50 km increases from 7.6% to 10.7% after the fault. This is because the current in the cable increases due to the fault, which increases the resistive losses.

Figure 5.7 shows the degree of unsymmery ($|\frac{I_-}{I_+}|$) for the current in the Scott–T transformer when there is a short–circuit in the middle of the pipe section at DEHBUS3. The fault is connected after 5 seconds.

The red line is the limit for maximum permissible continuous value of the negative sequence component. The black curve shows the change in degree of unsymmetry before and after the fault. The black box gives the value for the degree of unsymmetry which is 25.2% in the Scott–T transformer.

Figure 5.8 shows the degree of unsymmetry in the 100 km cable to the subsea load and in the line between the production source and BUS1.

The red line in Figure 5.8 is the limit of 15%. The blue curve is the degree of unsymmetry in the line between BUS1 and the grid, and the black curve is the degree of unsymmetry in the 100 km subsea cable. The diagram shows that $|\frac{I_-}{I_+}|$ for the grid side is as much as 30.4%, but only 0.5% in the 100 km subsea cable. There is a strong degree of unsymmetry in the three–phase power system on the grid connection side which causes the phase currents to differ in magnitude.

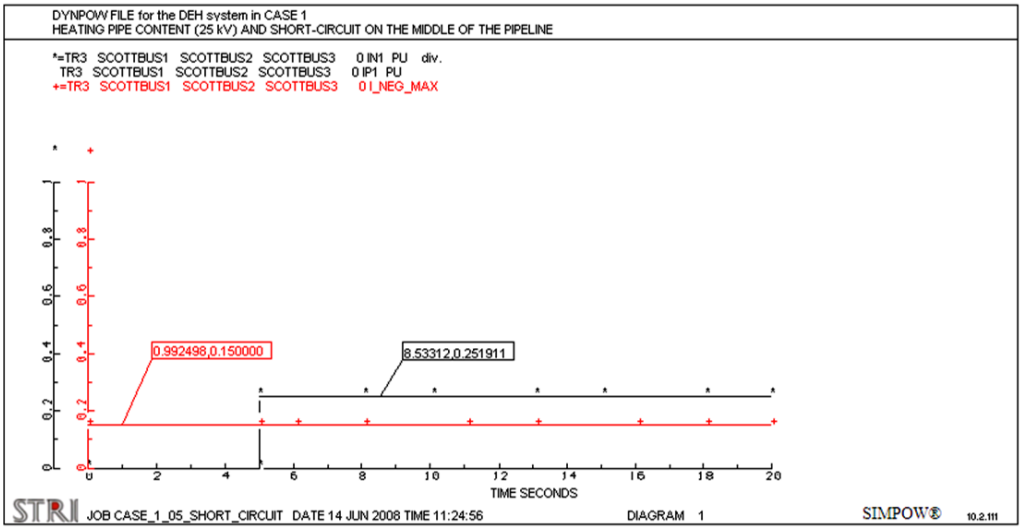

Figure 5.7: Degree of unsymmetry in the Scott–T transformer after the short–circuit in the middle of the pipe section at DEHBUS3

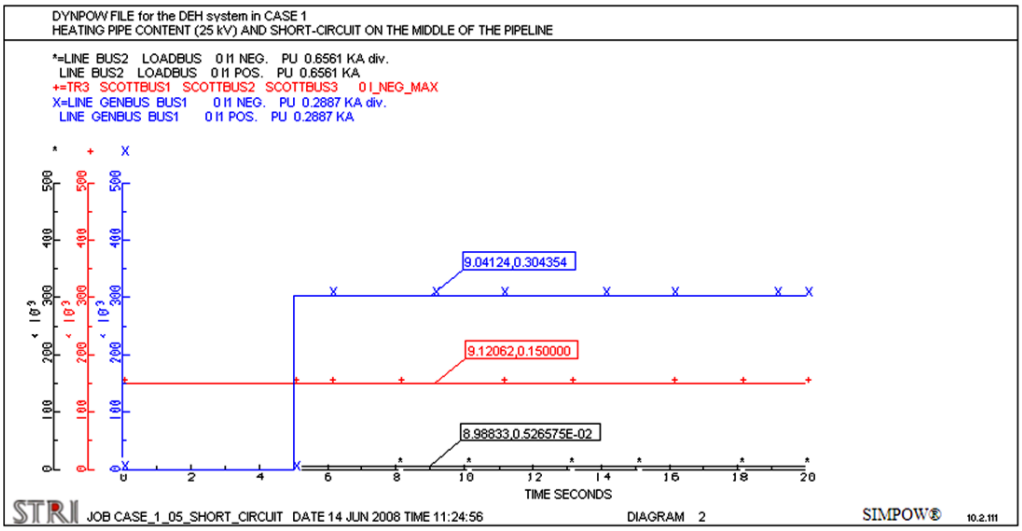

Figure 5.8: Degree of unsymmetry in the grid connection and in the cable to the LOADBUS after the fault in the middle of the pipe section

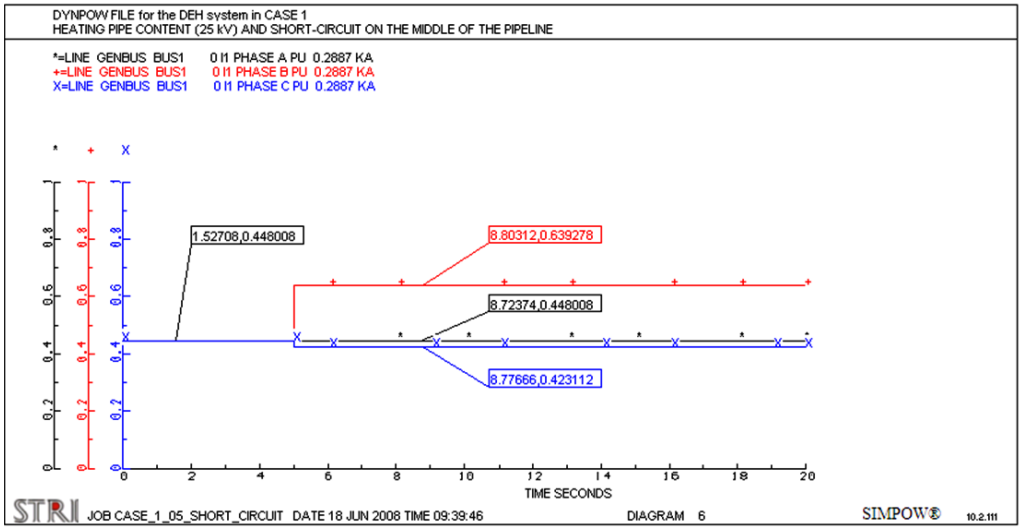

Figure 5.9: Phase currents in the grid connection after the fault in the middle of the pipe section at DEHBUS3

Figure 5.9 shows the phase currents in the line between GENBUS and BUS1. Note that they are equal before the fault, but differ in magnitude after the fault. This shows that the grid is loaded unsymmetrically.

Investigating the current in the system more closely, one possible reason to the large $|\frac{I_-}{I_+}|$ on the grid side is found. The positive– and negative sequence current in the 50 km cable to the DEH system are given in Figure 5.10.

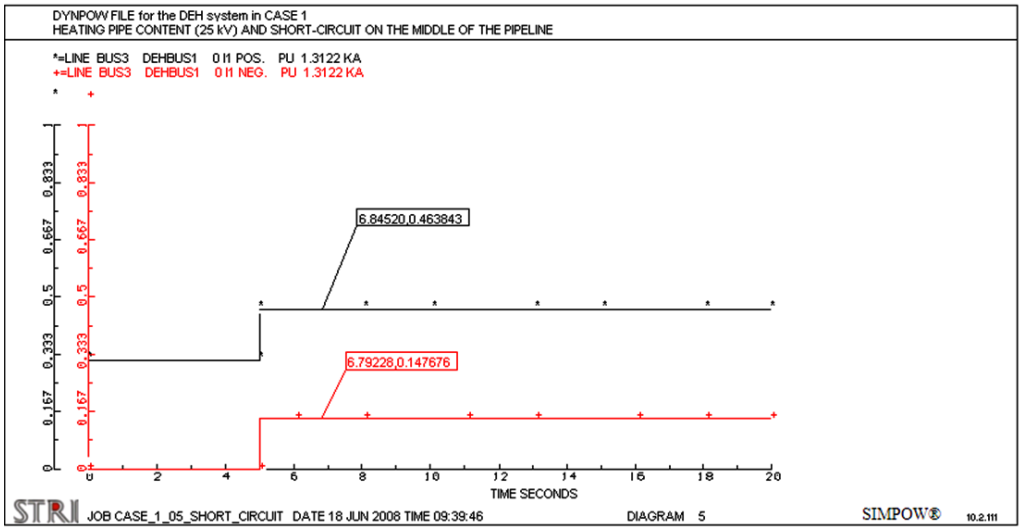

Figure 5.10: The physical value for I_+ and I_- in the 50 km cable to the DEH system after the short–circuit in the middle of the pipe section

The black curve is the positive sequence current in per unit, and the red line is for the negative sequence current in per unit. Note that the negative sequence current is 0.148 p.u.

Figure 5.11 shows the negative sequence component of the current in the line between

GENBUS and BUS1 and for the 100 km subsea cable.

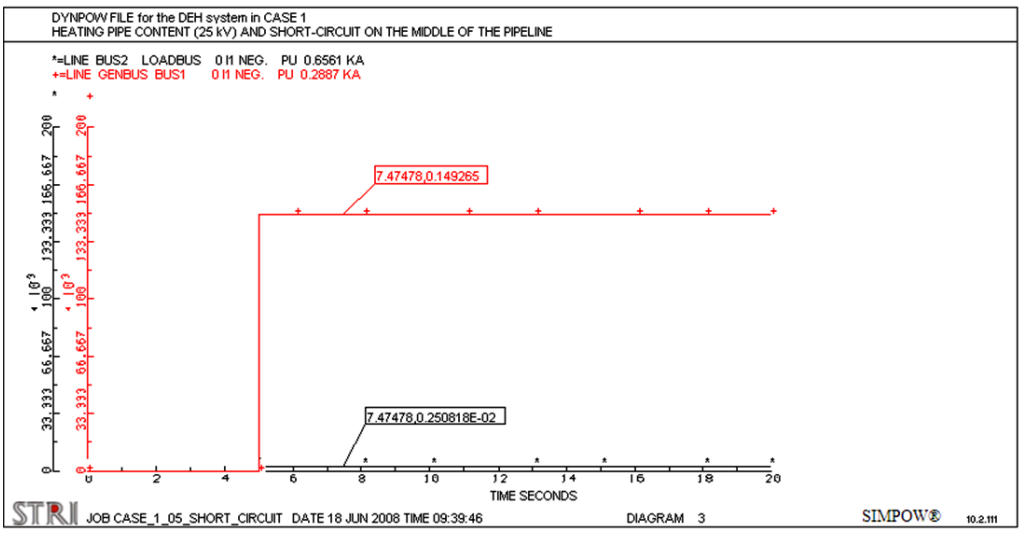

Figure 5.11: The physical value for I_- in the line connected to BUS1 and in the 100 km cable after the fault in the middle of the pipe section

The red box in Figure 5.11 shows the value for I_- in per unit for the line between GENBUS and BUS1 and the black box indicates the value for I_- in per unit for the 100 km cable. The negative sequence current in the line is 0.149 p.u which is almost the same as for the negative sequence current in the cable to the DEH system. The negative sequence current in the subsea cable is only 0.0025 pu. This means that the negative sequence current is only supplied to the DEH system from the production source which is defined as a swing bus. The 100 km subsea cable which is connected to the load does not ad any driving energy for the negative sequence current. This is because it is defined as a passive load without any rotating magnetic field which can set up a negative sequence voltage.

Short–circuit on a DEH load terminal

The node DEHBUS3 is short–circuited by using the Dynpow file given in Appendix F.1.5. The load flow result after the fault is given in Appendix G.1.5.

The voltage level at the faulted DEH load terminal is now zero. This is as expected, because the fault impedance is zero. The terminal voltage on DEHBUS2, is however stable at 20.76 kV which is the same as for normal operation. Due to the increased value of the current to the DEH system, the voltage drop from BUS3 to DEHBUS1 is larger than for normal operation.

The degree of unsymmetry in the Scott–T transformer is presented in Figure 5.12. The relation $|\frac{I_-}{I_+}|$ is now 67.3% for the current in the Scott–T transformer.

The degree of unsymmetry at the grid connection and in the 100 km subsea cable is shown in Figure 5.13.

The relationship $|\frac{I_-}{I_+}|$ is only 3% in the subsea cable, but as much as 86.7% at the grid connection. This is far beyond the limit for maximum negative sequence component. The

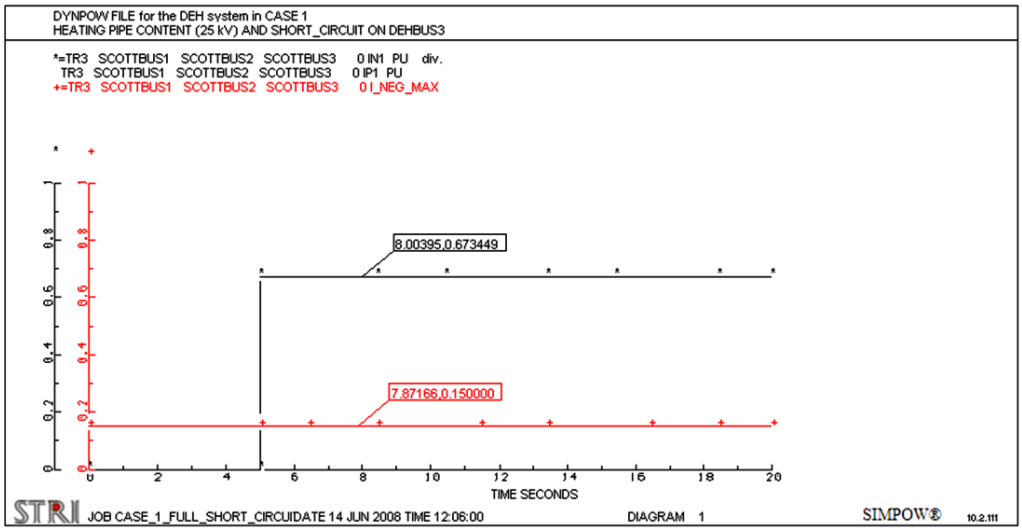

Figure 5.12: Degree of unsymmetry in the Scott–T transformer after the short–circuit on DEHBUS3

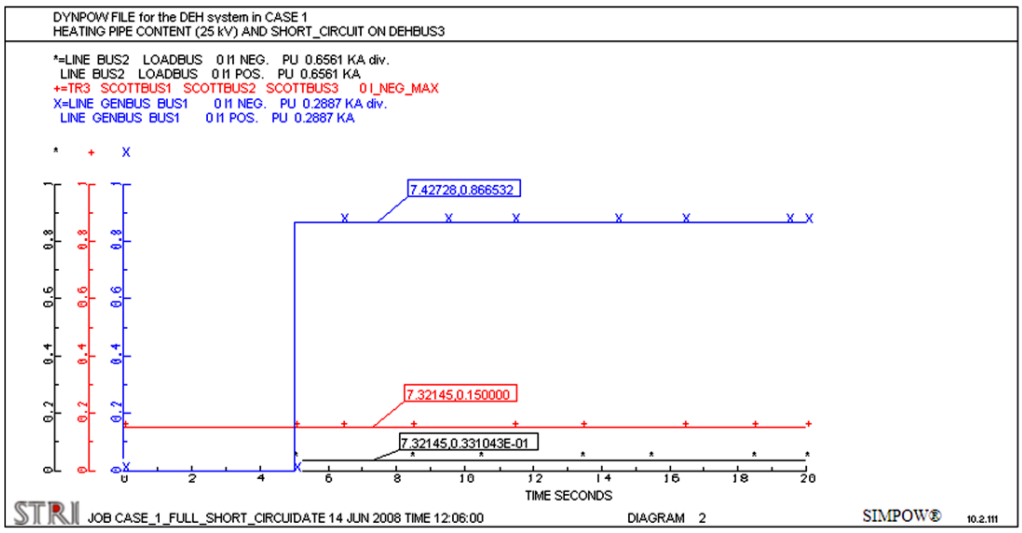

Figure 5.13: Degree of unsymmetry in the line connected to the grid and in the 100 km subsea cable after the short–circuit on DEHBUS3

large unsymmetry in the the line between the grid and BUS1 is most likely due to the large power delivered to the fault. During the fault, the reactive power delivered to the system increases from 10.6 Mvar to 131.9 Mvar, but the active power is only increased from 75.2 MW to 87.1 MW. This means that it is the reactive power that most likely contributes to the large unsymmetry and negative sequence component of the current. See, Figure G.5 in the appendix.

The value for the degree of unsymmetry is larger for the full short–circuit than for the short–circuit in the middle of the pipe section. This is natural seeing that the impedances are very different for the two situations. For the fault in the middle of the pipe section, the total impedance is the series connection of the transformers short–circuit impedance and the halve of the pipe section impedance. During the full short–circuit at DEHBUS3, the fault impedance is only represented by the short–circuit impedance of the Scott–T transformer.

Disconnecting one DEH section

The pipeline connected to DEHBUS3 is disconnected after 5 seconds by using the Dynpow file in Appendix F.1.6. The total simulation is run for 20 seconds. The load flow result is given in Appendix G.1.6.

The voltage level is now increased for load terminal DEHBUS3, but is the same for DEHBUS2. The voltage is increased in the rest of the system. Disconnection of one pipe section reduces the current, which reduces the voltage drops in the system. This makes the voltage levels increase. Looking at the reactive power, it is evident that the production source is consuming 36 Mvar after disconnecting the DEH pipe section.

Figure 5.14 shows the degree of unsymmetry in the Scott–T transformer when the pipe section at DEHBUS3 is disconnected.

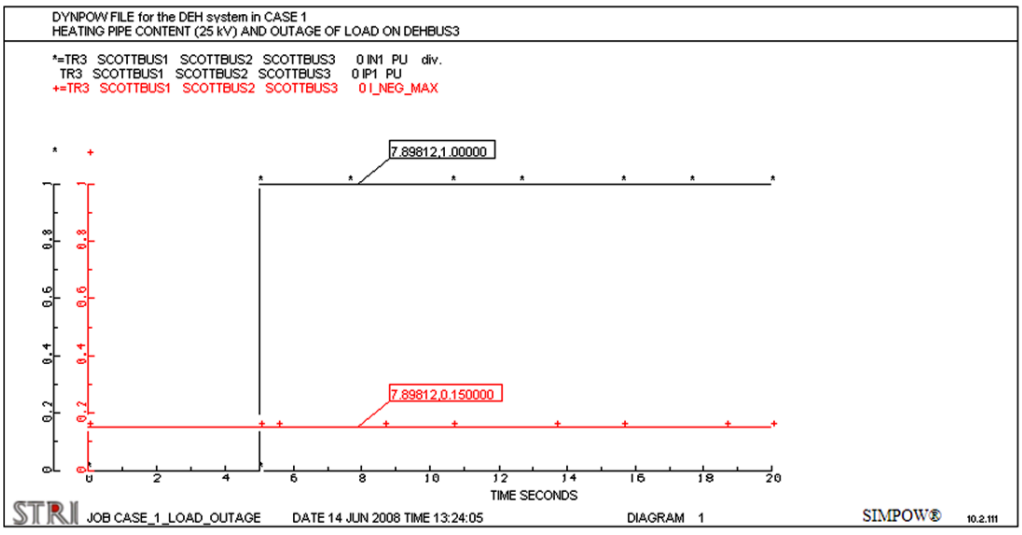

Figure 5.14: Degree of unsymmetry in the Scott–T when the pipeline at DEHBUS3 is disconnected

The diagram shows that the relationship between the negative and positive sequence component of the current is 1 when the Scott–T transformer is loaded only on one load

terminal. This means that the negative sequence component of the current is equal to the positive sequence component of the current.

The relationship $|\frac{I_-}{I_+}|$ for the current in the line between the production source and BUS1 and in the subsea cable is given in Figure 5.15.

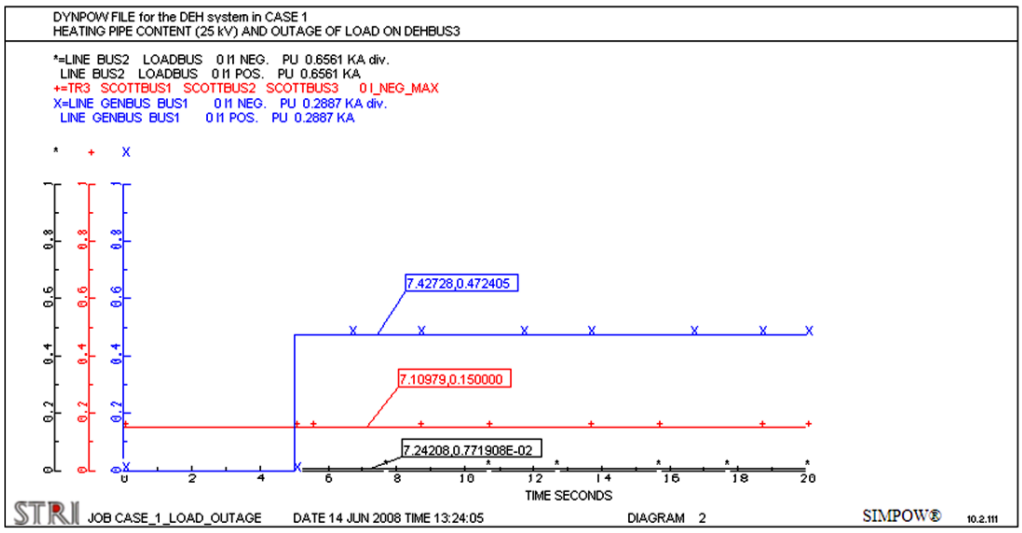

Figure 5.15: Degree of unsymmetry on the grid side and in the 100 km subsea cable when the pipeline at DEHBUS3 is disconnected

The degree of unsymmetry for the grid side is now 47.2% and 0.8% for the 100 km cable. The value for $\frac{I_-}{I_+}$ is still higher than the maximum limit, but is lower than during the short–circuit on the load terminal (86.7%). This can be explained by looking at the power flow. A short–circuit leads to more delivered power to the fault, than for a normal load situation. Seeing that the power to the faulted DEH system is higher than for the situation of disconnecting the load, the current is also higher. This makes the negative sequence component larger which results in a higher relation between $|\frac{I_-}{I_-}|$ as well.

5.2.5 Improving the system for Case 1

The simulations in the previous sections show the load flow results for different operational modes. In general, the voltage levels in the system are lower than required. Taking a closer look at the load flow result for the mode where both the subsea load and the DEH system are operating, this can be found, see Figure 5.2. For instance, the voltage level at DEHBUS2 and DEHBUS3 is only 20.76 kV, but should have been 25 kV. This results in a lower current than the required 1500 A for heating the pipe content.

One solution to the low voltage levels, is to increase the voltage at BUS3 where the 50 km subsea cable is connected. By increasing the voltage level, the magnitude of the current becomes lower which results in lower resistive losses in the system. Another solution for the analysis point of view, is to introduce a tap changer on the Scott–T transformer for regulating the voltage level. However, tap changers on a subsea transformer is not a good practical solution, as it requires complex equipment for operating in the harsh conditions at a subsea installation. On the other hand, tap changers can provide the optimal turn ratio for the Scott–T transformer during normal operation of the system in Case 1.

Another solution to the voltage drop across the cable, is to increase the cross section of the cables. Increasing the cross section reduces the resistance which gives a lower cable impedance and voltage drop. However, increasing the cross section has to be compared with other actions when it comes to the economical aspects.

A power system which is sensitive to voltage fluctuations should have an active voltage control which sets the voltage levels in the system according to the load flow. In addition, an advantage when it comes to stability is to ensure voltage control directly at the loads in the system. For Case 1, this means that at voltage control should be installed at the node LOADBUS.

Two improvements are introduced to the system in Case 1 for increasing the voltage levels in the system as well as improving the reactive power flow. Figure 5.2 shows that the DEH voltage levels are low. Tap changers in SIMPOW makes it possible to increase the voltage levels, as well as indicate which turn ratio the Scott–T transformer should have.

Reactive power compensation is done by including a shunt capacitor at the node LOADBUS. This compensates for the reactive power consumed by the load and reduces the transported apparent power in the long cable to the load. In addition, a shunt capacitor increases the voltage a the node, because the losses in the cable are reduced. A shunt capacitor could have been connected to the DEH pipe nodes as well, but the intention is that the pipeline load should consume the reactive power from the cables.

There is however one problem regarding the tap changers. The DSL model for the lossless Scott–T transformer does not include specifications for tap changers. This means that the Optpow calculation and the Dynpow calculation for the improved system do not give the same load flow result when changing the winding configuration. The turn ratio for the DSL model is based on the relationship between the primary nominal voltage and the two secondary nominal voltages, see Equation 5.3.

$$\begin{aligned} TAU_{12} &= \frac{U_{N1}}{U_{N2}} \\ TAU_{13} &= \frac{U_{N1}}{U_{N3}} \end{aligned} \tag{5.3}$$

However, the terminal voltage for the Scott–T's primary winding at SCOTTBUS1 ($(U_{N1}$) is the voltage level that Optpow uses as a base for finding the best turn ratio. After the turn ratio is changed, the two secondary load voltages are also changed. On the other hand, the calculations in Dynpow with the DSL model for the Scott–T, use the turn ratio in Equation 5.3 for calculating the two secondary load voltages. This makes the initial calculation terms different for the Optpow– and Dynpow load flow. In order to include the change in the turn ratio, the primary nominal voltage for the Scott–T transformer (U_{N1}) has to be changed in Optpow.

The difference between the specified value in Optpow for U_{N1} and the value from the load flow, is used as the point of departure for finding the optimized turn ratio for the Scott–T. Simulations show that when the nominal primary voltage U_{N1} is specified to be 66 kV in the Optpow file, the primary voltage in the load flow calculation is only 0.80 of the specified value. By reducing the value for U_{N1} by 80% in Optpow, the turn ratio is changed for the calculations in Dynpow.

The tap changers are specified for both the three–winding transformer and the Scott–T transformer, see the Optpow file in Appendix F.1.7. The shunt capacitor is 20 Mvar which is the reactive power required to the subsea load. The Dynpow file is the same as in Appendix F.1.1.

Figure 5.16 shows the simulation result from Dynpow after the tap changers and shunt capacitor are included. The SLD result is also given in Appendix G.1.7.

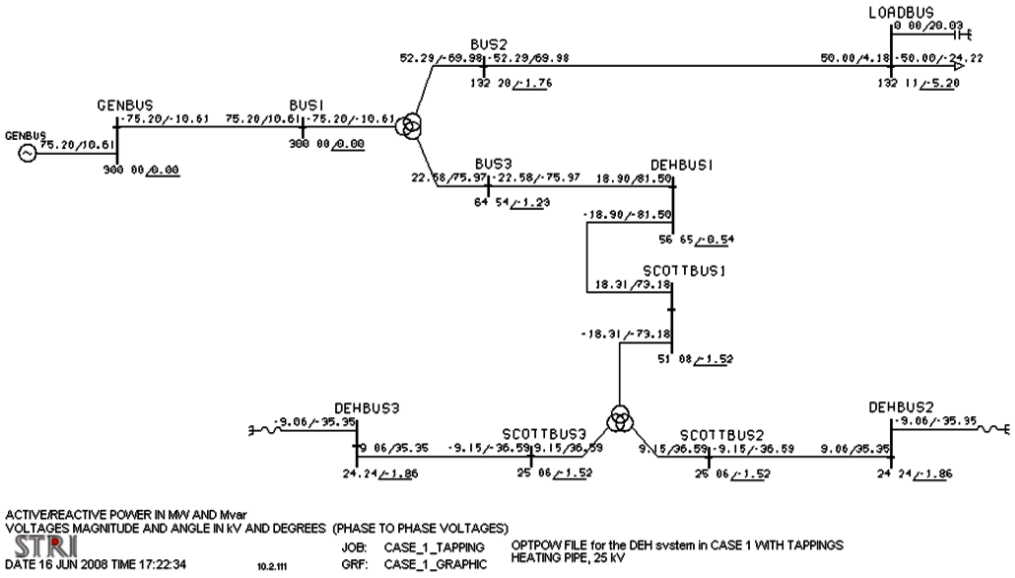

Figure 5.16: SLD result after improving the system in Case 1

The voltages at DEHBUS2 and DEHBUS3 are now 24.24 kV (0.97 pu) which makes the current equal to the required 1500 A. For the system without the improvements, the voltages are only 20.76 kV, see Figure 5.2. The shunt capacitor is specified in Optpow to produce 20 Mvar at LOADBUS. The voltage at the node LOADBUS is now 132 kV (1 pu) and the voltage drop across the 100 km subsea cable is now very low. In addition, due to the increased voltage levels in the system and the reactive power compensation, the swing bus at GENBUS delivers now 10.6 MVAr to the subsea installation. For the load flow in Chapter 5.2.1, it consumed 3.6 MVAr. This means that a compensation of 10.6 MVAr is required on the grid connection side to ensure a power factor of unity. However, increasing the voltage level at the pipe load increases the power. This makes the load current in the 50 km cable also increase which in turn increases the losses in the cable. Contrary to the 100 km cable, the voltage drop across the 50 km subsea cable is now 12.2%, which is a very large value.

The turn ratio for the Scott–T connection is calculated from the expression in Equation 5.4.

$$\begin{aligned} TAU_{12} = TAU_{13} &= \frac{U_{N1} \cdot 0.80}{U_{N2}} \\ TAU_{12} = TAU_{13} &= \frac{66 \cdot 0.80}{25} = 2.1 \end{aligned} \tag{5.4}$$

The turn ratio for the lossless Scott–T transformer is found by using Figure 2.4, see

Equation 5.5. TAU_{12} is the ratio for the "teaser" transformer and TAU_{13} is the ratio for the "main" transformer.

$$\begin{aligned} TAU_{12} &= \frac{\sqrt{3}}{2} \cdot \frac{N1}{N2} \\ TAU_{13} &= \frac{N1}{N3} \end{aligned} \tag{5.5}$$

The value for the turn ratios are then found by setting the value in Equation 5.4 equal to Equation 5.5.

5.3 Case 2

Figure 5.17 shows the single–line diagram for Case 2 in Chapter 4.1.2. The system consists of an onshore power system and an offshore subsea installation. The subsea installation includes a DEH system and a subsea load (compressor, pump etc).

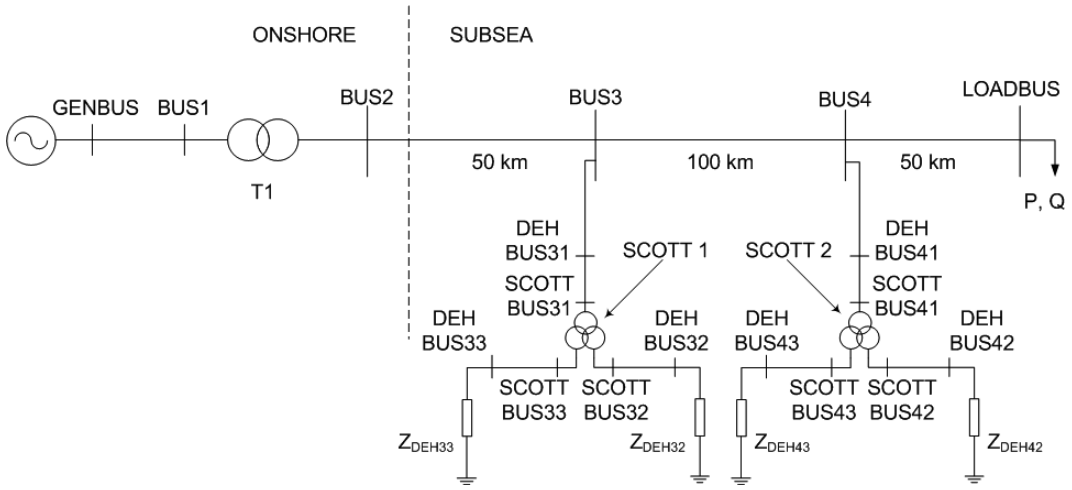

Figure 5.17: Single line diagram for Case 2

The subsea load (50 MW at a power factor of 0.9) connected to the node LOADBUS is located 200 km from the onshore installation. The two nodes BUS3 and BUS4 are branches for connecting the two Scott–T transformers and the DEH system to the power supply. The subsea cable parts between BUS2 and BUS3 are 50 km long, the distance between BUS3 and BUS4 is 100 km and it is 50 km from BUS4 to the subsea load connected to LOADBUS.

The two Scott–T transformers, SCOTT1 and SCOTT2 respectively, are directly connected to BUS3 and BUS4 by two lossless lines. The short–circuit impedances of the transformers are implemented by using lines between the nodes DEHBUS and SCOTTBUS. Transformer T1 is a two–winding transformer which connects the subsea installation and the onshore power system. The voltage level is 300 kV for the onshore power supply, and 132 kV for the subsea installation connected to the secondary side of T1.

In Case 2, the pipeline is 200 km and is sectioned in four parts of 50 km each. The impedance of the pipeline and the piggyback cable is given in Figure 5.17 by the param-

eters Z_{DEH32}, Z_{DEH33}, Z_{DEH42} and Z_{DEH43}. The data for the four pipe sections of 50 km in Case 2 are the same as given for Case 1 in Table 5.1.

The subsea cable used in the simulations, is the 132 kV cable in Table 5.2. The parameters required for the SIMPOW simulations are given in Appendix E.2.

The different modes that are analysed for Case 2 are:

1. Normal load on LOADBUS, and DEH system operating for heating (25 kV)
2. Disconnect load at LOADBUS, keep DEH system heating

In addition, tap changers and a shunt capacitor are implemented to the configuration for improving the load flow.

Two fault scenarios are included in the analysis of Case 2:

i. Short–circuit on DEHBUS42

ii. Only heating on pipe section at DEHBUS33

5.3.1 Normal load, DEH heating

The Optpow– and Dynpow file for Case 2 are based on the parameters in Appendix E.2 and are given in Appendix F.2. The two Scott–T transformers are implemented in the system by using the DSL model for the lossless Scott–T which is given in Appendix C.

The load flow result from Dynpow is presented in Figure 5.18. It is also given in a larger version in the appendix, see Figure G.8.

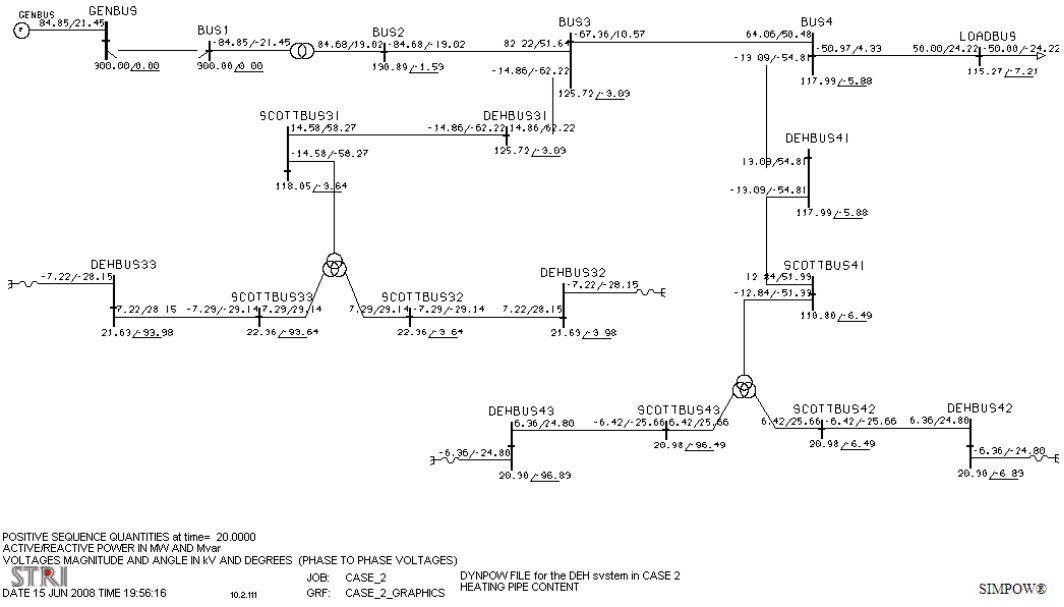

Figure 5.18: Load flow result for Case 2 for normal load and heating the pipe

The values in the figure are the power flow and the node voltage. The "lower" values are the node voltages (phase–to–phase, kV) and the "upper" values are the active– and reactive power (MW, Mvar).

The voltage drop across the total 200 km cable from BUS2 to LOADBUS is considerable for Case 2, see Equation 5.6.

$$U_{200-drop} = \frac{U_{BUS2} - U_{LOADBUS}}{U_{BUS2}} \qquad (5.6)$$
$$U_{200-drop} = 0.119 = 11.9\%$$

In addition, the first 50 km of the cable causes a voltage drop to BUS3. This reduces the primary voltage to SCOTT1 making the secondary terminal load voltages to the pipe sections only 21.63 kV. The terminal voltages for the SCOTT2 are only 20.3 kV. This results in a DEH current that is only 1340 A and 1260 A respectively. This is far lower than the 1500 A required for the mode of heating the pipe content from 4°C to 25°C within 48 hours.

Seeing that the voltage levels are too low for the DEH pipelines, tap changers and a shunt capacitor is implemented in the Optpow file. The same procedure, as shown for Case 1 in Section 5.2.5, is used for finding the most suitable turn ratios for the two Scott–T transformers in Case 2. The simulation for the improved system is given in Section 5.3.2.

Investigations on the degree of unsymmetry for Case 2, shows that the two Scott–T transformers provide balanced electrical power between the two–phase and three–phase system. The degree of unsymmetry is zero when the system is loaded with equal load impedances.

5.3.2 Improving the system for Case 2

The Optpow file for the improved system is based on the file given in Appendix F.2.1. The improvements for Case 2 are done by including tap changers and reactive compensation in the data groups "TRANSFORMERS", "SHUNT IMPEDANCES" and "POWER CONTROL", see Appendix F.2.2. The nominal primary voltage on the SCOTT1 transformer is set to 0.88 of the initial value and 0.82 for the SCOTT2 transformer. The shunt capacitor at LOADBUS is set at 40 Mvar. The value is chosen after simulating with different values.

The load flow result from Dynpow is presented in Figure 5.19 and in Appendix G.2.2.

The node voltages at the DEH pipelines are now almost equal to 25 kV, and provide a load current in the pipe sections of 1500 A. The turn ratio for this load flow, can be found by using the same procedure as explained in Section 5.2.5. The node voltage at LOADBUS is now 117.5 kV, compared to the former 115.3 kV.

Possible improvements are introduced here, but further upgrading is feasible. When it comes to such actions for improving the system, economical issues have to be included. For the system in Figure 5.19 it is possible to increase the node voltage at LOADBUS by increasing the value of the shunt capacitor. In addition, this decreases the reactive power supplied from the grid connection at BUS1. However, the costs for compensating subsea has to be evaluated and compared to the costs for reactive compensation onshore.

Another effort is to change the cross section of the subsea cable either for the total length or in between the nodes. Increasing the cross section reduces the resistance in the cable which gives a lower voltage drop across it. The introduced improvements give an idea

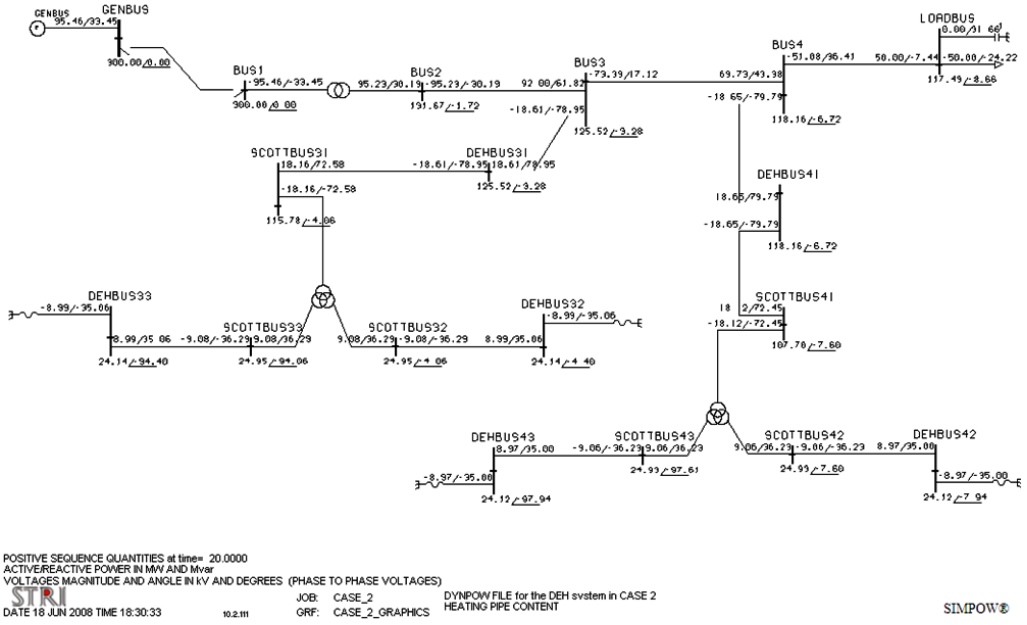

Figure 5.19: Load flow result for the Case 2 with tap changers and reactive compensation

of the possibilities, but is not further addressed. The load flow result in Figure 5.19 is therefore used in the further analysis.

5.3.3 Disconnect the subsea load, DEH heating

If an unexpected incident occurs during operation, the subsea field might have to shut down. The transportation of hydrocarbons in the pipe will then stop flowing and is cooled down. When the production is started again, the content needs to be heated in order to ensure a safe and reliable flow of the multiphase liquid. This mode of operation is now simulated.

The subsea load at LOADBUS is disconnected after 5 seconds by using the Dynpow file in Appendix F.2.3. In addition, the shunt capacitor is disconnected as it is regarded as a compensator for the reactive power consumption at the node. The Optpow file is the same as given for the simulation in Section 5.3.1 with the improvements given in Appendix F.2.2.

Figure 5.20 shows the load flow result from the simulation. See Appendix G.2.3 for a larger figure. The voltage at LOADBUS increases from 118 kV to 125 kV after the subsea load and shunt capacitor are disconnected. This is because there is no loading of the cable which causes a resistive voltage drop in the cable. In addition, the charging current of the cable increases the voltage. The values at the DEH loads are stable for this mode of operation. The pipe voltages are all close to 25 kV which gives the required current of 1500 A for heating the pipe. The reactive power at BUS1 is almost the same as before the disconnection.

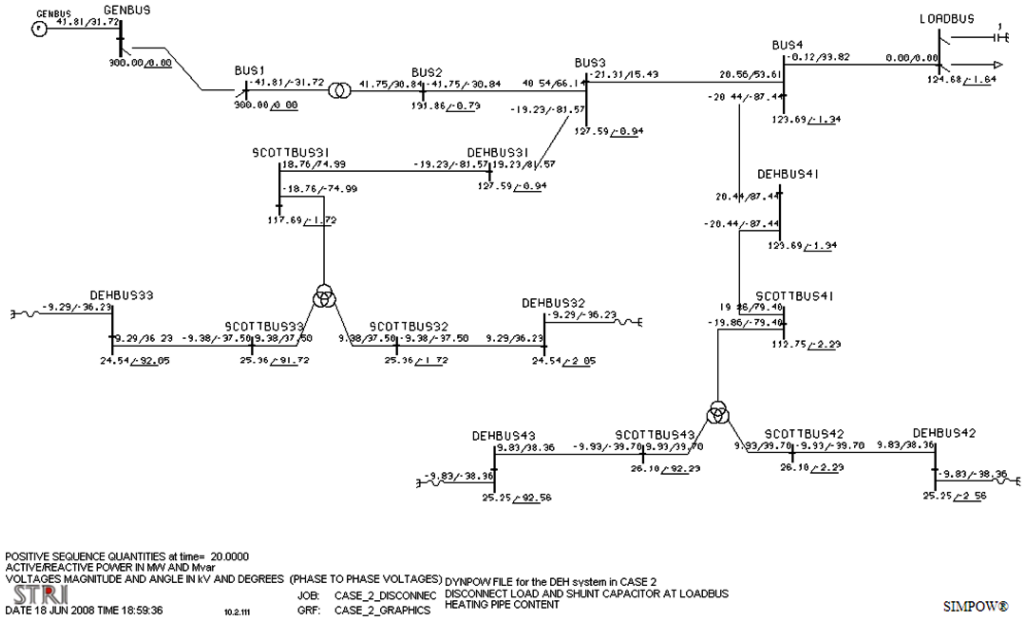

Figure 5.20: Load flow result when the load and shunt capacitor at LOADBUS are disconnected

5.3.4 Fault scenarios

Two different fault scenarios are analysed for Case 2. As explained earlier, a fault on the pipeline or in close proximity, can change the load impedance of the Scott–T transformers and result in unsymmetrical condition. The degree of unsymmetry is especially analysed at BUS1 and LOADBUS because these two nodes are connected to the grid and the subsea load.

A short–circuit is first connected to DEHBUS42. The degree of unsymmetry is investigated. However, a short–circuit is normally disconnected immediately as the large current causes thermal heating above the limits which damages the system components, but for a DEH system the fault current can be too small to detect for the protection and breakers. It is therefore analysed in the following. In addition, heating of only the pipe section at node DEHBUS33 is paid attention to.

Short–circuit at DEHBUS42

A short–circuit is connected to the node DEHBUS42 by using the Dynpow file give in Appendix F.2.4. The load flow result is given in Figure 5.21 and Appendix G.2.4.

The voltages along the 200 km subsea cable drop considerably after the short–circuit which is expected. The power supplied by the production source increases after the fault. However, the voltages at the DEH pipe sections do not follow the same pattern. The voltage at the pipe section next to the fault, DEHBUS43, is the same as before, but the load voltages at SCOTT1 are not equal to each other. The voltage level at DEHBUS33 is 24 kV, but the voltage at DEHBUS32 is only 19 kV. The reason for this is found by examining the phase currents in the system.

Figure 5.22 shows the phase currents for the lossless line between DEHBUS31 and BUS3.

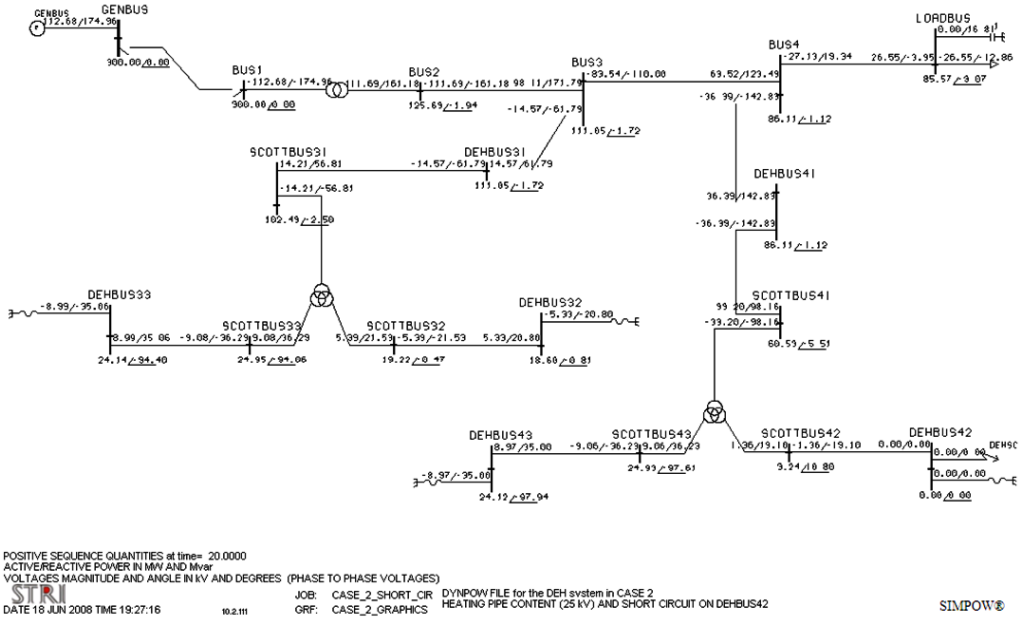

Figure 5.21: Load flow result after a short–circuit at DEHBUS42

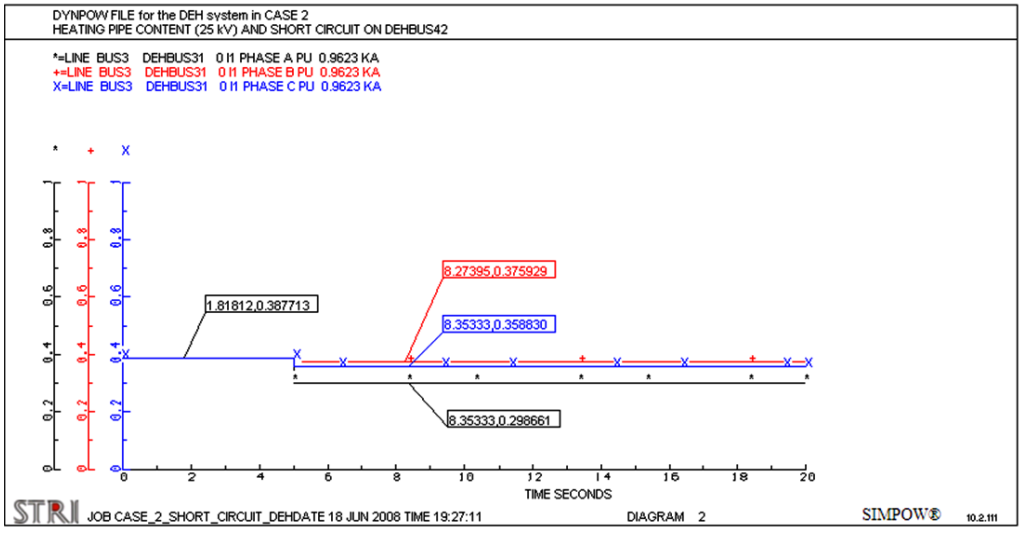

Figure 5.22: Phase currents in the three–phase connection between SCOTT1 and the subsea cable

This is the three–phase connection for the DEH-system at SCOTT1 to the subsea cable. The diagram shows that the phase currents are equal and symmetrical before the fault, but after the short–circuit they become different which points out the unsymmetrical conditions. In [6], it is stated that the Scott–T transformer provides balances electrical power between a three–phase and two–phase system and vice versa, but the right conditions have to be met. The short–circuit at DEHBUS42 gives unsymmetrical phase currents in the three–phase network. This means that the two–phase side on SCOTT1 does not become equal and 90 degrees out of phase. The two load voltages on SCOTT1 are in this mode 24 kV and 19 kV respectively. In addition, the phase angels are 94 degrees out of phase. This is due to the unsymmetrical conditions in the three–phase network.

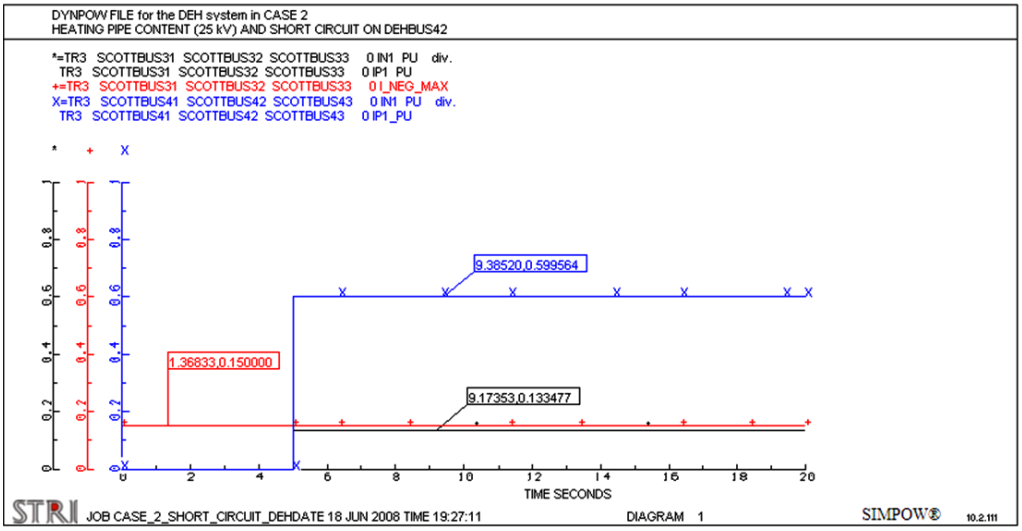

Figure 5.23: Degree of unsymmetry in the two Scott–T transformers after short–circuit at DEHBUS42

The degree of unsymmetry for the faulted SCOTT2 and the other Scott–T transformer is presented in Figure 5.23. The blue curve shows the degree of unsymmetry for the faulted SCOTT2 transformer. The red line is the limit for maximum negative sequence current and the black curve is the degree of unsymmetry for the other Scott–T transformer. The boxes give the coordinates of the points. The x–axis is the time in seconds and the y–axis is the degree of unsymmetry in per unit.

The value for the relation $|\frac{I_-}{I_+}|$ in SCOTT2 is 60% and 13% for SCOTT1. This shows that the fault causes unsymmetrical conditions both in the three–phase network, and in the two–phase side for the Scott–T transformer which is connected to the system.

The degree of unsymmetry in the line between BUS1 and GENBUS on the grid side and in the subsea cable between BUS4 and LOADBUS are shown in Figure 5.24. The blue graph is the degree of unsymmetry in the line connected to the grid, the black line is for the cable part between BUS4 and LOADBUS and the red straight line is the limit for the maximum allowed continuous negative sequence current. $|\frac{I_-}{I_+}|$ is 68.5% for the line at the production source and 38.9% for the cable to the subsea load.

For this fault, the degree of unsymmetry is quite large in the subsea cable connected to LOADBUS. This is most likely because the short–circuit at DEHBUS42 causes a huge

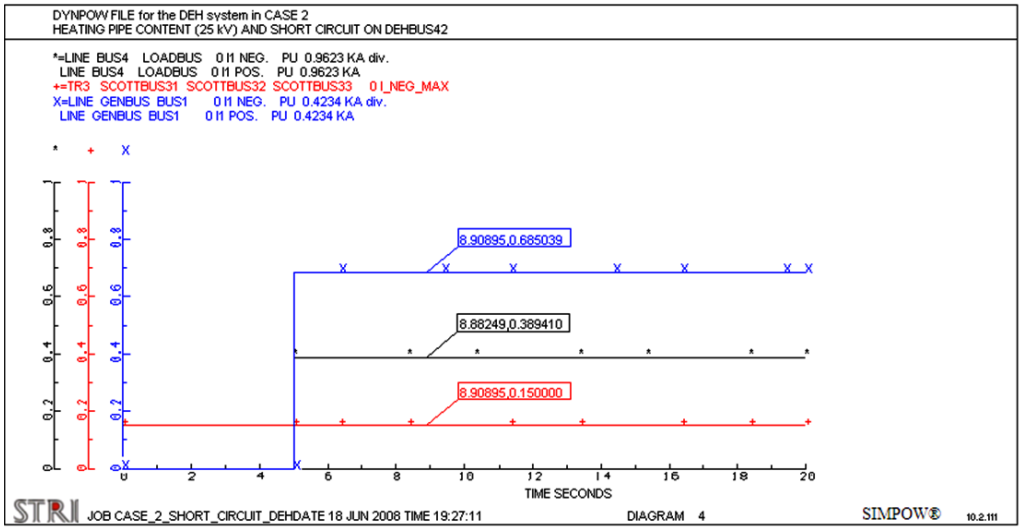

Figure 5.24: Degree of unsymmetry in the line to BUS1 and in the cable connected to the subsea load after the short–circuit at DEHBUS42

power flow to node BUS4. This results in a large contribution of negative sequence components to BUS4.

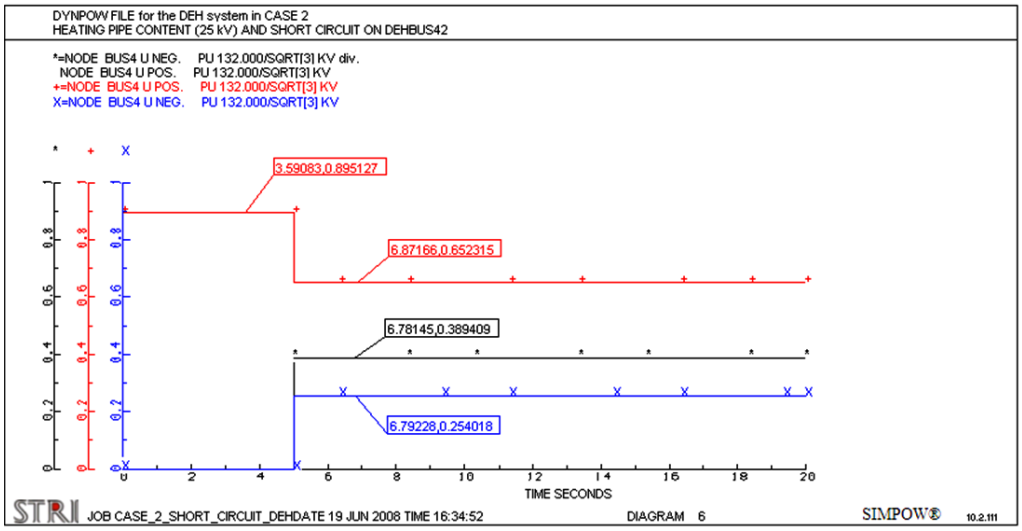

Figure 5.25: Voltages and voltage relationship at BUS4

Figure 5.25 shows the voltage relationship at BUS4. The red curve shows the change in per unit value of the positive sequence component for the node voltage after the short–circuit at DEHBUS42. The blue curve gives the negative sequence component of the node voltage in per unit and the black curve gives the relationship $|\frac{U_-}{U_+}|$. Note that the positive sequence drops after the fault, but the negative sequence of the voltage increases resulting in a degree of unsymmetry in the voltage of 39% which is the same as for the current in the cable to LOADBUS.

Loadshedding, only heating at DEHBUS33

For a certain period of time, it might be practical to only heat the last section of the 200 km pipeline. This mode of DEH operation can be applicable for early stages in the production and transportation of the multiphase liquid when the temperature of the oil and gas in the well is higher than the critical point of hydration. When the fluid enters the pipeline its temperature is high, but decreases as it is transported through the pipeline. If the thermal insulation of the pipe is not sufficient for preserving the heat, DEH is necessary, but maybe only for the last 50 km.

The Dynpow file in Appendix F.2.5 disconnects the three pipe sections at the nodes DEHBUS42, DEHBUS43 and DEHBUS32. The pipe section at DEHBUS33 is the only pipe connected for heating. Figure 5.26 shows the load flow result for this mode. The result is also given in Appendix G.2.5.

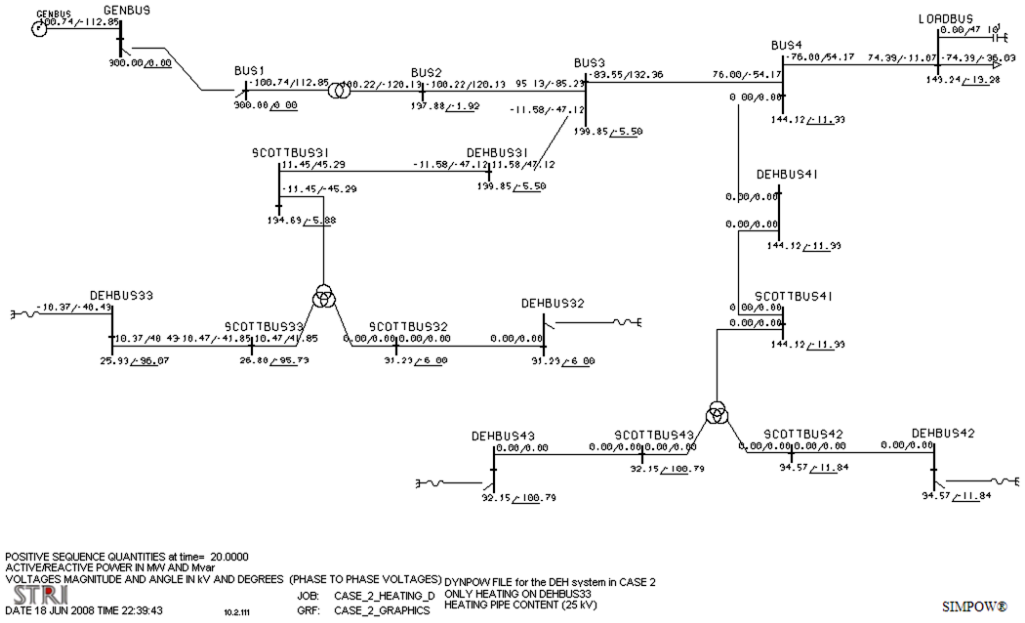

Figure 5.26: Load flow result when only the pipe section at DEHBUS33 is heated

The disconnection of the three DEH pipe sections results in a voltage increase in the system. The voltage at LOADBUS is now as much as 143 kV which is an increase of 8.3% compared to the nominal value of 132 kV. Due to the disconnection of the three pipe sections, a surplus of reactive power is present in the network. The cable is now almost unloaded and generates 113 Mvar into the grid connection at BUS1. The terminal voltages on the two Scott–T transformers are also increased, but they are not equal in magnitude. This is because the three–phase subsea system is not symmetrical.

The degree of unsymmetry for this situation is shown in Figure 5.27. Seeing that the SCOTT2 transformer is unloaded, the degree of unsymmetry is zero which the black line in the figure shows. The blue curve shows that the relation $|\frac{I_-}{I_+}|$ in SCOTT1 changes from 0 to 1 after the disconnection.

Figure 5.28 shows that the value for unsymmetry is 32% in the line connected to the grid. The black curve shows that the relationship $|\frac{I_-}{I_+}|$ is 3.6% for the current in the subsea

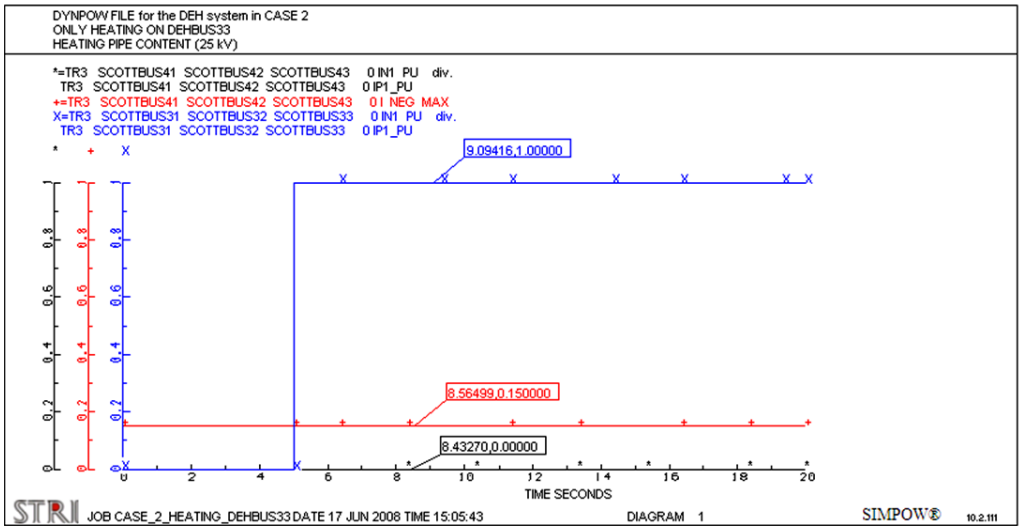

Figure 5.27: Degree of unsymmety in the two Scott–T transformers when only the section at DEHBUS33 is heated

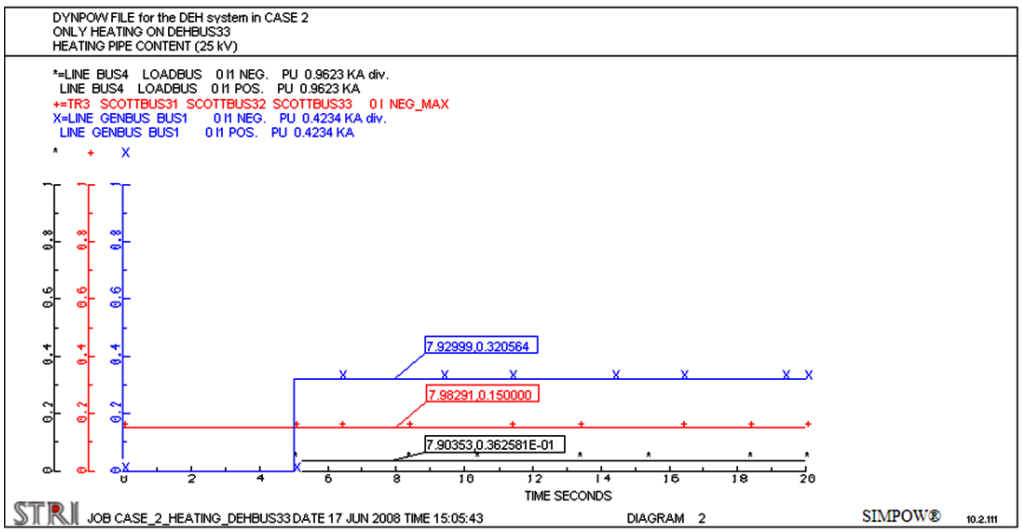

Figure 5.28: Degree of unsymmetry on the grid connection side and to the subsea load when only the pipe section at DEHBUS33 is heated

cable between BUS4 and LOADBUS.

As explained earlier the phase currents are different in magnitude and angle when the power system is unsymmetrical.

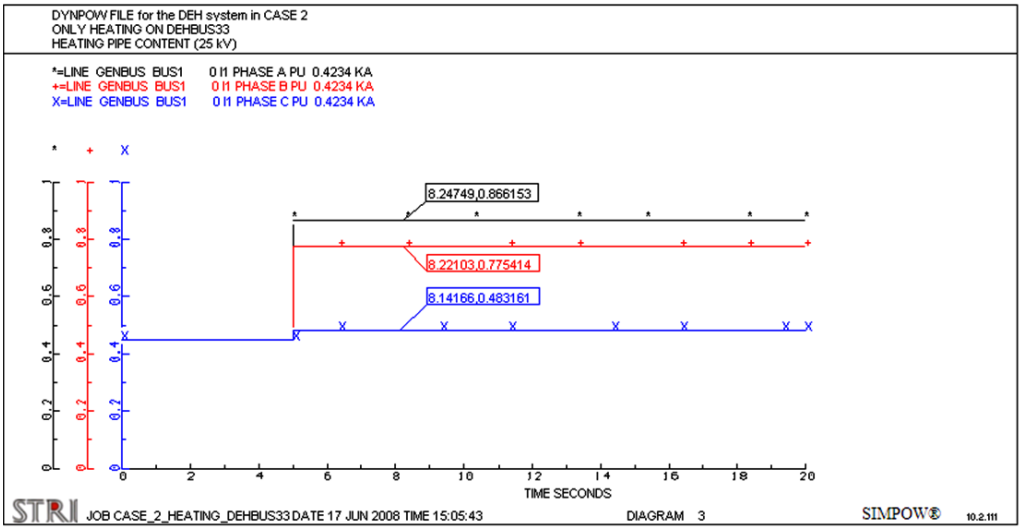

Figure 5.29: The phase currents in the line connected to the grid and BUS1 when only the pipe section at DEHBUS33 is heated

The three curves in Figure 5.29 show the change in the phase current in the line between GENBUS and BUS1 after the system is unsymmetrical. The black curve is the current i phase A, the red curve is for phase B and the blue curve shows the change in phase C. The values are given in per unit. Note that the phase currents are different from each other after the three pipe sections are disconnected. This is typical for an unsymmetrical system.

5.4 Summary of results

The objective of the simulations is to analyse the behavior of the DEH system configurations when the Scott–T transformer is implemented. The simulations carried out for Case 1 and Case 2 introduces some possible basic operation modes for the DEH system in addition to fault scenarios that may occur. The analysis is limited to the investigation of the voltage levels, reactive power and degree of unsymmetry, but it does show the characteristics of the power system. The most important observations from the simulations are given in this section.

Case 1

Table 5.3 summaries the results from the analysis of the different operational modes for Case 1. The two values in the column "DEHBUS voltage" indicate the voltages at DEHBUS3 and DEHBUS2 respectively. The values in the column "Q_{BUS1}" represent either the amount of excessive reactive power in the subsea system (positive value Q) or the required reactive power to the subsea system (negative Q).

Table 5.3: Summary of the analysis for Case 1

Operation mode	**LOADBUS voltage [kV]**	**DEHBUS voltage [kV]**	Q_{BUS1} **[Mvar]**	$\lvert\frac{I_-}{I_+}\rvert$ **Scott [%]**	$\lvert\frac{I_-}{I_+}\rvert$ **BUS1 [%]**	$\lvert\frac{I_-}{I_+}\rvert$ **LOAD-BUS [%]**
Normal load	131.1	20.8 - 20.8	3.6			
Disconnect subsea load	139.9	20.9 - 20.9	34.9			
Disconnect 100 km cable	0	20.5 - 20.5	-44.6			
Short–circuit in the middle of the pipe	130.5	17.4 - 20.8	-18.4	25	30	0.5
Short–circuit at DEHBUS3	127.0	0 - 20.8	-131.9	67	87	3.3
Disconnect pipe section at DEHBUS3	132.1	25.8 - 20.8	36.2	100	47	0.8
Improved system	132.1	24.2 - 24.2	-10.6			

The voltages for the configuration in Case 1 are initially too low for heating the pipe content. Tap changers and reactive power compensation are necessary to increase the voltage in the system.

The system simulations show that the pipeline consumes the reactive power produced by the subsea cables. By consuming the reactive power from the cables, the critical cable length can be increased. However, for certain modes, there is a lack of reactive power which has to be compensated by the swing bus connected to BUS1. This is particularly significant when the 100 km subsea cable is disconnected at BUS2. The required reactive power from the production source to the DEH system is then 45 Mvar. The fault scenarios do require more Q, but are considered to be disconnected when it occurs. Another remark is that BUS1 consumes almost the same amount of Q when the subsea load at LOADBUS is disconnected as it consumes when the pipe section at DEHBUS3 is disconnected.

The fault scenarios that are analysed show that a short–circuit in the middle of the pipeline and at the load terminal give a large degree of unsymmetry in the rest of the network. A short–circuit in the middle of the pipeline results in 30% unsymmetry in the three–phase power supply at the grid connection (BUS1). When disconnecting one of the pipe sections connected to the Scott–T transformer, there is also a large degree of unsymmetry (47%), which is above the limit for maximum allowed continuous negative current (15%). Looking at the node LOADBUS, the short–circuit at DEHBUS3 is the only fault that results in a degree of unsymmetry which may have conseqeunces.

Case 2

Table 5.4 presents the most important observations and results from the simulations of Case 2. The column "DEHBUS 100 [kV]" is the voltage level for the first 100 km pipeline (DEHBUS33 and DEHBUS32), and the column "DEHBUS 200 [kV]" is the voltage level for the last two pipe sections (DEHBUS43 and DEHBUS42).

Table 5.4: Summary of the analysis results for Case 2

Operation mode	**LOADBUS voltage [kV]**	**DEHBUS 100 voltage [kV]**	**DEHBUS 200 voltage [kV]**	Q_{BUS1} **[Mvar]**	$\frac{I_-}{I_+}$ **Scott [%]**	$\frac{I_-}{I_+}$ **BUS1 [%]**	$\frac{I_-}{I_+}$ **LOADBUS [%]**
Normal load	115.3	21.6 - 21.6	20.3 - 20.3	-21.5			
Improved system	117.5	24.1 - 24.1	24.1 - 24.1	-33.5			
Disconnect subsea load	124.7	24.5 - 24.5	25.3 - 25.3	-31.7			
Short–circut at DEHBUS42	85.6	24.1 - 18.6	24.1 - 0	-175.0	13 - 60	69	38.9
Heating only at DEHBUS33	143.2	25.9 - 31.2	32.2 - 34.6	112.9	100 - 0	32	3.6

The voltage levels for Case 2 are improved after introducing tap changers on the transformers in addition to reactive compensation at the subsea load. However, the voltage at LOADBUS increases to 143.2 kV when the there is only heating on one pipe section, DEHBUS33. This is 8.5% higher than the nominal value of 132 kV.

When it comes to the reactive power flow, Table 5.4 clearly indicates that the power system in Case 2 always requires reactive power compensation. For the operation of the improved system, the power factor at BUS1 is 0.945 (leading). When only the pipe section at DEHBUS33 is heated, the power factor changes considerably to 0.67 (lagging).

The voltage levels of the four pipe sections show that a short–circuit at DEHBUS42 causes negative sequence components of the current in the system. An interesting observation is that when the fault is on SCOTT2 transformer, the three–phase system becomes unsymmetrical. This causes unbalanced voltages at SCOTT1 as well. For the subsea cable connected to the LOADBUS, the degree of unsymmetry is largest when there is a short–circuit at DEHBUS42. It is then 38.9% which is far above the limit of 15%.

Chapter 6

Discussion

The DSL model and SIMPOW

The specially connected Scott–T transformer, is modelled by the use of Dynamic Simulation Language. The model is based on mathematical expressions which give the relationship for the currents and voltages in the Scott–T transformer. However, simplifications are introduced in the analysis for describing the transformer. The resistance and leakage reactance of the transformer are disregarded as well as the saturation of the cores. In addition, the magnetizing current is neglected. Based on these simplifications, the load voltages of the transformer are determined based on a no–load condition. The introduced simplifications introduce a degree of uncertainty, but the model does give the typical behavior of the Scott–T transformer. This is shown during the verification process of the lossless Scott–T transformer in Appendix C.1.1. The simulations on the lossless DSL model for Scott–T in SIMPOW give the same results for unbalanced loading as the results obtained in MATLAB.

The Scott–T transformer is implemented in SIMPOW by using Dynpow. This requires first a load flow calculation from Optpow to give the initial steady state of the power system. For the system simulations, the short circuit impedance of the transformer is represented by an impedance. This is not optimal, but does give an internal voltage drop in the transformer. The hand calculations in Chapter 3.4 shows that SIMPOW gives correct results for the Scott–T transformer when the losses are included.

The use of tap changers for the Scott–T is not optimal. Seeing that the DSL model does not include tap changing in Dynpow, the turn ratio for the Scott–T transformer is adapted by changing the ratio for the primary– and secondary nominal voltage ($\frac{U_{Np}}{U_{Ns}}$) in Optpow. This renders it impossible to change the turn ratio for the fault situations according to the given load flow. This weakens the result, but is a satisfactory adjustment on an analysis point of view.

Simulation results for Case 1 and Case 2

Case 1 and Case 2 are based on two DEH configurations that are established during discussions with the supervisors, but they are not the only configurations that can show to be suitable for subsea DEH systems. Economical issues are ignored in the analysis, as this is considered to be too detailed for a base study.

The input data that is used to describe the DEH pipeline and the system requirements are based on available information and typical data for a 40 km pipeline. The values are scaled up in order to be appropriate for the configurations in Case 1 and Case 2 which

have pipe sections of 50 km. The scaling of the data does give useful values, but closer analysis and research has to be carried out on the exact conditions for Case 1 and Case 2. The values used do not for instance consider the environmental conditions, for instance trenched pipeline, sea temperature etc, that applies for a 100 km or 200 km DEH system, nor the hydrate control philosophy for the condensate pipeline.

The electrical components such as the power supply onshore, the subsea cables and the subsea load are also specified by using typical values. The subsea cables in particular may prove to be unsuitable for an installation. The power supply is specified to be a swing bus, which is more or less impossible to install for practical use. However, the use of a swing bus does give a good base for the analysis, as the power flow for any operational mode is supplied. In addition, the subsea load at the far end of the cable is specified to be a passive load (50 MW, cosfi = 0.9) and does not contribute to a short–circuit or dynamical disturbances. This means that it does also not contribute to the negative sequence component in the power system. This is because there is no rotating magnetic field in the passive subsea load which can produces negative sequence components.

The simulations that are presented only consider the configurations for Case 1 and Case 2 with the given parameters and input data. The simulations modes specified give an indication for what to expect when implementing a Scott–T transformer in a DEH system, and especially what to expect for the worst case scenarios. However, the parameters for the components in the system affect the simulation results and must be specified for all individual cases.

The analysis of unsymmetrical variations is based on the ratio between the magnitude of the negative and the positive sequence component of the three–phase current. This is a suitable criteria for the degree of unsymmetry, which is explained in Chapter 2.4. The values obtained are valuable for understanding the principals of the Scott–T transformer, and indicate reliable results compared to the analysis in MATLAB as well as the theory.

Chapter 7

Conclusion

The DSL model and SIMPOW

The simulations in SIMPOW show that the DSL model for the Scott–T transformer give correct and reliable results for analysing the degree of unsymmetry in the transformer. The SIMPOW simulations in Chapter 3.3 give the same results as the MATLAB calculations obtained in the Specialisation Project. The simulations in SIMPOW on the Scott–T DSL model, show that the degree of unsymmetry is zero when the two load impedances of the transformer are equal. When the load impedance of one pipe is varied, the simulation proves that it can vary between 0.75 to 1.34 per unit of the other pipe impedance. The Scott–T transformer still provides electrical power between the two systems below the 15% limit for the degree of unsymmetry.

Simulation results for Case 1 and Case 2

The simulations carried out for Case 1 and Case 2 introduce two possible configurations for a DEH system with a subsea power supply. For normal operation of the subsea load and heating the pipe content, the results prove that tap changers are necessary to keep the Scott–T transformers secondary terminal voltage at 25 kV. This meets the requirement (1500 A) in both cases for heating the pipe content from 4°C to 25°C within 48 hours after a shutdown of the process.

The reactive power flow in Case 1 shows that the DEH system uses the produced reactive power from the two subsea cables. However, all system simulations indicates that reactive power compensation has to be included in order to have a power factor of unity at the grid connection (BUS1). If it is assumed that a short–circuit is removed instantaneously after the fault occurs, the most demanding situation for the reactive compensation is when one of the pipe sections are disconnected. Then, for the specified power system, there is a surplus of 36 Mvar at BUS1.

The degree of unsymmetry for Case 1 is zero for the operation of a normal subsea load (50 MW, cosfi=0.9) and heating of the pipe. This means that the Scott–T transformer provides balanced electrical power between the two–phase DEH system and the three–phase power supply. However, if a short–circuit occurs in the middle of a the pipeline, the ratio $|\frac{I_-}{I_+}|$ at the grid connection (BUS1) becomes greater than the limit of 15%. This applies also when one of the pipe sections are disconnected. The degree of unsymmetry is then of 100% in the Scott–T transformer and 47% at the grid connection.

The relationship $|\frac{I_-}{I_+}|$ is only of 3.3% in the subsea cable when there is a short–circuit at DEHBUS3, but as much as 87% at the grid connection. This is far beyond the limit

for maximum negative sequence component. The significant unsymmetry in the the line between the grid and BUS1 is most likely due to the large power delivered to the fault. During the fault, the reactive power delivered to the system increases from 10.6 Mvar to 131.9 Mvar, but the active power increases only from 75.2 MW to 87.1 MW. This means that it is most likely the reactive power that contributes to the consequent unsymmetry and negative sequence component of the current.

The simulation results from Case 2 show that the DEH system uses the reactive power from the cables, but requires additional compensation. When a shunt capacitor of 32 Mvar is installed next to the subsea load, the system simulation in Figure 5.19 shows that the there is a deficit of 34 Mvar in the subsea system seen from BUS1. On the contrary, when only the pipe section at DEHBUS33 is heated, there is a surplus of 113 Mvar in the system. This changes the power factor for the two situations at BUS1 from 0.944 (leading) to 0.67 (lagging) respectively.

Investigations on the degree of unsymmetry prove that the ratio $|\frac{I_-}{I_+}|$ is zero for Case 2 when the subsea load is running in normal conditions (50 MW, cosfi=0.9) and the DEH system is heating the pipe content.

An interesting result is obtained for the short–circuit at the load terminal DEHBUS42 for SCOTT2. Figure 5.22 shows that the phase currents in the three–phase subsea cable are symmetrical before the fault, but after the short–circuit they become different. This indicates unsymmetrical conditions. In [6], it is stated that the Scott–T transformer provides balanced electrical power between a three–phase and two–phase system and vice versa, but the right conditions have to be met. The short–circuit at DEHBUS42 gives unsymmetrical phase currents in the three–phase network. This results in an unbalanced two–phase side on SCOTT1. The load voltages are not equal in magnitude and dephased of 90 degrees, but are 24 kV and 19 kV respectively and dephased of 94 degrees. This is due to the unsymmetrical conditions in the three–phase network.

The simulations conclude that the Scott–T transformer provides symmetrical conditions for both configurations when the two load impedances are equal. However, Case 2 shows an important result when installing two Scott–T transformers in the same system. Unbalanced loading of one of the specially connected transformers gives unsymmetrical conditions in the three–phase system which results in unbalanced load voltages for the other Scott–T transformer.

The analysis is limited to the configurations given for Case 1 and Case 2, but shows typical results when an alternative transformer connection is implemented in a DEH system.

Further work

Further simulations and analysis is required for verifying the operational characteristics of a DEH system with the Scott–T transformer.

The DSL model for SIMPOW should be further developed to include tap changers and the short–circuit impedance of the Scott–T. To prevent the Optpow–Dynpow combination for including the Scott–T transformer, the transformer should be modelled and available in the SIMPOW library for the Optpow module.

Considering the input data and parameters, the dimensioning of the power supply and the Scott–T transformer should take into account all the DEH system uncertainties. In particular, the variations of the pipeline impedance and the variation of the electrical and magnetic parameters of the carbon steel should be evaluated. In addition, it may be necessary to include other parameters in SIMPOW to increase the reliability of the results. That is, specifying the subsea cables, subsea load and the production source according the the electrical components available in the market.

The operational modes that are analysed, are meant to show the limitations and restrictions for Case 1 and Case 2. Further analysis should include operational modes closer to normal operation, and especially investigate the results for possible variations in the pipeline impedance.

The alternative DEH configuration for Case 2 should also be investigated further and compared with the results obtained for the configuration analysed. In addition, the Le Blanc transformer introduced in Chapter 2.3 may, due to its winding connection, give both technical and economical advantages. This requires both electro technical– as well as economical analysis.

Bibliography

[1] Harald Kulbotten and Jens Kristian Lervik. Direct Electrical Heating System for Preventing Wax and Hydrates in Pipelines. *Project Memo*, October 2007.

[2] Ole-Johan Bjerknes. Proposal for student task, project master or thesis (Draft for comments), 2007.

[3] Thor Henriksen. DEH Power Supply – Transformer Couplings. Technical report, SINTEF Energy Research AS, 2007.

[4] Frode K. Novik. Subsea Power Supply and Electrical Heating of Pipelines. Technical report, NTNU, 2007.

[5] Nysveen, Kulbotten, Lervik, Børnes, Høyer-Hansen, and Bremnes. Direct Electrical Heating of Subsea Pipelines. Technology Development and Operating Experience. *IEEE transaction on industry applications*, 2007.

[6] A. C. Franklin and D. P. Franklin. *The J&P Transformer Book*. Butterworth & Co. Ltd., 11 edition, 1983.

[7] Brush Electrical Machines LTD. Permissible duration of negative sequence current. Diagram.

[8] Discourses with Senior Scientist Thor Henriksen, SINTEF Energy Research, January 2008.

[9] Simpow. Website, 16.04.2008. `http://www.stri.se/metadot/index.pl?id=2221&isa=Category&op=show`.

[10] STRI AB. *SIMPOW, User Manual (Beta release)*, 2004.

[11] Stephen J. Chapman. *ELECTRIC MACHINERY and POWER SYSTEM, FUNDAMENTALS*. McGraw–Hill, 2002.

[12] Professor Arne Nysveen. TET4195 High voltage equipment, Power Transformer. Compendium, Spring 2007.

[13] Discourses with Professor Nysveen (NTNU), 2008.

[14] Discourses with Atle H. Børnes, StatoilHydro, April 2008.

[15] Discourses with ProfessorNysveen (NTNU) and Bjerknes (Aker Solutions), February 2008.

[16] Cable document supplied by Aker Solutions. E–mail, 2008.

[17] Hadi Saadat. *Power system analysis*. McGraw–Hill, 2 edition, 2004.

Appendices

Appendix A

Permissible duration of I_2

Figure A.1 shows the permissible duration of negative sequence current [7].

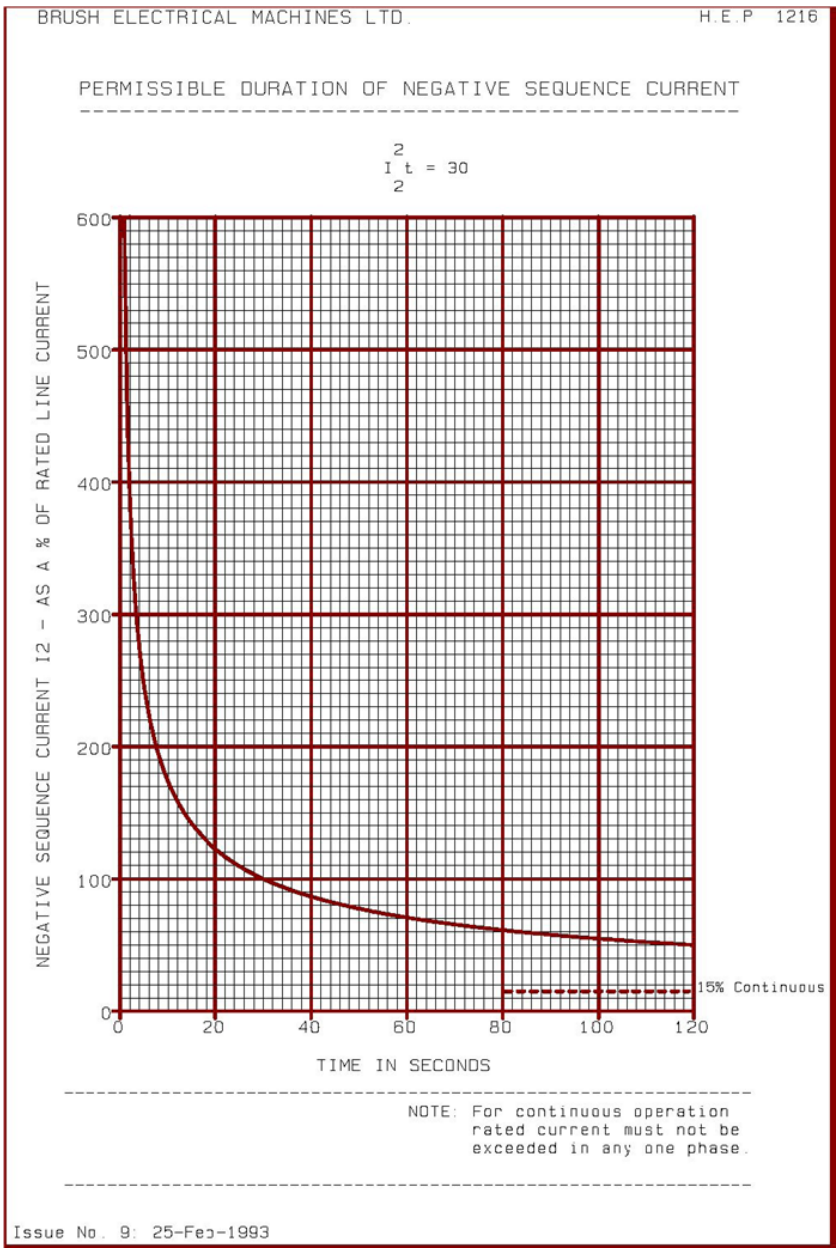

Figure A.1: Permissible duration of negative sequence current

Appendix B

MATLAB program

B.1 Simulating the degree of unsymmetry

The program code for simulating the degree of unsymmetry in Chapter 2.4 when the length of one load is varied (Z_1), is given below.

```
% Aggregated simulation of the Scott-T and Le Blanc when the loads are
% inductive and the length (Z_1) is varying

clear all

% a-operator

a = -0.5 + j*(sqrt(3)/2) ;  % a-operator
a2 = -0.5 - j*(sqrt(3)/2) ; % a-operator

% SCOTT-T: General inputs

m = (sqrt(3)/2) ;           % turn ratio m
V1 = 1 ;                    % Load voltage 1
V2 = j*V1 ;                 % Load voltage 2

% LE BLANC: General inputs

n = sqrt(3) ;                   % turn ratio n
s = 3 ;                         % turn ratio s
r = 3/2 ;                       % turn ratio r
U1 = 3/n ;                      % Load voltage 1
U2 = -j*(1/s + 1/r)*sqrt(3);    % Load voltage 2

%%%%%%% Specifications of load impedances Z1 and Z2

R1 = 0.301 ;           % R of loadimpedance 1
R2 = 0.301 ;            % R of loadimpedance 2
X1 = 0.954 ; %0.954   % X of loadimpedance 1
X2 =0.954 ; %0.954    % X of loadimpedance 2

Z1 = R1+j*X1 ;

%%%%%%% SCOTT-T

%%%%%%% Specifications of the variable and currents

for q1=1:501
    sImp1(q1,1) = (q1+9)*0.01*Z1 ;     % Value to be varied
    I1(q1,1) = V1/(sImp1(q1,1)) ; % Load current 1
```

```
    I2 = V2/(R2+j*X2) ;             % Load current 2

    IA(q1,1) = I1(q1,1) ;
    IB(q1,1) = ((-I1(q1,1))/2) - m*I2 ;
    IC(q1,1) = ((-I1(q1,1))/2) + m*I2 ;

    Imin(q1,1) = (1/3)*(IA(q1,1) + IB(q1,1)*a2+ IC(q1,1)*a) ;
    Ipos(q1,1) = (1/3)*(IA(q1,1) + IB(q1,1)*a+ IC(q1,1)*a2) ;
    y(q1,1)= abs(Imin(q1,1)/Ipos(q1,1)) ;
end

% Loop which finds the intersection (value of R1 at intersection)

min=50;
mini=0;

for q2 = 1:501
    if y(q2,1) < min
        min = y(q2,1);
        mini = q2-1;
    else
    end
end

for q3 = 1:mini
    if y(q3,1) > 0.15
        yes = 0;
    else
        yes = sImp1(q3,1);
        break
    end
end

for q4 = mini:501
    if y(q4,1) < 0.15
        no = 0;
    else
        no = sImp1(q4-1,1);
        break
    end
end

sImp1=abs(sImp1);

%%%%%%% LE BLANC

%%%%%%% Specifications of the variable and currents

for i1=1:501
    Imp1(i1,1) = (i1+9)*0.01*Z1 ;     % Value to be varied
    I1(i1,1) = U1/(Imp1(i1,1)) ; % Load current 1
    I2 = U2/(R2+j*X2) ;             % Load current 2

    IA(i1,1) = I1(i1,1)*(2/sqrt(3)) ;
    IB(i1,1) = I2 - I1(i1,1)*(1/sqrt(3))  ;
    IC(i1,1) = - I1(i1,1)*(1/sqrt(3)) - I2 ;

    Imin(i1,1) = (1/3)*(IA(i1,1) + IB(i1,1)*a2+ IC(i1,1)*a) ;
    Ipos(i1,1) = (1/3)*(IA(i1,1) + IB(i1,1)*a+ IC(i1,1)*a2) ;
    z(i1,1)= abs(Imin(i1,1)/Ipos(i1,1)) ;
```

```
end

% Loop which finds the intersection (value of R1 at intersection)

min=50;
mini=0;

for i2 = 1:501
    if z(i2,1) < min
        min = z(i2,1);
        mini = i2-1;
    else
    end
end

for i3 = 1:mini
    if z(i3,1) > 0.15
        rock = 0;
    else
        rock = Imp1(i3,1);
        break
    end
end

for i4 = mini:501
    if z(i4,1) < 0.15
        roll = 0;
    else
        roll = Imp1(i4-1,1);
        break
    end
end

Imp1=abs(Imp1);

%%%%%%% Specifications of function to be plotted

u = 0.15        % Max value of usymmetry

%%%%%%% SCOTT-T and LE BLANC plot

plot(sImp1(:,1),y(:,1),':b',Imp1(:,1),z(:,1),'-.g',sImp1(:,1),u,'-r')

% The absolute value of the degree of unsymmetry as a
% function of varying R1

xlabel('Z_1 [p.u]') %Name of the x-axis
ylabel('Imin/Ipos')
legend ('SCOTT-T Degree of unsymmetry','LE BLANC Degree of unsymmetry',
'Max allowed unsymmetry')

%%%%%%% Coordinates of the intersection between 0.15 and the degree of
%%%%%%% unsymmetry

Q = [yes no]

P = [rock roll]
```

Appendix C

Dynamic Simulation Language

This appendix gives the lossless DSL model for the Scott–T transformer. In addition, an example is included where the lossless DSL model is compared with hand calculations.

C.1 DSL for Scott–T

The DSL model for the lossless Scott–T transformer is given below. Note that the resistance and leakage reactance of the transformer are ignored as well as disregarding the saturation of the core. The comments after "!!" are included to describe the purpose and function of the equations or expressions.

```
!! Modelleing of the Scott-T transformer for simulations in
!! SIMPOW using Dynamic Simulation Language (DSL)

PROCESS SCOTT(BUS1,BUS2,BUS3,UN1,UN2,UN3)

REAL UN1,UN2,UN3,TAU12/*/,TAU13/*/,I2RE,I2IM,I3RE,I3IM
EXTERNAL UN1,UN2,UN3
STATE I2RE,I2IM,I3RE,I3IM

AC BUS1,BUS2,BUS3
AC_CURRENT I1/BUS1/
AC_CURRENT I2/BUS2/
AC_CURRENT I3/BUS3/

REAL  P1,P2,P3, Q2, Q3, IBASE, IP1_PU, IN1_PU, IO1_PU, IP1H_PU,
& IN1H_PU, IO1H_PU, IP1_A, IN1_A, IO1_A, I_NEG_MAX

PLOT    P1,P2,P3,Q2,Q3,IP1_PU,IN1_PU,IO1_PU,IP1_A,IN1_A,IO1_A,I_NEG_MAX

!! Calculations for the teaser- and main transformer ratio of the Scott-T:
!! (UB has to be included for situations where UN is unequal to UB)

IF (START) THEN
 TAU12 = (UN1/(UBASE(BUS1))/(UN2/UBASE(BUS2)))
 TAU13 = (UN1/(UBASE(BUS1))/(UN3/UBASE(BUS3)))
ENDIF

!! Implicit equations for determining the load currents of the Scott-T:

IF (TRANSTA) THEN

!! 1. Calculate the current on the secondary side
```

```
I2RE: UPRE(BUS2) = (2/SQRT(3))*(1/TAU12)* 1/SQRT(3) *
   & (UARE(BUS1)-(UBRE(BUS1)/2)-(UCRE(BUS1)/2))
I2IM: UPIM(BUS2) = (2/SQRT(3))*(1/TAU12)* 1/SQRT(3) *
   &(UAIM(BUS1)-(UBIM(BUS1)/2)-(UCIM(BUS1)/2))
I3RE: UPRE(BUS3) = (1/TAU13)* 1/SQRT(3) *
   & (UBRE(BUS1)-UCRE(BUS1))
I3IM: UPIM(BUS3) = (1/TAU13)* 1/SQRT(3) *
   & (UBIM(BUS1)-UCIM(BUS1))

!! 2. Inject the secondary current into the transformer

IPRE(I2) = I2RE
IPIM(I2) = I2IM
IPRE(I3) = I3RE
IPIM(I3) = I3IM

!! 3. Inject the primary current into the transformer

IPRE(I1): (1/SQRT(3))*IPRE(I1) = (1/SQRT(3))*(-(1/TAU12)*I2RE +
& (1/TAU13)*I3IM)
INRE(I1): (1/SQRT(3))*IPIM(I1) = (1/SQRT(3))*(-(1/TAU12)*I2IM -
   & (1/TAU13)*I3RE)

IPIM(I1): (1/SQRT(3))*INRE(I1) = (1/SQRT(3))*(-(1/TAU12)*I2RE -
   & (1/TAU13)*I3IM)
INIM(I1): (1/SQRT(3))*INIM(I1) = (1/SQRT(3))*(-(1/TAU12)*I2IM +
   & (1/TAU13)*I3RE)

IORE(I1) = 0
IOIM(I1) = 0

!! Determination of number of phases and sequence
!! components of the load currents

IF (.NOT. ONE_PHASE(BUS2)) THEN
  INRE(I2) = 0
  INIM(I2) = 0
  IORE(I2) = 0
  IOIM(I2) = 0
ENDIF

IF (.NOT. ONE_PHASE(BUS3)) THEN
  INRE(I3) = 0
  INRE(I3) = 0
  IORE(I3) = 0
  IORE(I3) = 0
ENDIF

!! Equations for plotting the sequence components of the primary
!! current into the transformer

IP1H_PU = IPRE(I1)**2+IPIM(I1)**2

IF (IP1H_PU .LE. 0) THEN
  IP1_PU = 0
ELSE
  IP1_PU = SQRT(IP1H_PU)
ENDIF

IN1H_PU = INRE(I1)**2+INIM(I1)**2
```

```
IF (IN1H_PU .LE. 0) THEN
  IN1_PU = 0
ELSE
  IN1_PU = SQRT(IN1H_PU)
ENDIF

IO1H_PU = IORE(I1)**2+IOIM(I1)**2

IF (IO1H_PU .LE. 0) THEN
  IO1_PU = 0
ELSE
  IO1_PU = SQRT(IO1H_PU)
ENDIF

!! Equation for calculating the base value of the current into
!! the primary side of the transformer

IBASE = SBASE/(UBASE(BUS1)*SQRT(3))

!! Equations for plotting the physical value of the primary current
!! into the transformer in Ampere

IP1_A = IP1_PU*IBASE
IN1_A = IN1_PU*IBASE
IO1_A = IO1_PU*IBASE

!! Equation for plotting the power into the transformer primary

P1 = UPIM(BUS1)*_PIM(I1) + UPRE(BUS1)*_PRE(I1) !! + UO(BUS1)*IO(I1)

!! Equation for drawing the max permissible continous negative
!! sequence current of 15%

I_NEG_MAX = 0.15

!! Equation for plotting the power to the load at Bus 2 (in per unit)

P2 = (UPRE(BUS2)*_PRE(I2)) + (UPIM(BUS2)*_PIM(I2))

!! Equation for plotting the power to the load at Bus 3 (in per unit)

P3 = (UPRE(BUS3)*_PRE(I3)) + (UPIM(BUS3)*_PIM(I3))

!! Equation for plotting Q2 (in per unit)

Q2 = (UPIM(BUS2)*_PRE(I2)) - (UPRE(BUS2)*_PIM(I2))

!! Equation for plotting Q3 (in per unit)

Q3 = (UPIM(BUS3)*_PRE(I3)) - (UPRE(BUS3)*_PIM(I3))

ENDIF

END
```

C.1.1 Verifying the lossless model for the Scott–T transformer with hand calculations

The model used for the hand calculations and in the SIMPOW simulations is given in Figure C.1. The objective is to carry out both hand calculations as well as simulations in SIMPOW which gives equal results. By comparing the results, the DSL model is verified.

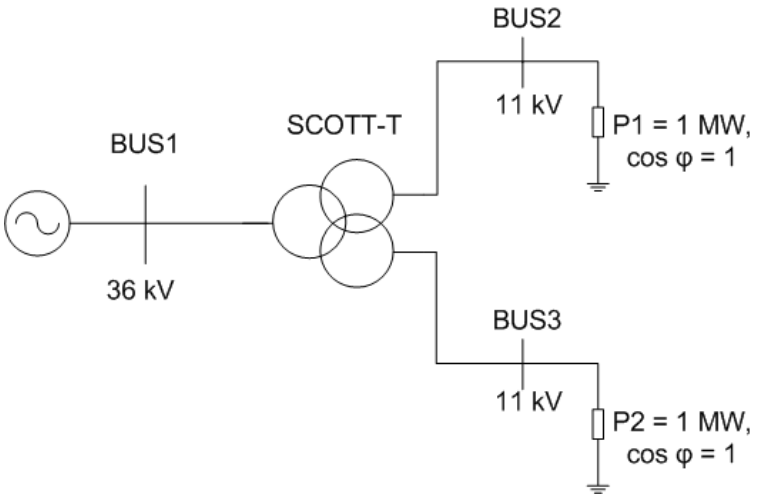

Figure C.1: SLD for the hand calculations and simulations

The Scott–T transformer is directly connected to the voltage source and to the two loads on the secondary side. The Scott–T is assumed lossless, which means that the resistances, reactances as well as the magnetising current are ignored. The three–phase model is given in Figure C.2.

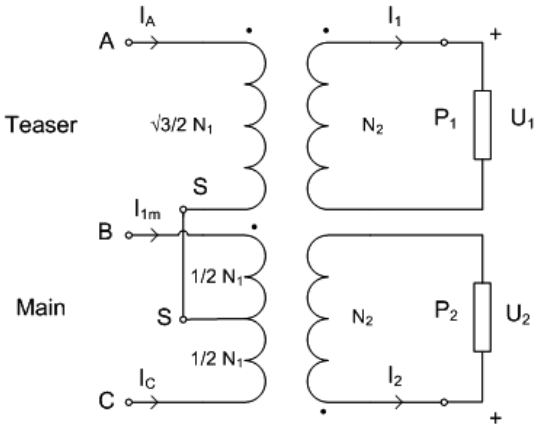

Figure C.2: Three–phase model for calculations with the lossless Scott–T

The notation β in the calculations is the turn ration $\frac{N_2}{N_1} = \frac{11}{36} = 0.306$. Note also that the power factor of the system is one, which means that the there is only active power transferred in the system. The calculations will therefore only consider the amplitude of the values and not the angles as well.

The expressions for the phase currents on the primary side are given in Equation C.1.

$$
\begin{aligned}
I_A &= \frac{2}{\sqrt{3}}\beta\vec{I_1} = 1.15\beta\vec{I_1} \\
I_B &= \sqrt{\vec{I_{1m}}^{\,2} + (\frac{\vec{I_A}}{2})^2} \\
I_C &= \sqrt{\vec{I_{1m}}^{\,2} + (\frac{\vec{I_A}}{2})^2}
\end{aligned}
\tag{C.1}
$$

I_{1m} is the current in the main transformer on the primary side and I_1 is the load current in the secondary teaser winding, see Figure C.2. The voltages and currents are represented as phasors as given in Figure C.3.

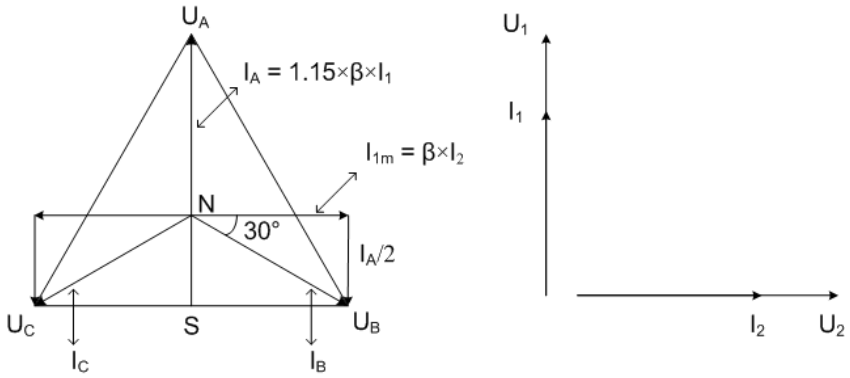

Figure C.3: Phasor diagram for voltages and currents in the Scott–T transformer

The load currents I_1 and I_2 are calculated as follows:

$$
I_1 = I_2 = \frac{P_1}{U_1} = \frac{1MW}{11kV} = 90.9\text{A} \tag{C.2}
$$

This gives the phase current I_A on the primary side keeping the turn ratio $\beta = 0.306$ in mind:

$$
I_A = 1.15 \cdot 0.306 \cdot 90.9 \approx 32\text{A} \tag{C.3}
$$

The current I_{1m} through the main primary transformer is:

$$
I_{1m} = \beta \cdot I_2 = 0.306 \cdot 90.9A = 27.8\text{A} \tag{C.4}
$$

The primary phase currents I_B and I_C can also be found by putting the calculated values into Equation C.1. The result is presented in Equation C.5.

$$
\begin{aligned}
I_B &= \sqrt{(27.8)^2 + (\frac{32}{2})^2} = 32\text{A} \\
I_C &= \sqrt{(27.8)^2 + (\frac{32}{2})^2} = 32\text{A}
\end{aligned}
\tag{C.5}
$$

The calculations show that the primary phase currents are equal and there is no unbalance in the system.

Optpow file and simulations

The Optpow file with comments for the same system as for the hand calculations is given below. The comments after "!!" are included to describe the defined variables. It is however not possible to include the Scott–T in the Optpow file, due to the lack of a predefined model for the specially connected transformer. As explained in Chapter 3.2, the Scott–T has to be modelled by DSL and included in the Dynpow module in SIMPOW. But first a load flow calculation has to be done to make a base for the Dynpow simulations.

```
OPTPOW FILE for simulations with the lossless Scott-T transformer.
Verification of handcalculations
**

GENERAL
 SN=2 !! Base value for the power in  MVA
END

NODES
 GENBUS  UB=36 !! UB is the base voltage at each node in kV
 BUS1    UB=36
 BUS2    UB=11  PHASE=1
 BUS3    UB=11  PHASE=1
END

LINES
 GENBUS  BUS1  TYPE=0   !! The line has no resistance or reactance
END

LOADS
 BUS2  P=1   COSFI=1
 BUS3  P=1   COSFI=1
END

TRANSFORMERS
 BUS1  BUS2  BUS3  NW=3               !! 3 winding transformer
 SN=2  UN1=36  UN2=11  UN3=11            !! Nominal values
 ER12=0  ER13=0  ER23=0               !! Lossless
 EX12=0.00001  EX13=0.00001  EX23=0.00001 !! Lossless, but EX cannot be zero
END

POWER CONTROL   !! The node GENBUS is a swing bus (Constant U, FI)
 GENBUS  TYPE=NODE  RTYP=SW  U=36  FI=0
END

END
```

When the Optpow simulation is done, it is possible to present the load flow results in a single–line diagram (SLD), see Figure C.4.

The values presented in the SLD is the current in ampere and the voltage in kV phase–to–phase value. Note that the values are the same as calculated for the currents and for the specified voltages. However, the two secondary load voltages are equal in both

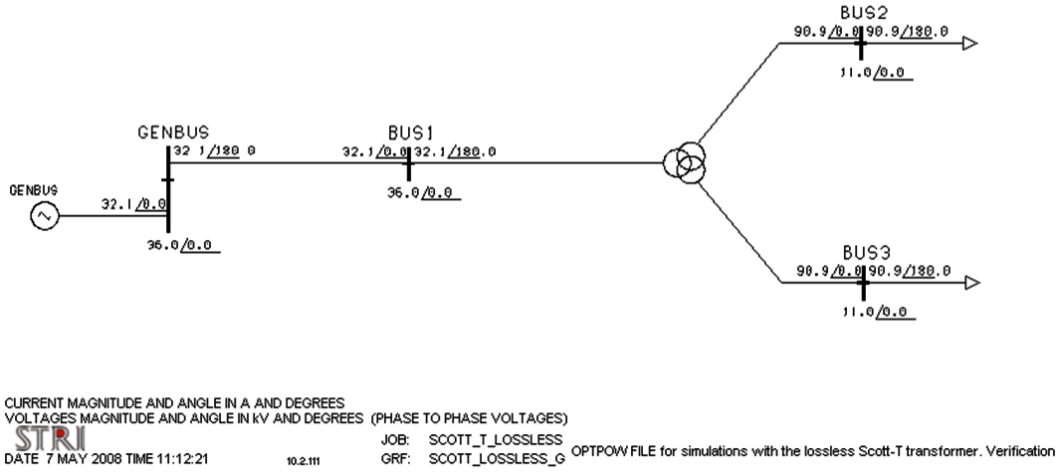

Figure C.4: Load flow calculations from Optpow

amplitude and phase. As explained in Chapter 2, the two load voltages of the Scott–T transformer should be same in amplitude, but 90 degrees phase shifted from each other. This result is expected from the simulations in Dynpow on the same model.

Dynpow file and simulations

The Dynpow file for simulations with the lossless Scott–T is given below. The comments after !! are included to describe the data groups.

```
DYNPOW FILE for simulations with the lossless Scott-T transformer
**

CONTROL DATA
 TEND=4.0  XTRACE=1  EDSL=3  DDSL=3  !! The simulations are performed in 4 seconds
END

NODES
 GENBUS  TYPE=1          !! Infinite voltage source with constant
END                      !! voltage and angle at node GENBUS

TRANSFORMERS
 BUS1  BUS2  BUS3  NW=3  TYPE=DSL/SCOTT  !! The DSL file is implemented
END                                      !! in the Dynpow calculations

DSL-TYPES
 SCOTT(BUS1,BUS2,BUS3,UN1,UN2,UN3)  !! Name of process and predefined
END                                 !! parameters and variables in DSL

END
```

The SLD result from the Dynpow calculations is presented in Figure C.5.

The values for the currents are presented in ampere and in kV for the phase–to–phase voltage. Note that the load voltage at BUS3 is now 90 degrees phase shifted, and the values for the current and the voltages are the same as for both the Optpow– and hand calculations. This shows that the DSL model for the lossless Scott–T complies with the

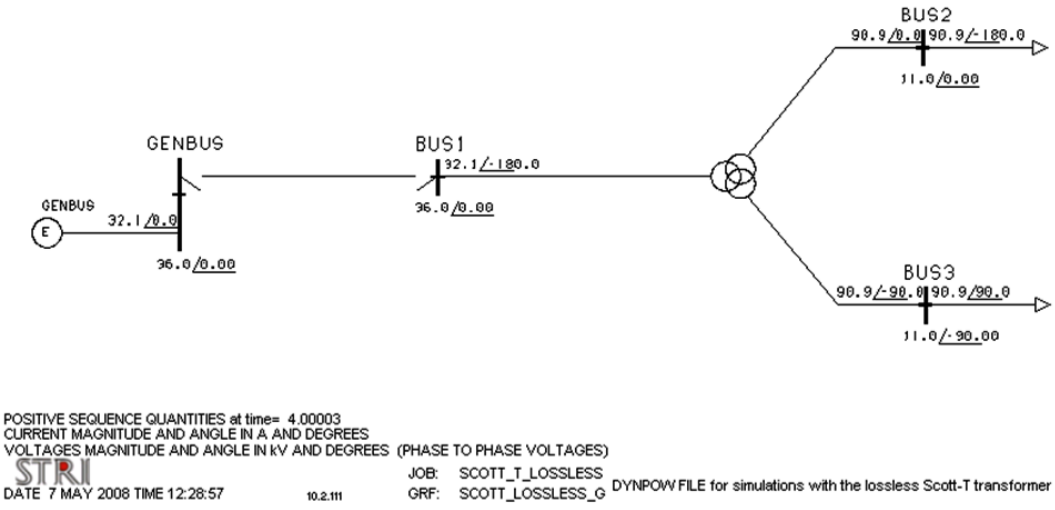

Figure C.5: Load flow calculations from Dynpow

analysis of the Scott–T in Chapter 2.2. It is however also evident do investigate the degree of unsymmetry, to verify that the model is correct in that matter as well.

By selecting "Curves" in the Dynpow window, it is possible to plot the parameters specified for plotting in the DSL model. In addition, values for the other components can of course also be presented as well. Figure C.6 shows the plot for the primary phase currents I_A, I_B and I_C into the transformer. In addition, Figure C.7 shows the values for the symmetrical components of the current in the Scott–T transformer. These are defined as IP1_A, IN1_A and I01_A in the DSL file.

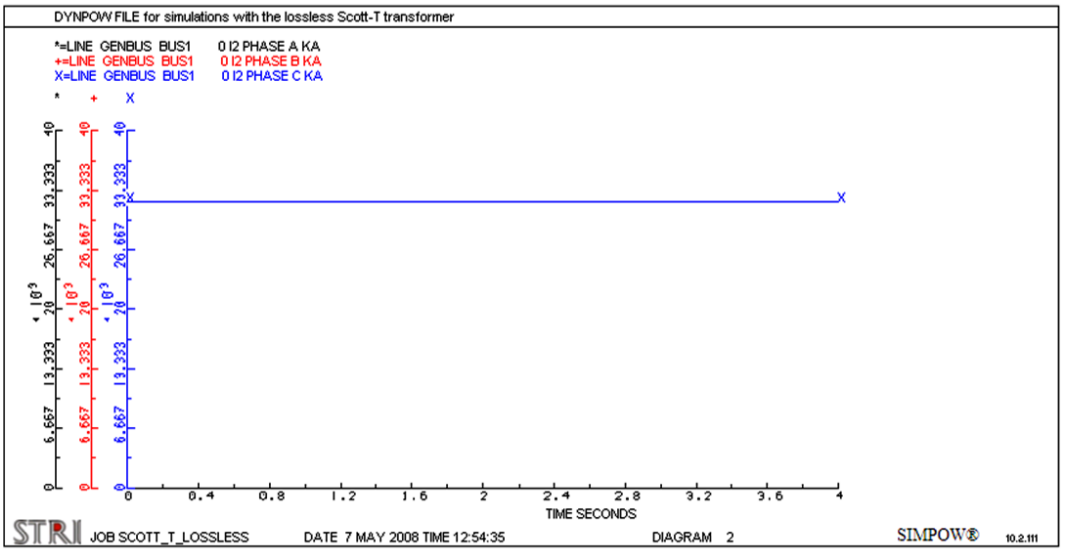

Figure C.6: The primary phase currents into the transformer

The value for the primary phase currents are plotted in kA in Figure C.6. The values are 32 A for the phase currents, which is the same as for the hand calculated result.

Note that the positive sequence component of the current is 32 A in Figure C.7, but

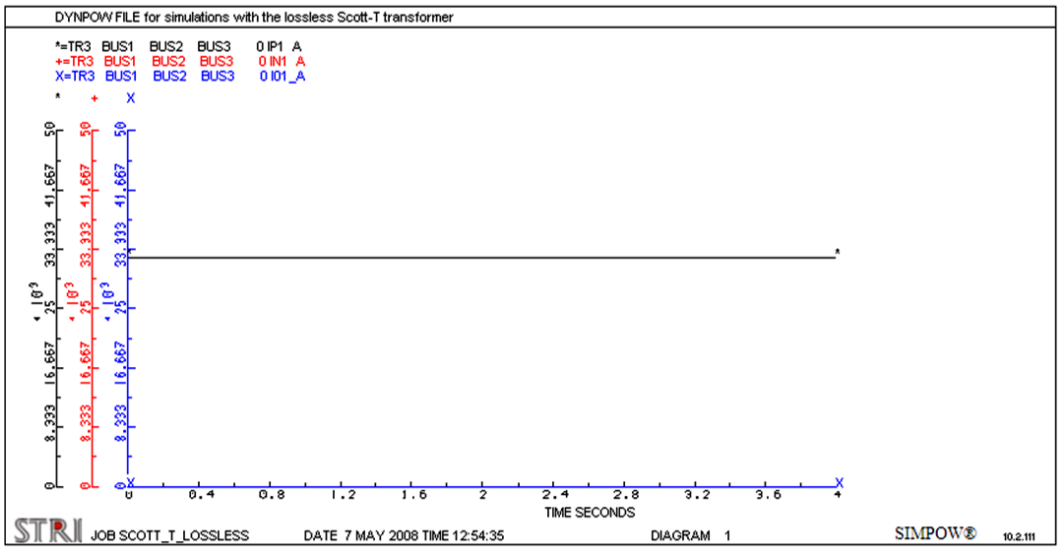

Figure C.7: The positive–, negative– and zero sequence component of the load current in the transformer

the negative sequence is zero. This means that the degree of unsymmetry is zero. The zero sequence is always zero for this system, seeing that there is now connection through ground in the transformer. It is however included in the plot to state its value and verify the equations in the DSL model.

The results from the Optpow– and Dynpow simulations are equal to the hand calculated values. It is therefore proven that the model is correct.

Appendix D

Simulation files for the transformer

The simulation files for Chapter 3.3 for comparing the MATLAB results with the simulations in SIMPOW are given in this appendix. In addition, the Optpow– and Dynpow files for the model when including the short–circuit impedances are given.

The comments after "!!" are included to describe the data groups in the files. The DSL model for the simulations are given in Appendix C.

D.1 Changes in unsymmetry for the Scott–T transformer when the active power at BUS2 changes

Optpow

The values from Chapter 3.3 are implemented in the Optpow file.

```
OPTPOW FILE for comparing the simulations
in SIMPOW with MATLAB results
**

GENERAL
 SN=2                !! Base value for the power in MVA
END

NODES
 GENBUS  UB=36        !! UB is the base voltage at each node in kV
 BUS1    UB=36
 BUS2    UB=18  PHASE=1
 BUS3    UB=18  PHASE=1
END

LINES
 GENBUS  BUS1  TYPE=0  !! The line has no resistance or reactance
END

LOADS
 BUS2  P=0.6  COSFI=0.3
 BUS3  P=0.6  COSFI=0.3
END

TRANSFORMER
```

```
 BUS1  BUS2  BUS3  NW=3
     SN=2  UN1=36  UN2=18  UN3=18
     ER12=0  ER13=0  ER23=0
     EX12=0.00001  EX13=0.00001  EX23=0.00001
END

POWER CONTROL
 GENBUS  TYPE=NODE  RTYP=SW  U=36  FI=0  !! Node GENBUS is a swing bus
END

END
```

Dynpow

The Dynpow file for the simulations when varying the active part of the load at Bus 2 is given here. Note the data groups "LOADS" and "TABLES" which define the load variations.

```
DYNPOW FILE for comparing the simulations in SIMPOW with MATLAB results
**

CONTROL DATA
 TEND=20  XTRACE=1  EDSL=3  DDSL=3
END

NODES
 GENBUS  TYPE=1
END

TRANSFORMERS
 BUS1  BUS2  BUS3  NW=3  TYPE=DSL/SCOTT
END

DSL-TYPES
 SCOTT(BUS1,BUS2,BUS3,UN1,UN2,UN3)
END

LOADS
 BUS2  PTAB 1   !! Vary the active power at Bus 2 in Table 1
END

TABLES
 1  TYPE=0 F  0.  0.1  !! Table 1,function of time, steps 0.1 second
       1.  0.1         !! At 1 second, P=0.1 per unit
       20. 5.1         !! At 20 seconds, P=5.1 per unit
END

END
```

D.2 Changes in unsymmetry for the Scott–T transformer when the reactive power at BUS2 changes

The variance for Q2 is $[0.1Q3 - 5.1Q3]$ which in per unit is $[0.095 - 4.865]$.

Optpow

The Optpow file is the same as for the previous simulation when the active power at BUS2 changes.

Dynpow

The variations of the reactive power at BUS2 is specified in "LOADS" and "TABLES".

```
DYNPOW FILE for comparing the simulations in SIMPOW with MATLAB results
**

CONTROL DATA
 TEND=20  XTRACE=1  EDSL=3  DDSL=3
END

NODES
 GENBUS  TYPE=1
END

TRANSFORMERS
 BUS1  BUS2  BUS3  NW=3  TYPE=DSL/SCOTT
END

DSL-TYPES
 SCOTT(BUS1,BUS2,BUS3,UN1,UN2,UN3)
END

LOADS
 BUS2  QTAB 1 !! QTAB is the definition for varying the reative power
END

TABLES
 1  TYPE=0 F  0.  0.1
       1.  0.1
       20. 5.1
END

END
```

D.3 Changes in unsymmetry for the Scott–T transformer when the total impedance at BUS2 changes

Optpow

The Optpow file is the same as for the previous simulation when the active power at BUS2 changes.

Dynpow

The active and reactive power are varied from 0.1 per unit to 5.1 per unit. See the data groups "LOADS" and "TABLES".

```
DYNPOW FILE for comparing the simulations in SIMPOW with MATLAB results
**

CONTROL DATA
 TEND=20  XTRACE=1  EDSL=3  DDSL=3
END

NODES
 GENBUS  TYPE=1
END

TRANSFORMERS
 BUS1  BUS2  BUS3  NW=3  TYPE=DSL/SCOTT
END

DSL-TYPES
 SCOTT(BUS1,BUS2,BUS3,UN1,UN2,UN3)
END

LOADS
 BUS2  QTAB 1   !! QTAB is the definition for varying the reative power
 BUS2  PTAB 1   !! PTAB is the definition for varying the reative power
END

TABLES
 1  TYPE=0 F  0.  0.1
       1.  0.1
       20. 5.1
END

END
```

D.4 Verifying the Scott–T model including the short–circuit impedance with hand calculations

The Optpow– and Dynpow files for comparing the hand calculations in Chapter 3.4 with simulations in SIMPOW are given here. Note that the values for lines representing the

short–circuit impedance are the same as calculated in Chapter 3.4. The DSL model for Scott–T in the Dynpow file is the same as before.

Optpow

The impedance values for the lines are the same as the short–circuit impedance that is calculated.

```
OPTPOW FILE for including ER and EX in the Scott-T transformer
**

GENERAL
 SN=2
END

NODES
 GENBUS  UB=36
 IMPBUS1 UB=36
 IMPBUS2 UB=18  PHASE=1
 IMPBUS3 UB=18  PHASE=1
 BUS1    UB=36
 BUS2    UB=18  PHASE=1
 BUS3    UB=18  PHASE=1
END

LINES
 GENBUS   IMPBUS1  TYPE=0                   !! R and X is zero
 IMPBUS1  BUS1     TYPE=1  R=3.24  X=45.36
 BUS2     IMPBUS2  TYPE=1  R=0.81  X=11.34
 BUS3     IMPBUS3  TYPE=1  R=0.81  X=11.34
END

TRANSFORMER
 BUS1  BUS2  BUS3  NW=3
     SN=2  UN1=36  UN2=18  UN3=18
     ER12=0  ER13=0  ER23=0
     EX12=0.00001  EX13=0.00001  EX23=0.00001
END

POWER CONTROL
 GENBUS  TYPE=NODE  RTYP=SW  U=36  FI=0
END

END
```

Dynpow

The short–circuit of the secondary windings are given in the data group "FAULTS" and the specification of the fault is given in "RUN INSTRUCTION".

```
DYNPOW FILE for including R and X in the Scott-T transformer
**

CONTROL DATA
```

```
 TEND=20  XTRACE=-1  EDSL=3  DDSL=3
END

NODES
 GENBUS   TYPE=1
END

TRANSFORMERS
 BUS1  BUS2  BUS3  NW=3  TYPE=DSL/SCOTT
END

DSL-TYPES
 SCOTT(BUS1,BUS2,BUS3,UN1,UN2,UN3)
END

FAULTS
 IMP2SC  TYPE=3PSG  NODE=IMPBUS2
 IMP3SC  TYPE=3PSG  NODE=IMPBUS3
END

RUN INSTRUCTION
 AT 5  INST=CONNECT  FAUL=IMP2SC
 AT 5  INST=CONNECT  FAUL=IMP3SC
END

END
```

Appendix E

Input data for SIMPOW

In order to carry out system simulations in SIMPOW, the modules Optpow and Dynpow requires input data for the electrical equipment and topology for Case 1 and Case 2. The parameters for the different data groups in SIMPOW are given in this appendix.

E.1 Case 1

The cable data given in Table 5.2 are re–calculated in order to be used in SIMPOW. In addition, the parameters for the different data groups in Optpow are given.

E.1.1 Calculations for cable data

The cable data for the 100 km cable and the 50 km long cable in Case 1 is given in Table E.1.

Table E.1: Parameters for the subsea cables in Case 1

Subsea cable	**Cable type**	**Rated voltage**	**AC-resistance at 90°C**	**Capacitance (per phase)**	**Inductance (per phase)**	**Rated current at 90°C**
100 km	3x240mm^2 Cu	132 kV	0.097 Ω/km	0.14 μF/km	0.46 mH/km	500 A
50 km	3x630mm^2 Cu	66 kV	0.040 Ω/km	0.27 μF/km	0.35 mH/km	750 A

According to [17], lines between 80 km and 250 km in length are termed medium length lines. For medium length lines, half of the shunt capacitance may be considered to be lumped at each end of the line. This is referred to as the nominal π–model and is shown in Figure E.1[17].

The two cables in Case 1 are both modelled as a π–model for the system simulations. According to the SIMPOW–manual, a line specified as type 2 is a π–model which is described with resistance (R in Ω/km), inductance (X in Ω/km) and susceptance (B in S/km).

From Table E.1 it is evident that the inductance and susceptance have to be re–calculated for adjusting to the required input data in SIMPOW.

The inductance is calculated according Equation E.1 and the susceptance as in Equation E.2. The system frequency is 50 Hz.

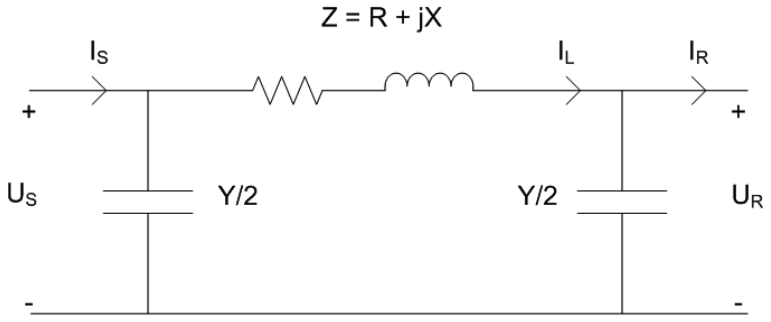

Figure E.1: Nominal π-model for medium length line

$$X_L = j\omega L \tag{E.1}$$

$$\begin{aligned} B &= \frac{1}{X_C} \\ X_C &= \frac{1}{j\omega C} \end{aligned} \tag{E.2}$$

The cable input data for the SIMPOW files are given in Table E.2

Table E.2: Cable input data for SIMPOW

Subsea cable	**AC-resistance at 90°C**	**Inductance (per phase)**	**Capacitance (per phase)**	**Reactance**	**Susceptance**
100 km	0.097 Ω/km	0.46 mH/km	0.14 μF/km	0.145 Ω/km	4.398e-5 S/km
50 km	0.040 Ω/km	0.35 mH/km	0.27 μF/km	0.110 Ω/km	8.482e-5 S/km

E.1.2 Parameters for the data groups in Optpow

The parameters for normal operation of the DEH system is given in this part.

The transformers

The Scott–T transformer in Case 1 transforms the voltage supplied at SCOTTBUS1 to the two secondary terminals SCOTTBUS1 and SCOTTBUS2, see Figure 5.1. The nominal voltages U_{N1}, U_{N2} and U_{N3} for the Scott–T are specified in Optpow according to the nominal voltage levels at BUS3 and the required output voltages of the DEH system which are given in Table 5.1.

The base power, S_N, for the Scott–T transformer is calculated by using the highest required DEH voltage, the DEH impedance and the required current for heating the pipeline, see Equation E.3.

$$\begin{aligned} S_N &= U_{DEH} \cdot I^*_{DEH} \\ S_N &== \frac{U^2_{DEH}}{Z^*_{DEH}} \\ S_N &= 38.8e^{-75.62} MVA \end{aligned} \tag{E.3}$$

Seeing that there are two pipelines to be heated, the base power for the Scott–T is multiplied by 2. As a result, 80 MVA is set as the base power. The base power for the three–winding transformer, S_{N3w}, is estimated by using Equation E.4 which adds the base power for the Scott–T transformer and the subsea load. This is also used as the total system base power.

$$\begin{aligned} S_{N3w} &= S_N + S_{subsea} \\ S_{N3w} &= 80MVA + \frac{P}{cosfi} \\ S_{N3w} &= 80MVA + \frac{50}{0.9} \\ S_{N3w} &= 135.6MVA \end{aligned} \tag{E.4}$$

The base power for the total system and the three–winding transformer are set equal to 150 MVA. The base power and the nominal voltages for the Scott–T and the three–winding transformer are given in Table E.3.

Table E.3: SIMPOW input data for the two transformers

Transformer	S_N	U_{N1}	U_{N2}	U_{N3}
3–winding	150 MVA	300 kV	132 kV	66 kV
Scott–T	80 MVA	66 kV	22.5 kV/25.0 kV (maintain/heating)	22.5 kV/25.0 kV (maintain/heating)

The short–circuit impedance which are given by three lines are calculated by considering the transformer values. The values for ER and EX for the Scott–T transformer are given in per unit of the transformer nominal values in Chapter 3.4 and are equal to $Z_{SC} = ER + jEX = 0.005 + j0.07 p.u.$

The reference values for the short–circuit impedance are calculated in Equation E.5. Further, the simulations are only carried out for heating the pipeline at 25 kV, and the short–circuit impedances are calculated by using that voltage level.

$$\begin{aligned} Z_{Base1} &= \frac{U^2_{N1}}{S_N} = 54.45\Omega \\ Z_{Base2} &= \frac{U^2_{N2}}{S_N} = 7.81\Omega \\ Z_{Base3} &= Z_{Base2} = 7.81\Omega \end{aligned} \tag{E.5}$$

The short–circuit impedances are then calculated into physical values by using Equation E.6.

$$\begin{aligned} Z_{SC1} &= Z_{Base1} \cdot Z_{SC} = 0.272 + j3.815\Omega \\ Z_{SC2} &= Z_{Base2} \cdot Z_{SC} = 0.039 + j0.547\Omega \\ Z_{SC3} &= Z_{SC2} = 0.039 + j0.547\Omega \end{aligned} \tag{E.6}$$

The short–circuit impedance of the Scott–T transformer is modelled as lines and the input data are given in Table E.6. The short–circuit impedance of the tree–winding transformer is also set equal to $ER + jEX = 0.005 + j0.07$ of the transformer base power. The inputs for the data group "TRANSFORMERS" is based on Table E.3 and is given in Table E.4.

Table E.4: Parameters for the data group "TRANSFORMERS"

Nodes	S_N **[MVA]**	U_{N1}**[kV]**	U_{N2}**[kV]**	U_{N3}**[kV]**	**ER[p.u]**	**EX[p.u]**
BUS1, BUS2, BUS3	150	300	132	66	0.005	0.07
SCOTTBUS1, SCOTTBUS2, SCOTTBUS3	80	66	22.5/25	22.5/25	0	0

The nodes

Table E.5 summaries the required input data for data groups "NODES" in SIMPOW for Case 1. Figure 5.1 shows the system topology for Case 1 and the names of the nodes.

Table E.5: Parameters for the data group "NODES"

NODE	**Base voltage [kV]**	**Number of phases**
GENBUS	$U_B = 300$	3
BUS1	$U_B = 300$	3
BUS2	$U_B = 132$	3
LOADBUS	$U_B = 132$	3
BUS3	$U_B = 66$	3
DEHBUS1	$U_B = 66$	3
SCOTTBUS1	$U_B = 66$	3
SCOTTBUS2	$U_B = 22.5/25$	1
SCOTTBUS3	$U_B = 22.5/25$	1
DEHBUS2	$U_B = 22.5/25$	1
DEHBUS3	$U_B = 22.5/25$	1

It is worth repeating that the base value does not have any affect on the load flow, only the representation of the values in per unit. Therefore, the base values are specified to be the same as the nominal voltages in the system. The base value for the DEH terminals are specified according to the mode of operation (maintaining or heating).

The lines

Table E.6 gives the lines that connect the nodes for Case 1.

Type 0 is a line without R and X, type 2 is the nominal π–model for a medium line length and type 1 is including R and X. For further details, see [10]. The three lines which are specified type 1, are the three lines representing the short–circuit impedance of the Scott–T transformer.

Table E.6: Parameters for the data group "LINES"

Node 1	Node 2	Type	Length [km]	Resistance [Ω/km]	Reactance [Ω/km]	Susceptance [S/km]
GENBUS1	BUS1	0				
BUS2	LOADBUS	2	100	0.097	0.145	4.398E-5
BUS3	DEHBUS1	2	50	0.040	0.110	8.482E-5
DEHBUS1	SCOTTBUS1	1	1	0.272	3.815	
SCOTTBUS2	DEHBUS2	1	1	0.039	0.547	
SCOTTBUS3	DEHBUS3	1	1	0.039	0.547	

The subsea load

The input data for the subsea load is specified in the data group "LOADS", see Table E.7.

Table E.7: Parameters for the data group "LOADS"

Node	Power [MW]	Power factor
LOADBUS	50	0.9

DEH impedance

The two DEH impedances for representing the the piggyback cable and the pipeline, are connected to the system in the data group "SHUNT IMPEDANCES", see Table E.8.

Table E.8: Parameters for the data group "SHUNT IMPEDANCES"

Node	Resistance [Ω]	Reactance [Ω]
DEHBUS2	4.0	15.6
DEHBUS3	4.0	15.6

Power control

In addition to the topology of the power system, a production source is specified. For the system simulations it is practical to specify a swing bus which has a constant voltage and phase angle and can produce or consume the power as necessary. This makes it possible to investigate the flow of reactive power. The data group "POWER CONTROL" is given in Table E.9.

E.2 Case 2

The necessary calculations for the configuration in Case 2 are presented as well as the parameters for the different data groups in SIMPOW.

Table E.9: Parameters for the data group "POWER CONTROL"

Node	TYPE	RTYP	Voltage [kV]	Phase angle FI
GENBUS	NODE	SW	300	0

E.2.1 Parameters for the data groups in Optpow

The transformers

The short–circuit impedance for the two specially connected transformer is $Z_{SC} = 0.005 + j0.07$ of the transformer base value. The base power for the Scott–T transformers is the same as for Case 1 because the load conditions are equal. It is therefore specified to be 80 MVA. However, the two Scott–T transformers in Case 2 transforms a nominal voltage of 132 kV to 25 kV when heating the pipe content. This makes the primary short–circuit impedance different. It is calculated in Equation E.7.

$$Z_{Base1} = \frac{U_{N1}^2}{S_N} = 217.8\Omega \tag{E.7}$$

The short–circuit impedances for the Scott–T transformers are given in Equation E.8.

$$\begin{aligned} Z_{SC1} &= ZBase1 \cdot Z_{SC} = 1.089 + j15.246 \\ Z_{SC2} &= ZBase2 \cdot Z_{SC} = 0.039 + j0.547 \\ Z_{SC3} &= ZBase3 \cdot Z_{SC} = 0.039 + j0.547 \end{aligned} \tag{E.8}$$

Transformer T1 base power is calculated in Equation E.9.

$$\begin{aligned} S_{T1} &= S_{subsea} + S_{Scott1} + S_{Scott2} \\ S_{T1} &= \frac{50}{0.9} + 80MVA + 80MVA \\ S_{T1} &= 216MVA \\ \Rightarrow S_{T1} &= 220MVA \end{aligned} \tag{E.9}$$

The base power and the nominal values for the transformers in Case 2 are given in Table E.10.

Table E.10: Parameters for the data group "TRANSFORMERS"

Nodes	S_N [MVA]	U_{N1}[kV]	U_{N2}[kV]	U_{N3}[kV]	ER[p.u]	EX[p.u]
BUS1, BUS2	220	300	132		0.005	0.07
SCOTTBUS31, SCOTTBUS32, SCOTTBUS33	80	132	22.5/25	22.5/25	0	0
SCOTTBUS31, SCOTTBUS32, SCOTTBUS33	80	132	22.5/25	22.5/25	0	0

The short–circuit impedance for the Scott–T transformers is given in the data group "LINES" in Optpow, see Table E.12.

The nodes

Figure 5.17 shows the name for the nodes in Case 2. Table E.11 gives the nodes that are specified in Optpow and the data group "NODES".

Table E.11: Parameters for the data group "NODES"

NODE	Base voltage [kV]	Number of phases
GENBUS	$U_B = 300$	3
BUS1	$U_B = 300$	3
BUS2	$U_B = 132$	3
BUS3	$U_B = 132$	3
BUS4	$U_B = 132$	3
LOADBUS	$U_B = 132$	3
DEHBUS31	$U_B = 132$	3
SCOTTBUS31	$U_B = 132$	3
SCOTTBUS32	$U_B = 22.5/25$	1
SCOTTBUS33	$U_B = 22.5/25$	1
DEHBUS32	$U_B = 22.5/25$	1
DEHBUS33	$U_B = 22.5/25$	1
DEHBUS41	$U_B = 132$	3
SCOTTBUS41	$U_B = 132$	3
SCOTTBUS42	$U_B = 22.5/25$	1
SCOTTBUS43	$U_B = 22.5/25$	1
DEHBUS42	$U_B = 22.5/25$	1
DEHBUS43	$U_B = 22.5/25$	1

The lines

The lines connecting the nodes are given in Table E.12. Note also that the short–circuit impedance for SCOTT1 and SCOTT2 are given in the table as lines.

Table E.12: Parameters for the data group "LINES"

Node 1	Node 2	Type	Length [km]	Resistance [Ω/km]	Reactance [Ω/km]	Susceptance [S/km]
GENBUS1	BUS1	0				
BUS2	BUS3	2	50	0.097	0.145	4.398E-5
BUS3	BUS4	2	100	0.097	0.145	4.398E-5
BUS4	LOADBUS	2	50	0.097	0.145	4.398E-5
BUS3	DEHBUS31	0				
BUS4	DEHBUS41	0				
DEHBUS31	SCOTTBUS31	1	1	1.089	15.246	
SCOTTBUS32	DEHBUS32	1	1	0.039	0.547	
SCOTTBUS33	DEHBUS33	1	1	0.039	0.547	
DEHBUS41	SCOTTBUS41	1	1	1.089	15.246	
SCOTTBUS42	DEHBUS42	1	1	0.039	0.547	
SCOTTBUS43	DEHBUS43	1	1	0.039	0.547	

The subsea load

The subsea load is the same as given in Table E.7.

DEH impedance

The DEH impedance is specified in the data group "SHUNT IMPEDANCES" and is given in Table E.13.

Table E.13: Parameters for the data group "SHUNT IMPEDANCES"

Node	Resistance [Ω]	Reactance [Ω]
DEHBUS32	4.0	15.6
DEHBUS33	4.0	15.6
DEHBUS42	4.0	15.6
DEHBUS43	4.0	15.6

Power control

The production source at GENBUS is specified in "POWER CONTROL" as a swing bus with constant voltage and power angle, see Table E.9.

Appendix F

SIMPOW files for the system simulations

The Optpow– and Dynpow files for the simulations in Chapter 5 are given in this appendix.

F.1 Case 1

F.1.1 Normal operation

The voltage at the DEH terminals is 25 kV and the impedance of the DEH loads is $Z = 4.0 + j15.6\Omega$.

Optpow

The Optpow file establishes the topology and branches for Case 1 and calculates the steady state solution. In addition, it gives the initial condition for the Dynpow file in which the Scott-T is implemented into the system. Comments in the Optpow file after "!!" are included to describe the data groups. For further details, see the SIMPOW manual [10].

```
OPTPOW FILE for the DEH system in CASE 1.
HEATING PIPE, 25 kV
**

GENERAL
 SN=150
END


NODES
 GENBUS     UB=300
 BUS1       UB=300
 BUS2       UB=132
 LOADBUS   UB=132
 BUS3       UB=66
 DEHBUS1    UB=66
 SCOTTBUS1  UB=66
 SCOTTBUS2  UB=25  PHASE=1  !! 25 kV for heating
 SCOTTBUS3  UB=25  PHASE=1
```

```
 DEHBUS2    UB=25  PHASE=1
 DEHBUS3    UB=25  PHASE=1
END


LINES
 GENBUS  BUS1        TYPE=0
 BUS2  LOADBUS       TYPE=2  L=100  R=0.097  X=0.145  B=4.398E-5
 BUS3  DEHBUS1       TYPE=2  L=50   R=0.040  X=0.110  B=8.482E-5
 DEHBUS1  SCOTTBUS1  TYPE=1  L=1    R=0.272  X=3.815
 SCOTTBUS2  DEHBUS2  TYPE=1  L=1    R=0.039  X=0.547
 SCOTTBUS3  DEHBUS3  TYPE=1  L=1    R=0.039  X=0.547
END


TRANSFORMERS
 BUS1  BUS2  BUS3  NW=3
     SN=150   UN1=300  UN2=132  UN3=66
     ER12=0.005  ER13=0.005  ER23=0.005
     EX12=0.07  EX13=0.07  EX23=0.07

 SCOTTBUS1  SCOTTBUS2  SCOTTBUS3  NW=3
     SN=80  UN1=66  UN2=25  UN3=25
     ER12=0  ER13=0  ER23=0
     EX12=0.00001  EX13=0.00001  EX23=0.00001
END


LOADS
 LOADBUS  P=50  COSFI=0.9  !!Subsea load 100 km from shore (motors, pumps etc)
END


SHUNT IMPEDANCES
 DEHBUS2  R=4.0  X=15.6  !!Impedance of piggyback cable and pipeline
 DEHBUS3  R=4.0  X=15.6
END

POWER CONTROL
 GENBUS  TYPE=NODE  RTYP=SW  U=300  FI=0 !!The node GENBUS is a swing bus
END

END
```

Dynpow

The lossless DSL model for the Scott–T transformer is implemented in the data group "TRANSFORMERS", and the simulation is run in 20 seconds.

```
DYNPOW FILE for the DEH system in CASE 1
HEATING PIPE CONTENT, 25 kV
**

CONTROL DATA
 TEND=20  XTRACE=-1  EDSL=3  DDSL=3
END
```

```
NODES
 GENBUS   TYPE=1
END

TRANSFORMERS
 SCOTTBUS1  SCOTTBUS2  SCOTTBUS3  NW=3  TYPE=DSL/SCOTT
END

DSL-TYPES
 SCOTT(BUS1,BUS2,BUS3,UN1,UN2,UN3)
END

END
```

F.1.2 Disconnecting the subsaea load, DEH heating

Dynpow

The disconnection of the subsea load at LOADBUS is done in Dynpow, see the data group "RUN INSTRUCTION".

```
DYNPOW FILE for the DEH system in CASE 1
HEATING PIPE CONTENT, 25 kV AND DISCONNECTING SUBSEA LOAD
**

CONTROL DATA
 TEND=20  XTRACE=-1  EDSL=3  DDSL=3
END

NODES
 GENBUS   TYPE=1
END

TRANSFORMERS
 SCOTTBUS1  SCOTTBUS2  SCOTTBUS3  NW=3  TYPE=DSL/SCOTT
END

DSL-TYPES
 SCOTT(BUS1,BUS2,BUS3,UN1,UN2,UN3)
END

RUN INSTRUCTION
 AT 5  INST=DISCONNECT  LOAD  LOADBUS
END

END
```

F.1.3 Disconnecting cable at BUS2, DEH heating

The Dynpow file for the simulations in Chapter 5.2.3 is given below. The disconnection of the subsea cable between BUS2 and LOADBUS is done in "RUN INSTRUCTION".

Dynpow

```
DYNPOW FILE for the DEH system in CASE 1
HEATING PIPE CONTENT, 25 kV AND DISCONNECTING THE 100 KM CABLE
**

CONTROL DATA
 TEND=20  XTRACE=-1  EDSL=3  DDSL=3
END

NODES
 GENBUS   TYPE=1
END

TRANSFORMERS
 SCOTTBUS1  SCOTTBUS2  SCOTTBUS3  NW=3  TYPE=DSL/SCOTT
END

DSL-TYPES
 SCOTT(BUS1,BUS2,BUS3,UN1,UN2,UN3)
END

RUN INSTRUCTION
 AT 5  INST=DISCONNECT  LINE  BUS2 LOADBUS
END

END
```

F.1.4 Short–circuit in the middle of the pipeline

The Dynpow file for the short–circuit in the middle of the pipeline is given here.

Dynpow

```
DYNPOW FILE for the DEH system in CASE 1
HEATING PIPE CONTENT (25 kV) AND SHORT-CIRCUIT ON THE MIDDLE OF THE PIPELINE
**

CONTROL DATA
 TEND=20  XTRACE=-1  EDSL=3  DDSL=3
END

NODES
 GENBUS   TYPE=1
END

TRANSFORMERS
 SCOTTBUS1  SCOTTBUS2  SCOTTBUS3  NW=3  TYPE=DSL/SCOTT
END

DSL-TYPES
 SCOTT(BUS1,BUS2,BUS3,UN1,UN2,UN3)
END
```

```
SHUNT IMPEDANCES
 DEHBUS3  NO=1  R=4.0  X=15.6
END

RUN INSTRUCTION
 AT 5 INST=CONNECT  SHUN=DEHBUS3  NO=1
END

END
```

F.1.5 Short–circuit on a DEH load terminal

The Optpow file is the same as for normal load flow, but the Dynpow file is changed to short–circuit the node DEHBUS3

Dynpow

```
DYNPOW FILE for the DEH system in CASE 1
MAINTAINING TEMPERATURE AND SHORT_CIRCUIT ON DEHBUS3
**

CONTROL DATA
 TEND=20  XTRACE=-1  EDSL=3  DDSL=3
END

NODES
 GENBUS   TYPE=1
END

TRANSFORMERS
 SCOTTBUS1  SCOTTBUS2  SCOTTBUS3  NW=3  TYPE=DSL/SCOTT
END

DSL-TYPES
 SCOTT(BUS1,BUS2,BUS3,UN1,UN2,UN3)
END

FAULTS
 DEHSC  TYPE=3PSG  NODE=DEHBUS3
END

RUN INSTRUCTION
 AT 5  INST=CONNECT  FAUL=DEHSC
END

END
```

F.1.6 Disconnecting one DEH load

The Optpow file is the same as used before. The Dynpow however, is changed to simulate the situation when the load at DEHBUS3 is disconnected.

Dynpow

```
DYNPOW FILE for the DEH system in CASE 1
MAINTAINING TEMPERATURE AND OUTAGE OF LOAD ON DEHBUS3
**

CONTROL DATA
 TEND=10  XTRACE=-1  EDSL=3  DDSL=3
END

NODES
 GENBUS   TYPE=1
END

TRANSFORMERS
 SCOTTBUS1  SCOTTBUS2  SCOTTBUS3  NW=3  TYPE=DSL/SCOTT
END

DSL-TYPES
 SCOTT(BUS1,BUS2,BUS3,UN1,UN2,UN3)
END

RUN INSTRUCTION
 AT 5  INST=DISCONNECT  SHUN=DEHBUS3
END

END
```

F.1.7 Improving the system

The Optpow file for specifying the tap changers for the transformers and the shunt capacitor at LOADBUS is given here. The tap changers for the transformers are given a very large step–span. This is done for the sake of analysis, and render the possibility to have the turn ratio which is required. See [10] for further information on the input parameters. The Dynpow file is the same as for the normal simulation given in Appendix F.1.1.

Optpow

```
OPTPOW FILE for the DEH system in CASE 1 WITH TAPPINGS
HEATING PIPE, 25 kV
**

CONTROL DATA
 TAUCHECK=NO
END

GENERAL
 SN=150
END


NODES
 GENBUS     UB=300
 BUS1       UB=300
```

```
 BUS2       UB=132
 LOADBUS    UB=132
 BUS3       UB=66
 DEHBUS1    UB=66
 SCOTTBUS1  UB=66
 SCOTTBUS2  UB=25  PHASE=1  !! 25 kV for heating
 SCOTTBUS3  UB=25  PHASE=1
 DEHBUS2    UB=25  PHASE=1
 DEHBUS3    UB=25  PHASE=1
END


LINES
 GENBUS     BUS1       TYPE=0
 BUS2       LOADBUS    TYPE=2  L=100  R=0.097  X=0.145  B=4.398E-5
 BUS3       DEHBUS1    TYPE=2  L=50   R=0.040  X=0.110  B=8.482E-5
 DEHBUS1    SCOTTBUS1  TYPE=1  L=1    R=0.272  X=3.815
 SCOTTBUS2  DEHBUS2    TYPE=1  L=1    R=0.039  X=0.547
 SCOTTBUS3  DEHBUS3    TYPE=1  L=1    R=0.039  X=0.547
END


TRANSFORMERS
 BUS1  BUS2  BUS3  NW=3
     SN=150   UN1=300  UN2=132  UN3=66
     TAPSIDE=23 1STEP=0.01  +N1STEP=100  -N1STEP=100
     2STEP=0.01  +N2STEP=100  -N2STEP=100  3STEP=0.01  +N3STEP=100  -N3STEP=100
     ER12=0.005  ER13=0.005  ER23=0.005
     EX12=0.07   EX13=0.07   EX23=0.07

 SCOTTBUS1  SCOTTBUS2  SCOTTBUS3  NW=3
     SN=80  UN1=53  UN2=25  UN3=25
     TAPSIDE=23 1STEP=0.01  +N1STEP=100 -N1STEP=100
     2STEP=0.01  +N2STEP=100  -N2STEP=100  3STEP=0.01  +N3STEP=100  -N3STEP=100
     ER12=0  ER13=0  ER23=0
     EX12=0.00001    EX13=0.00001  EX23=0.00001
END

LOADS
 LOADBUS  P=50  COSFI=0.9  MP=0  MQ=0
END


SHUNT IMPEDANCES
 DEHBUS2  R=4.0  X=15.6  !! Impedance of piggyback cable and pipeline
 DEHBUS3  R=4.0  X=15.6
 LOADBUS  Q=-20
END

POWER CONTROL
 GENBUS  TYPE=NODE  RTYP=SW  U=300  FI=0
 BUS1  BUS2  BUS3  TYPE=TR3  R2TYP=UFI  U2=132  R3TYP=UFI  U3=66
 SCOTTBUS1  SCOTTBUS2  SCOTTBUS3  TYPE=TR3  R2TYP=UFI  U2=25  R3TYP=UFI  U3=25
END

END
```

F.2 Case 2

The simulation files for Case 2 are given here.

F.2.1 Normal load, DEH heating

Optpow

```
OPTPOW FILE for the DEH system in CASE 2
HEATING PIPE CONTENT 25 kV
**

GENERAL
 SN=220
END


NODES
 GENBUS     UB=300
 BUS1       UB=300
 BUS2       UB=132
 BUS3       UB=132
 BUS4       UB=132
 LOADBUS    UB=132

 DEHBUS31    UB=132
 SCOTTBUS31  UB=132
 SCOTTBUS32  UB=25  PHASE=1  !! 25 kV for  heating
 SCOTTBUS33  UB=25  PHASE=1
 DEHBUS32    UB=25  PHASE=1
 DEHBUS33    UB=25  PHASE=1

 DEHBUS41    UB=132
 SCOTTBUS41  UB=132
 SCOTTBUS42  UB=25  PHASE=1  !! 25 kV for  heating
 SCOTTBUS43  UB=25  PHASE=1
 DEHBUS42    UB=25  PHASE=1
 DEHBUS43    UB=25  PHASE=1

END


LINES
 GENBUS  BUS1      TYPE=0
 BUS2    BUS3      TYPE=2  L=50   R=0.097  X=0.145  B=4.398E-5
 BUS3    BUS4      TYPE=2  L=100  R=0.097  X=0.145  B=4.398E-5
 BUS4    LOADBUS   TYPE=2  L=50   R=0.097  X=0.145  B=4.398E-5

 BUS3        DEHBUS31    TYPE=0
 DEHBUS31    SCOTTBUS31  TYPE=1  L=1    R=1.089  X=15.246
 SCOTTBUS32  DEHBUS32    TYPE=1  L=1    R=0.039  X=0.547
 SCOTTBUS33  DEHBUS33    TYPE=1  L=1    R=0.039  X=0.547

 BUS4        DEHBUS41    TYPE=0
 DEHBUS41    SCOTTBUS41  TYPE=1  L=1    R=1.089  X=15.246
 SCOTTBUS42  DEHBUS42    TYPE=1  L=1    R=0.039  X=0.547
```

```
 SCOTTBUS43  DEHBUS43    TYPE=1  L=1    R=0.039  X=0.547

END


TRANSFORMERS
 BUS1  BUS2
     SN=220   UN1=300  UN2=132
     ER12=0.005  EX12=0.07

 SCOTTBUS31  SCOTTBUS32  SCOTTBUS33  NW=3
     SN=80  UN1=132  UN2=25  UN3=25
     ER12=0  ER13=0  ER23=0
     EX12=0.00001  EX13=0.00001  EX23=0.00001

 SCOTTBUS41  SCOTTBUS42  SCOTTBUS43  NW=3
     SN=80  UN1=132  UN2=25  UN3=25
     ER12=0  ER13=0  ER23=0
     EX12=0.00001  EX13=0.00001  EX23=0.00001
END


LOADS
 LOADBUS  P=50  COSFI=0.9  !!Subsea load 100 km from shore (motors, pumps etc)
END


SHUNT IMPEDANCES
 DEHBUS32  R=4.0  X=15.6  !!Impedance of piggyback cable and pipeline
 DEHBUS33  R=4.0  X=15.6
 DEHBUS42  R=4.0  X=15.6
 DEHBUS43  R=4.0  X=15.6
END

POWER CONTROL
 GENBUS  TYPE=NODE  RTYP=SW  U=300  FI=0   !!The node GENBUS is a swing bus
END

END
```

Dynpow

```
DYNPOW FILE for the DEH system in CASE 2
HEATING PIPE CONTENT
**

CONTROL DATA
 TEND=20  XTRACE=-1  EDSL=3  DDSL=3
END

NODES
 GENBUS   TYPE=1
END

TRANSFORMERS
 SCOTTBUS31  SCOTTBUS32  SCOTTBUS33  NW=3  TYPE=DSL/SCOTT
 SCOTTBUS41  SCOTTBUS42  SCOTTBUS43  NW=3  TYPE=DSL/SCOTT
```

```
END

DSL-TYPES
 SCOTT(BUS1,BUS2,BUS3,UN1,UN2,UN3)
END

END
```

F.2.2 Improving the system for Case 2

The data groups in Optpow for improving Case 2 are given below.

Optpow

```
TRANSFORMERS
 BUS1  BUS2
     SN=220   UN1=300  UN2=132
     TAPSIDE=2  STEP=0.01  +NSTEP=30  -NSTEP=30
     ER12=0.005  EX12=0.07

 SCOTTBUS31  SCOTTBUS32  SCOTTBUS33  NW=3
     TAPSIDE=23 1STEP=0.01  +N1STEP=70  -N1STEP=70  2STEP=0.01
     +N2STEP=70  -N2STEP=70  3STEP=0.01  +N3STEP=70  -N3STEP=70
     SN=80  UN1=118  UN2=25  UN3=25
     ER12=0  ER13=0  ER23=0
     EX12=0.00001  EX13=0.00001  EX23=0.00001

 SCOTTBUS41  SCOTTBUS42  SCOTTBUS43  NW=3
     TAPSIDE=23 1STEP=0.01  +N1STEP=70  -N1STEP=70  2STEP=0.01
     +N2STEP=70  -N2STEP=70  3STEP=0.01  +N3STEP=70  -N3STEP=70
     SN=80  UN1=118  UN2=25  UN3=25
     ER12=0  ER13=0  ER23=0
     EX12=0.00001  EX13=0.00001  EX23=0.00001
END

SHUNT IMPEDANCES
 DEHBUS32  R=4.0  X=15.6  !!Impedance of piggyback cable and pipeline
 DEHBUS33  R=4.0  X=15.6
 DEHBUS42  R=4.0  X=15.6
 DEHBUS43  R=4.0  X=15.6

 LOADBUS   NO=1  Q=-40  !! Reactive compensation
END

POWER CONTROL
 GENBUS      TYPE=NODE   RTYP=SW     U=300  FI=0   !!The node GENBUS is a swing bus
 BUS1  BUS2  TYPE=TREG   RTYP=UFI    U=132  FI=0
 SCOTTBUS31  SCOTTBUS32  SCOTTBUS33  TYPE=TR3  R2TYP=UFI  U2=25  R3TYP=UFI  U3=25
 SCOTTBUS41  SCOTTBUS42  SCOTTBUS43  TYPE=TR3  R2TYP=UFI  U2=25  R3TYP=UFI  U3=25
END
```

F.2.3 Disconnect the subsea load, DEH heating

The Dynpow file for disconnecting the load and shunt capacitor is given here.

Dynpow

```
DYNPOW FILE for the DEH system in CASE 2
DISCONNECT LOAD AND SHUNT CAPACITOR AT LOADBUS
HEATING PIPE CONTENT
**

CONTROL DATA
 TEND=20  XTRACE=-1  EDSL=3  DDSL=3
END

NODES
 GENBUS   TYPE=1
END

TRANSFORMERS
 SCOTTBUS31  SCOTTBUS32  SCOTTBUS33  NW=3  TYPE=DSL/SCOTT
 SCOTTBUS41  SCOTTBUS42  SCOTTBUS43  NW=3  TYPE=DSL/SCOTT
END

DSL-TYPES
 SCOTT(BUS1,BUS2,BUS3,UN1,UN2,UN3)
END

RUN INSTRUCTIONS
 AT 5  INST=DISCONNECT  LOAD=LOADBUS
 AT 5  INST=DISCONNECT  SHUN=LOADBUS  NO=1
END

END
```

F.2.4 Short–circuit on DEHBUS42

The Dynpow file for the short–circuit is given here.

Dynpow

```
DYNPOW FILE for the DEH system in CASE 2
HEATING PIPE CONTENT (25 kV) AND SHORT CIRCUIT ON DEHBUS42
**

CONTROL DATA
 TEND=20  XTRACE=-1  EDSL=3  DDSL=3
END

NODES
 GENBUS   TYPE=1
END
```

```
TRANSFORMERS
 SCOTTBUS31  SCOTTBUS32  SCOTTBUS33  NW=3  TYPE=DSL/SCOTT
 SCOTTBUS41  SCOTTBUS42  SCOTTBUS43  NW=3  TYPE=DSL/SCOTT
END

DSL-TYPES
 SCOTT(BUS1,BUS2,BUS3,UN1,UN2,UN3)
END

FAULTS
 DEHSC  TYPE=3PSG  NODE=DEHBUS42
END

RUN INSTRUCTION
 AT 5  INST=CONNECT  FAUL=DEHSC
END

END
```

F.2.5 Loadshedding, only heating on DEHBUS33

The Dynpow file for the mode where only the pipe section at DEHBUS33 is heated, is given here.

Dynpow

```
DYNPOW FILE for the DEH system in CASE 2
ONLY HEATING ON DEHBUS33
HEATING PIPE CONTENT (25 kV)
**

CONTROL DATA
 TEND=20  XTRACE=-1  EDSL=3  DDSL=3
END

NODES
 GENBUS   TYPE=1
END

TRANSFORMERS
 SCOTTBUS31  SCOTTBUS32  SCOTTBUS33  NW=3  TYPE=DSL/SCOTT
 SCOTTBUS41  SCOTTBUS42  SCOTTBUS43  NW=3  TYPE=DSL/SCOTT
END

DSL-TYPES
 SCOTT(BUS1,BUS2,BUS3,UN1,UN2,UN3)
END

RUN INSTRUCTION
 AT 5  INST=DISCONNECT  SHUN=DEHBUS42
 AT 5  INST=DISCONNECT  SHUN=DEHBUS43
 AT 5  INST=DISCONNECT  SHUN=DEHBUS32
END
```

```
END
```

Appendix G

Simulation results

This appendix gives the results obtained from the simulations in Chapter 5.

G.1 Case 1

G.1.1 Normal load, DEH heating

The Dynpow load flow result from Chapter 5.2.1 is given in Figure G.1.

G.1.2 Disconnecting the subsea load, DEH heating

The load flow result from Chapter 5.2.2 is given in Figure G.2.

G.1.3 Disconnecting the cable at BUS2, DEH heating

The load flow result from Chapter 5.2.3 is given in Figure G.3

G.1.4 Short–circuit in the middle of a pipeline

Figure G.4 shows the load flow result from the simulation when there is a short–circuit in the middle of the pipeline.

G.1.5 Short–circuit on a DEH load terminal

The simulation result from the short–circuit at DEHBUS3 is given in Figure G.5.

G.1.6 Disconnecting one DEH load

Figure G.6 shows the values for the voltages and the power flow in the system when the pipeline at DEHBUS3 is disconnected.

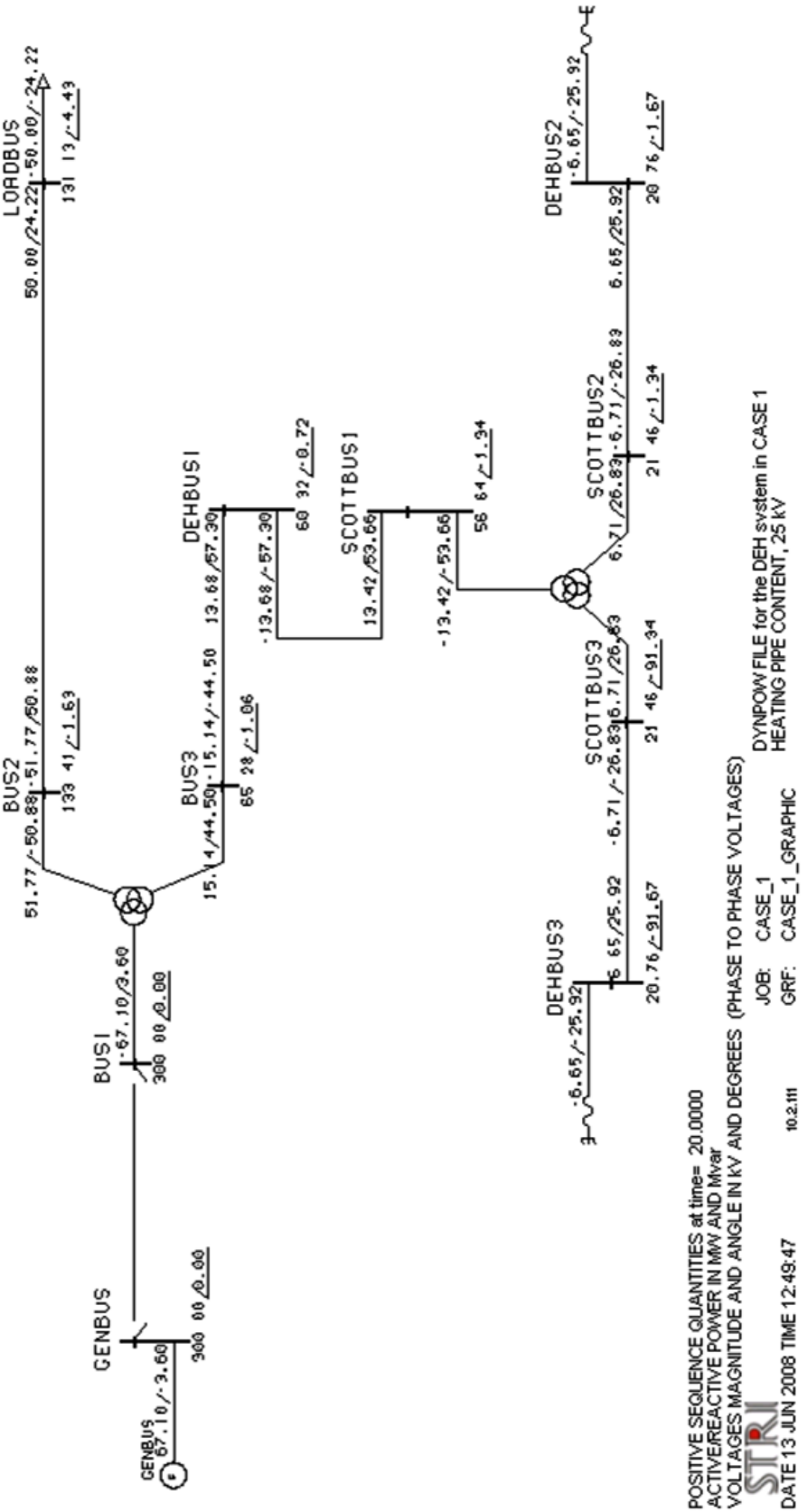

Figure G.1: Load flow result for Case 1 for normal load and heating the pipeline

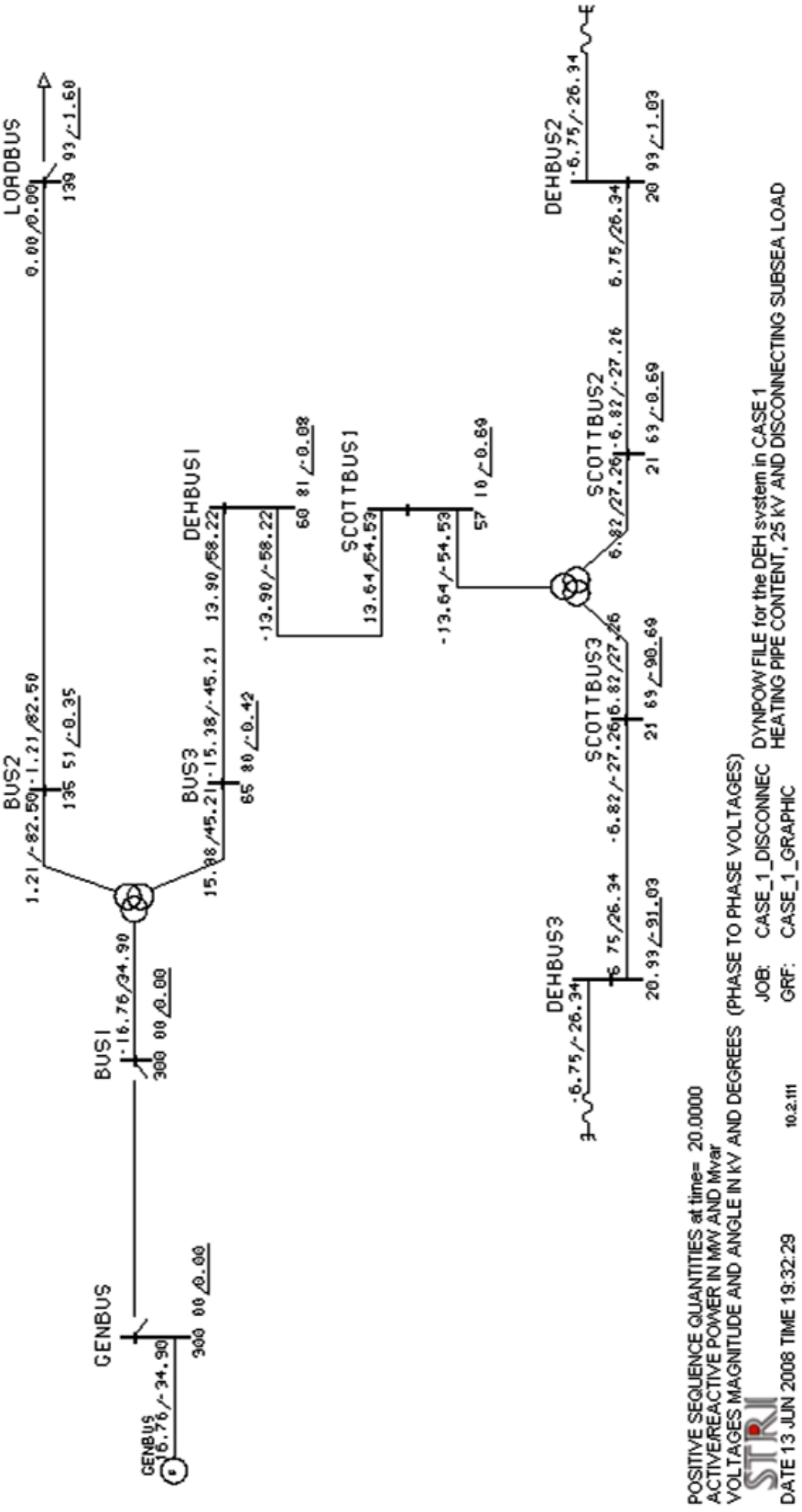

Figure G.2: Load flow result for Case 1 when the subsea load at LOADBUS is disconnected

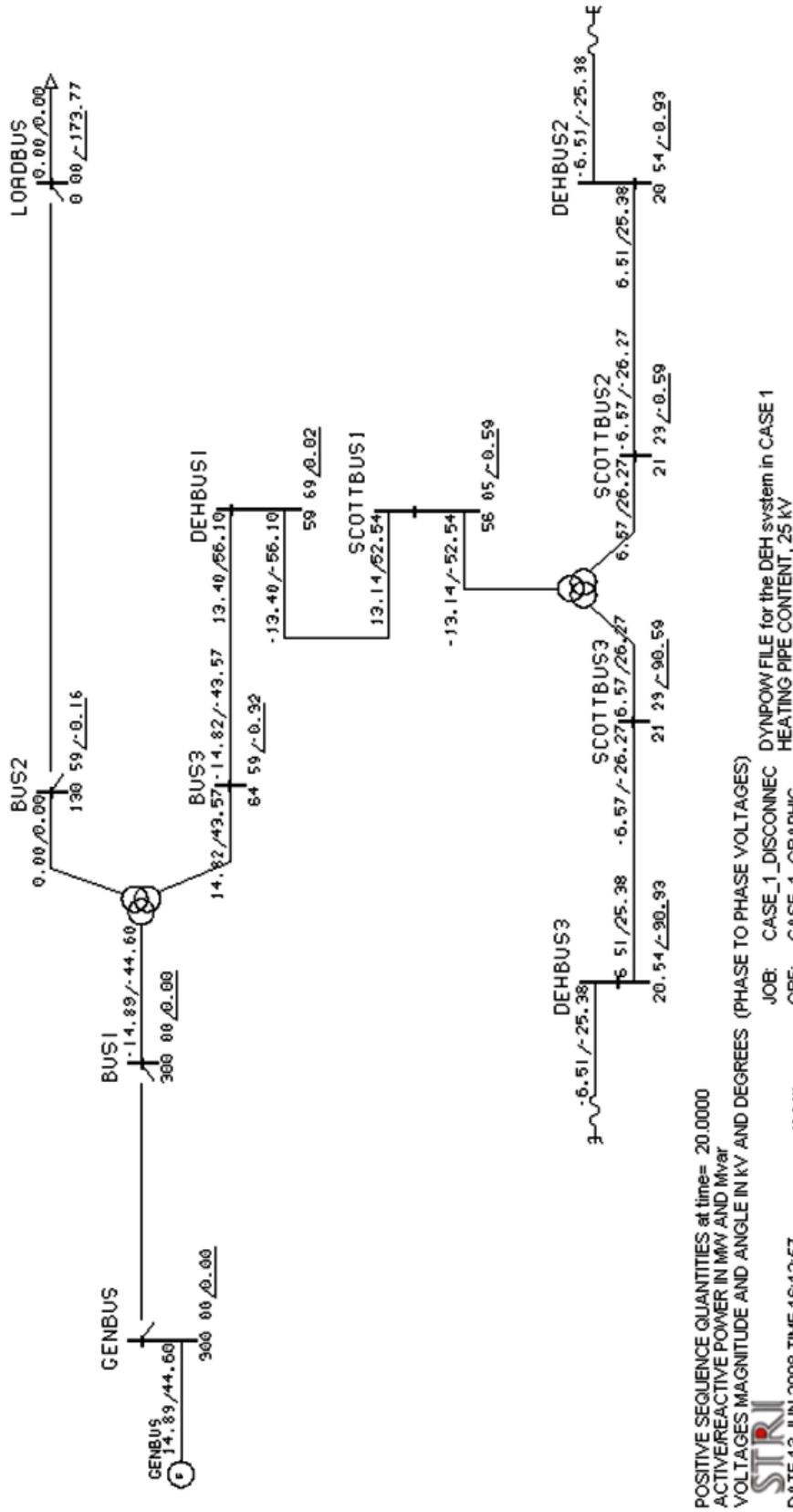

Figure G.3: Load flow result for Case 1 when the 100 km subsea cable at BUS2 is disconnected

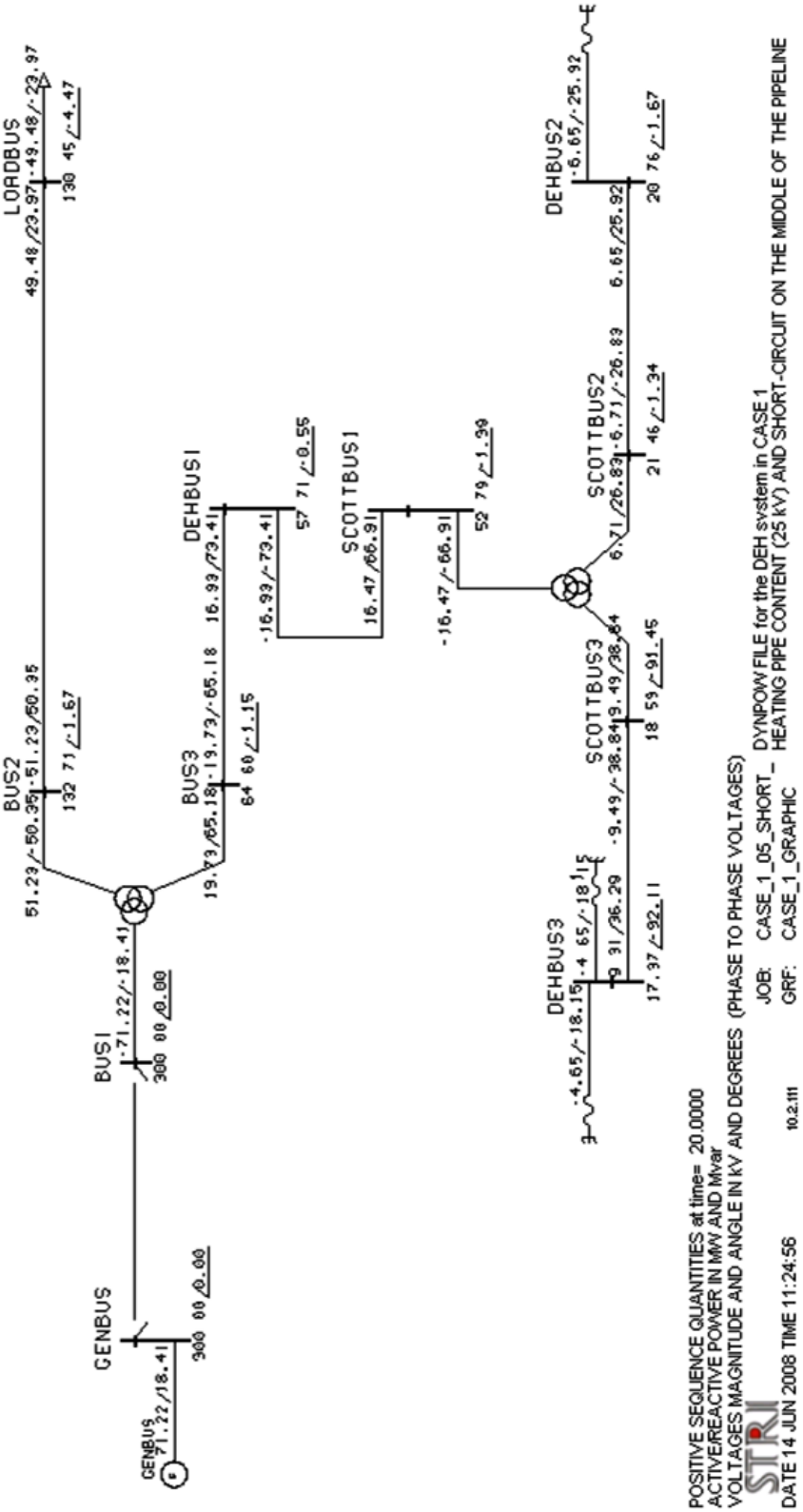

Figure G.4: Load flow result for Case 1 when there is a short–circuit in the middle of the pipeline at DEHBUS3

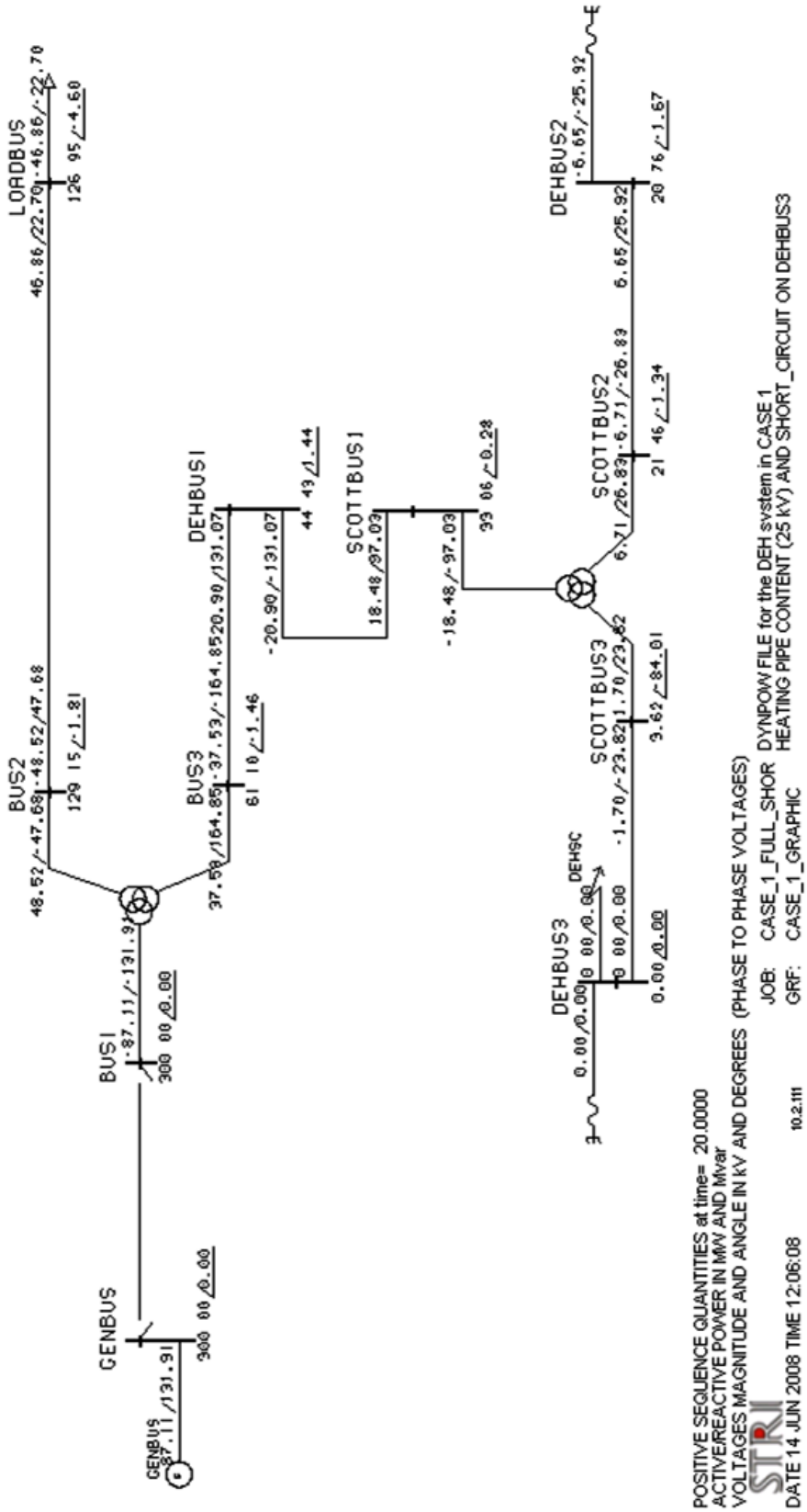

Figure G.5: SLD result after the short–circuit on DEHBUS3

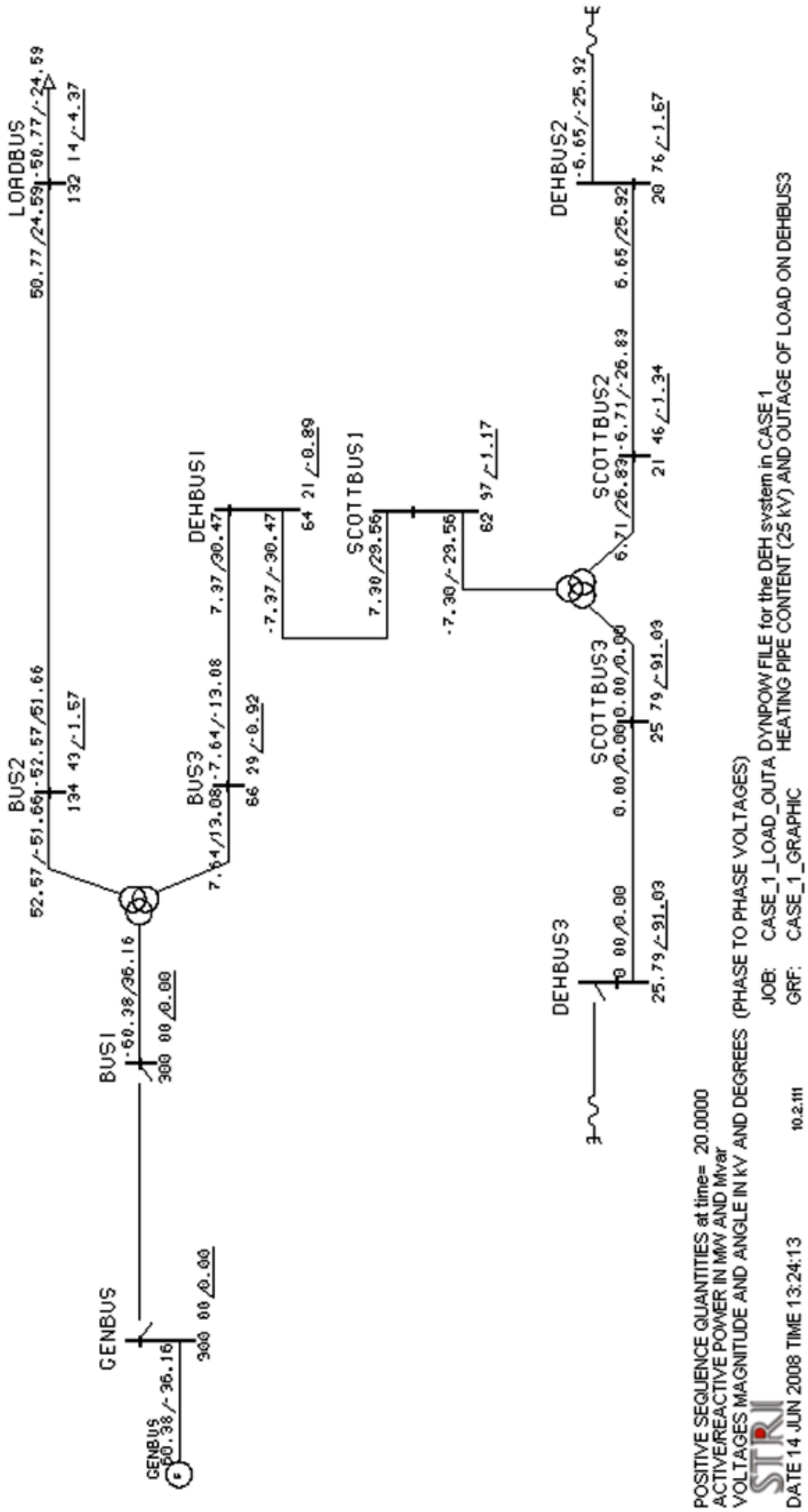

Figure G.6: SLD result after the pipeline at DEHBUS3 is disconnected

G.1.7 Improving the system for Case 1

Figure G.7 shows the load flow result when the tap changers and shunt capacitor are used.

G.2 Case 2

G.2.1 Normal load, DEH heating

Figure G.8 shows the load flow result for Case 2 for the mode where the load and DEH system is operating.

G.2.2 Improving the system for Case 2

Figure G.9 shows the load flow result when the tap changers and shunt capacitor are used in Case 2.

G.2.3 Disconnect the subsea load, DEH heating

The load flow result from Dynpow when the subsea load at LOADBUS is disconnected is given in Figure G.10

G.2.4 Short–circuit on DEHBUS42

The load flow for the short–circuit on DEHBUS42 is given in Figure G.11.

G.2.5 Loadshedding, only heating on DEHBUS33

Figure G.12 presents a larger version of the load flow presented for Case 2 and the mode where only heating is connected to DEHBUS33.

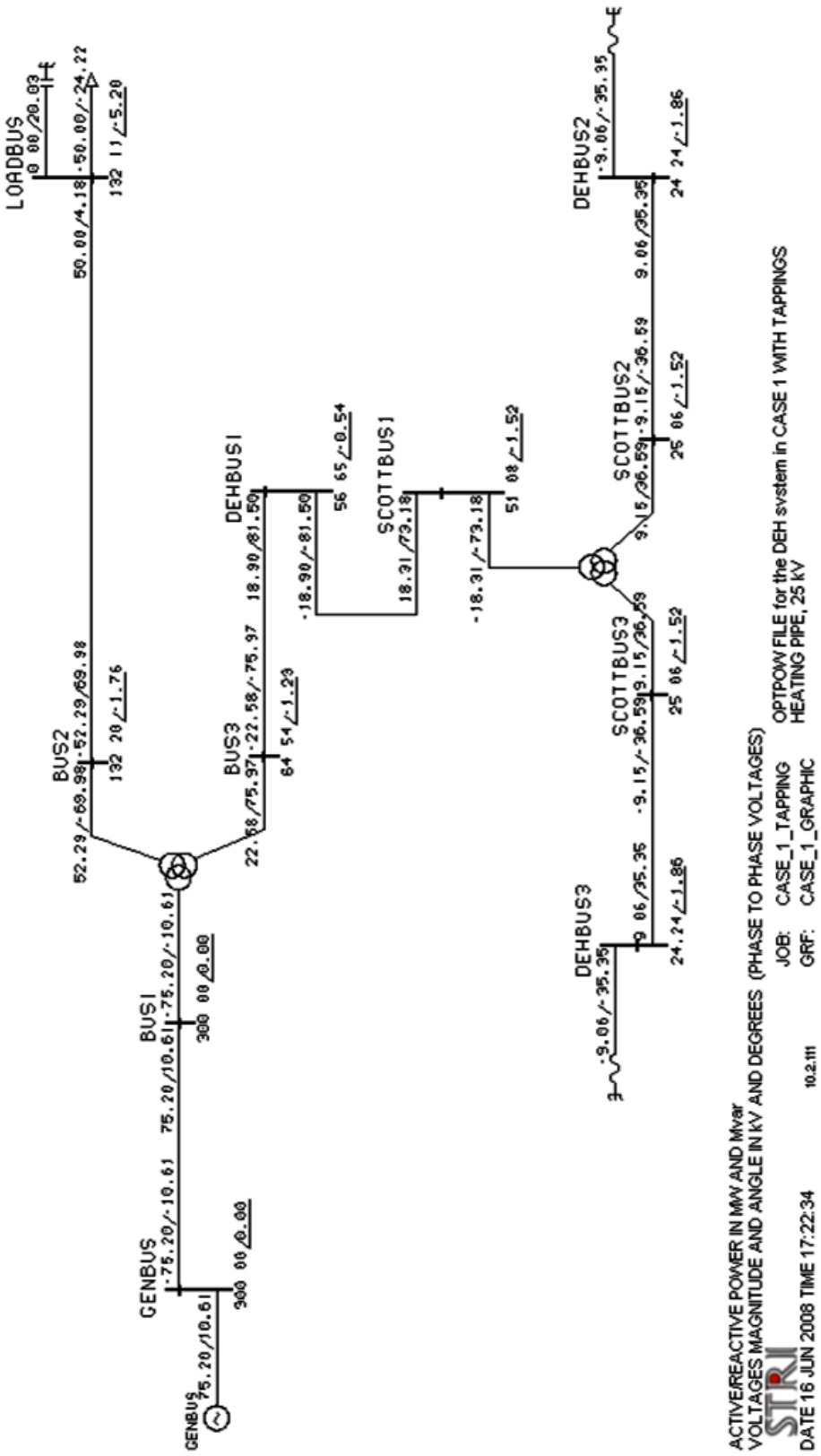

Figure G.7: SLD result after improving the system for Case 1

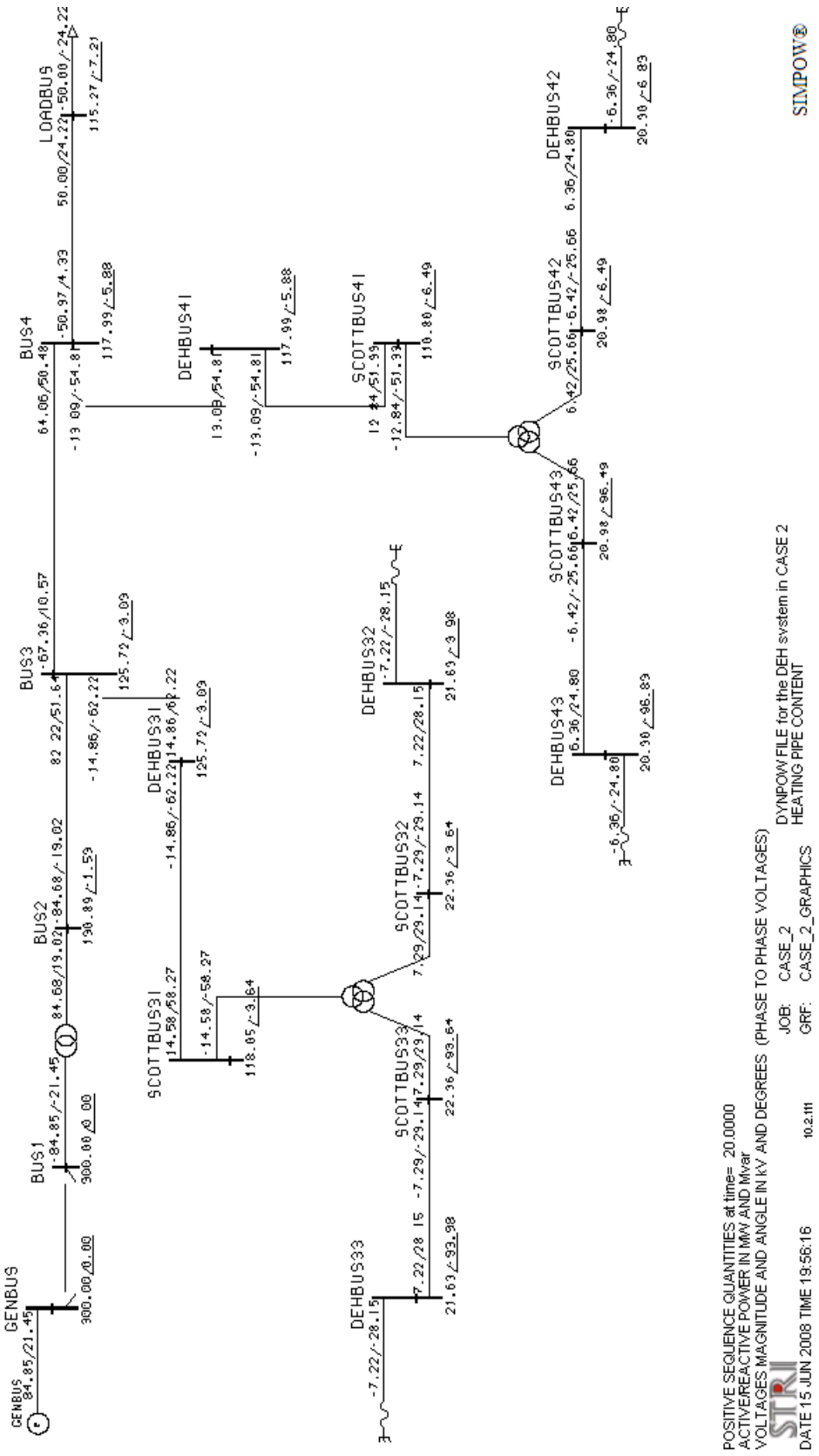

Figure G.8: Load flow result for Case 2 for normal load and heating the pipe

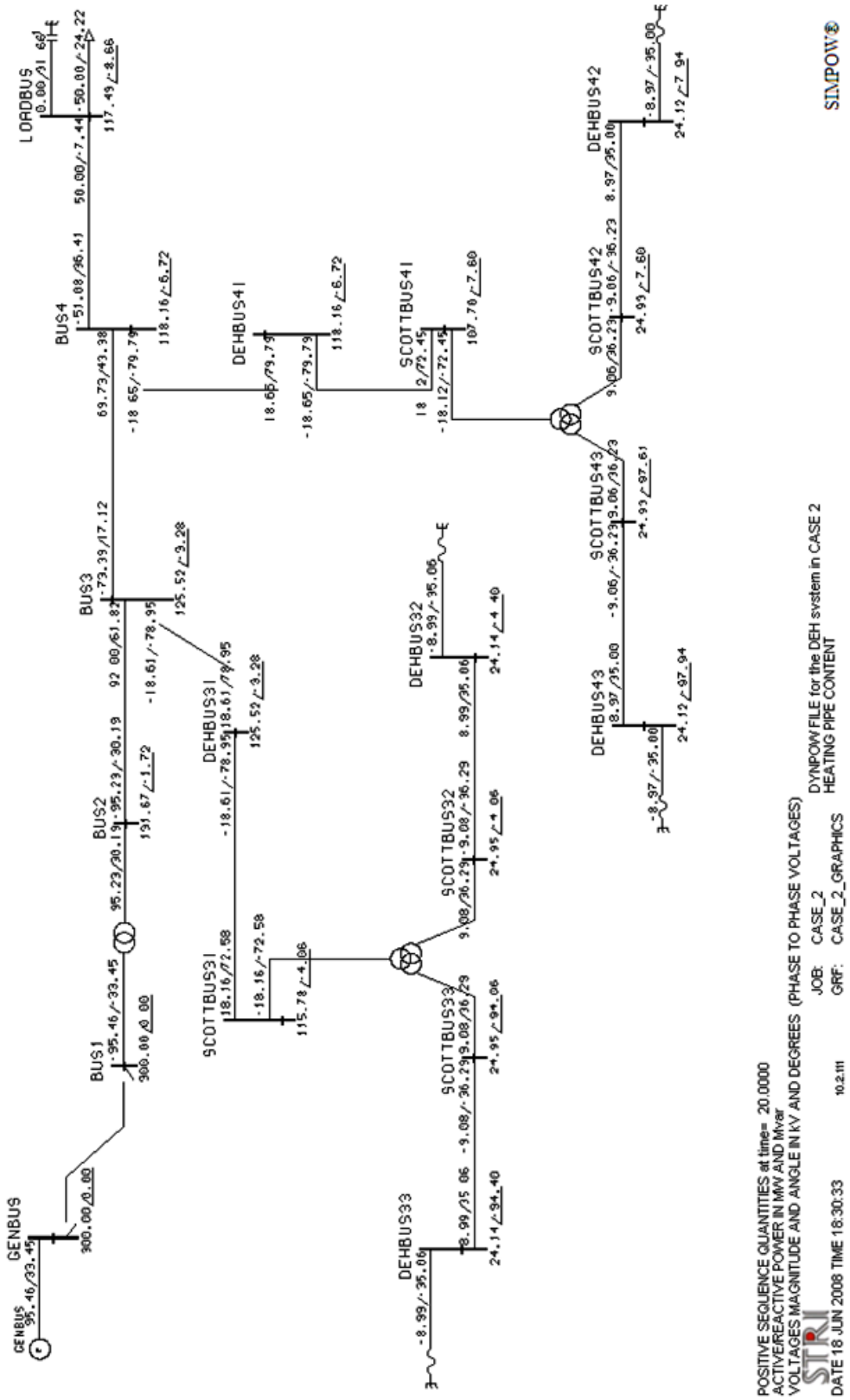

Figure G.9: SLD result after improving the system for Case 2

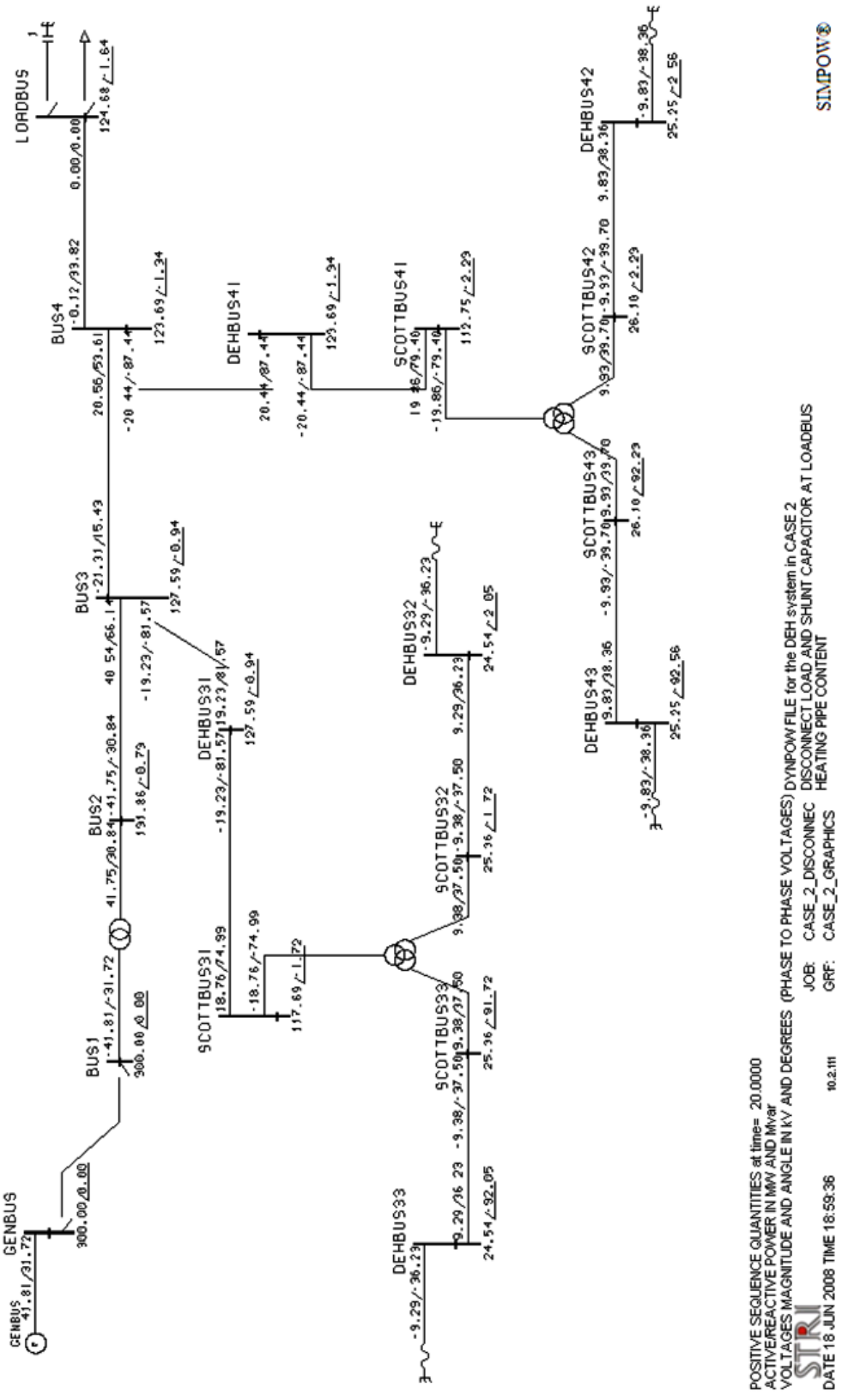

Figure G.10: SLD result after disconnecting the subsea load and shunt capacitor at LOADBUS

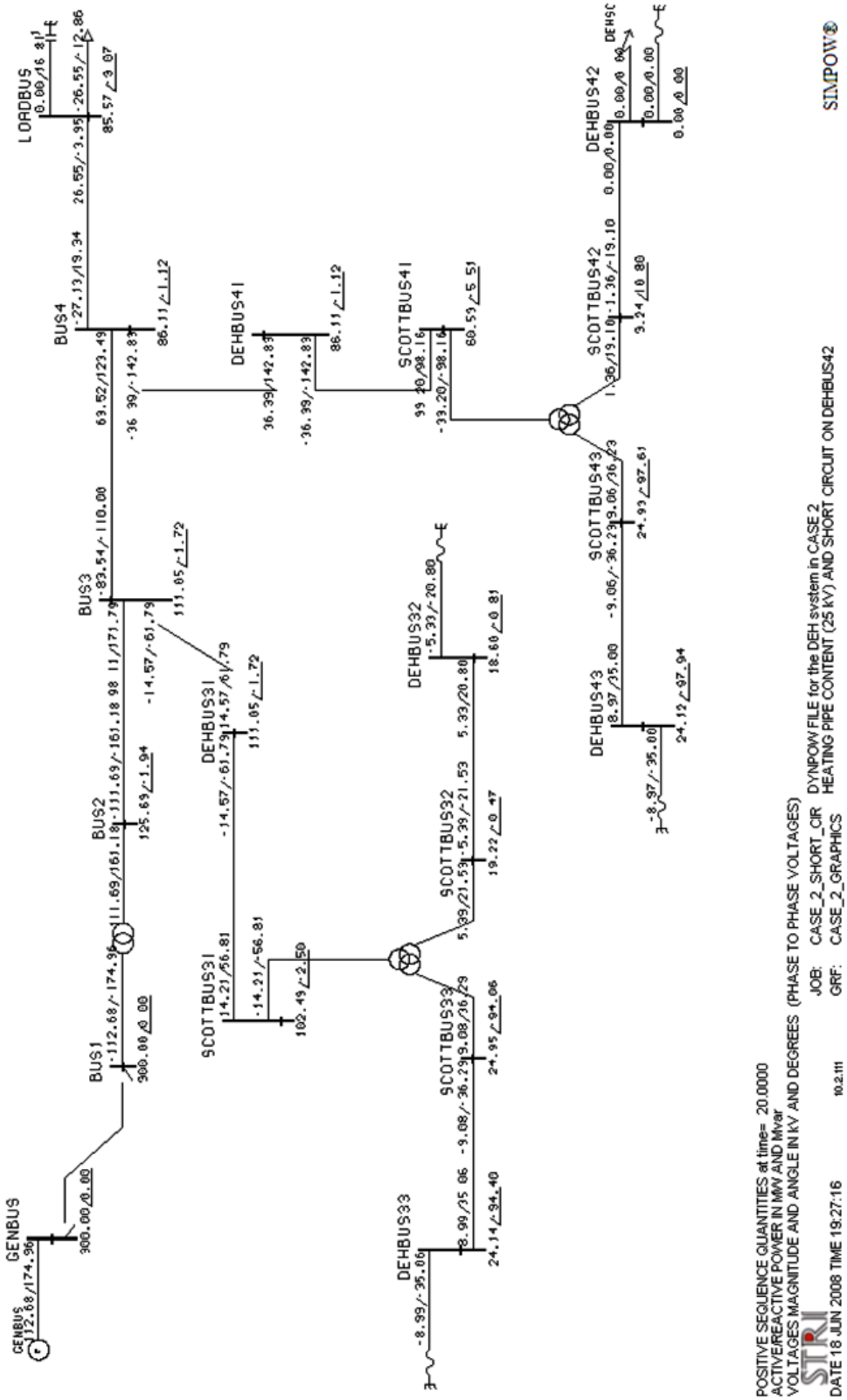

Figure G.11: Load flow result after a short–circuit on DEHBUS42

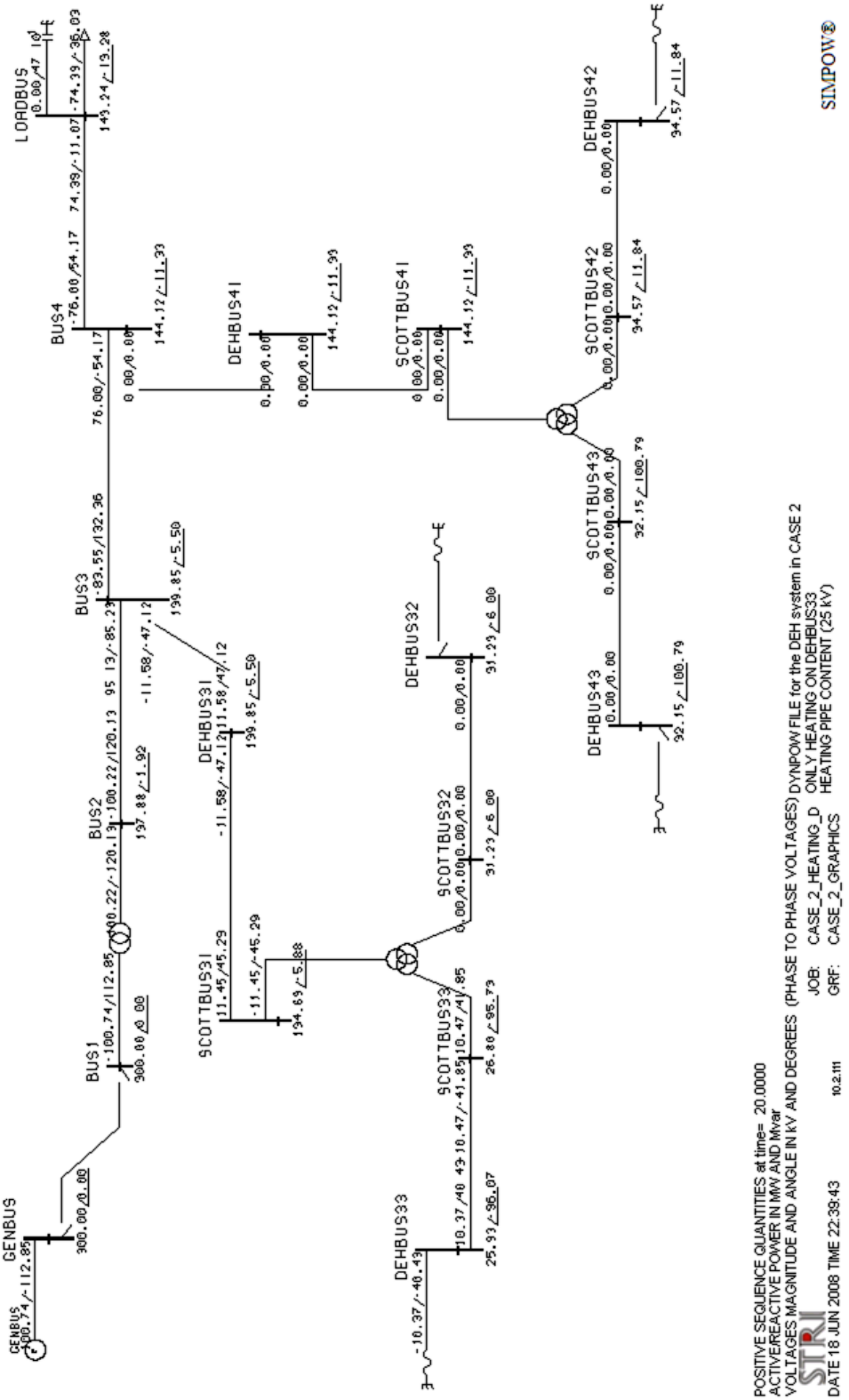

Figure G.12: Load flow result when only the pipe section at DEHBUS33 is heated